

博士(人間科学)学位論文

In vivo activation properties of
human skeletal muscle using mfMRI

(mfMRI を用いたヒト生体における骨格筋の活動特性)

2007 年 1 月

早稲田大学大学院 人間科学研究科

衣笠 竜太

Kinugasa, Ryuta

ABSTRACT

The goal of this dissertation was to investigate the *in vivo* activation properties of human skeletal muscle. The specific aims were 1) to establish the methodology for quantitative assessment of the size of activated volumes within muscles, the distribution of intramuscular activation, and the level of that activation, 2) to examine the activation properties in the synergistic triceps surae muscles at a given workload, and 3) to examine changes in activation properties in the medial gastrocnemius and soleus muscles with increasing workload. The results showed that muscle functional magnetic resonance imaging is a useful tool for quantitatively assessing three-dimensional data revealing muscle activation properties at various spatial resolutions.

During the calf-raise exercise employed in the present studies, muscle activation within the three triceps surae muscles differed with respect to the size and location of the activated regions and the level of that activation. When the required force level was increased, the number and species of activated fibers and their spatial distribution within the triceps surae muscles were regulated selectively, depending upon the level of force required. These findings shed new light on the mechanism of activation of human skeletal muscles.

ACKNOWLEDGEMENTS

This dissertation would not exist without the help and encouragement of many people. First of all I would like to express my deepest gratitude to my advisor, Professor Tetsuo Fukunaga, for his guidance in making this dissertation possible. Fukunaga's intelligence, vision and wisdom have been a tremendous source of inspiration to me throughout all stages of this study. I have learned a lot from him not only about exercise physiology and biomechanics, but also about life in general.

I would also like thank my second advisor Professor Yasuo Kawakami for his support, encouragement and help in putting things in perspective. I wish to express my warm gratitude to Professor Kazuyuki Kanosue and Associate Professor Hiroshi Akima at Nagoya University for their valuable comments and criticism on the manuscript of this dissertation.

I gratefully acknowledge the contributions of Shigeru Yoneyama, President of the Maxnet Co., Ltd., and Hauke Bartsch, of Mercury Computer Systems Co., Ltd., and I began this project in 2003. Since then, Yoneyama and Bartsch helped with development of numerous three-dimensional models of activation mapping that was used in this dissertation.

Final thanks go to my family and friends, for all of their support throughout the years, thanks for instilling in me belief that I can do anything I set my mind to. Without them by my side this work would not have been possible.

This dissertation was supported by the Japan Science Society, Kozuki Foundation, and Asahi Glass Foundation.

CONTENTS

ABSTRACT

ACKNOWLEDGEMENTS

CONTENTS

FIGURES

TABLES

ORIGINAL PAPERS

CHAPTER 1: Introduction-----	1
Activation of a muscle-----	2
Magnetic resonance imaging-----	4
Triceps surae muscles-----	9
Summary and Conclusions-----	10
CHAPTER 2: Neuromuscular activation of triceps surae using muscle functional MRI and EMG	
Introduction-----	14
Methods-----	15
Results-----	19
Discussion-----	23
CHAPTER 3: Quantitative assessment of skeletal muscle activation using muscle functional MRI	
Introduction-----	27
Methods-----	29
Results-----	35
Discussion-----	39

CHAPTER 4: Muscle activation and its distribution within human triceps
surae muscles

Introduction-----	45
Methods-----	47
Results-----	54
Discussion-----	59

CHAPTER 5: Load-specific distribution of muscle activity in human medial
gastrocnemius and soleus muscles

Introduction-----	64
Methods-----	66
Results-----	71
Discussion-----	77

CHAPTER 6: Mapping activation levels of skeletal muscle in healthy
volunteers: an MRI study

Introduction-----	83
Methods-----	84
Results-----	89
Discussion-----	94

CHAPTER 7: Conclusion----- 98

CHAPTER 8: Bibliography----- 103

FIGURES

- 1-1 The basic biological components of the neuromuscular system.
- 1-2 A 1.5-Tesla magnetic resonance scanner.
- 1-3 T1 recovery curve and T2 decay curve.
- 1-4 Typical example of pre- and post-exercise MR images and that T2 values in the quadriceps femoris muscles.

- 2-1 Representative post-exercise MR images at three workloads.
- 2-2 Changes in the % change in T2 and iEMG with the three workloads.
- 2-3 Relationship between the % change in T2 and iEMG in each triceps surae muscle.
- 2-4 Relationship between the % change in T2 and iEMG in all six subjects.

- 3-1 Illustration of the method for determining “active region” of a muscle.
- 3-2 Representative accumulated MR images and 3-D reconstructed MR images in the calf muscle.
- 3-3 Relationship between actual volume and reconstructed volume.
- 3-4 Relationship between the % activated volume and normalized iEMG or % workload in the MG.
- 3-5 Relationship between the % activated volume and normalized iEMG in all six subjects.
- 3-6 Representative T2-weighted MR images at pre- and post-exercise, and 3-D

- activation mapping in the MG.
- 3-7 Series of % activated area along the X-, Y-, and Z-axes in the MG.
- 4-1 Schematic illustration of calf-raise exercise.
- 4-2 Representative 3-D activation mapping after calf-raise exercise and an anatomical image in the triceps surae muscles.
- 4-3 Example of representative segments along three planes.
- 4-4 Series of anatomical and activated areas along the length in each triceps surae muscle.
- 4-5 Series of % activated area along the length in each triceps surae muscle.
- 4-6 The % activated volume of lateral and medial regions, anterior and posterior regions, and proximal and distal regions in each triceps surae muscle.
- 5-1 Representative 3-D activation mapping in the MG and Sol after plantar flexion exercise with loads of 25% and 75% 12 RM.
- 5-2 Series of activated areas in the MG along the X-, Y-, and Z-axes at 25% and 75% 12 RM.
- 5-3 Series of activated areas in the Sol along the X-, Y-, and Z-axes at 25% and 75% 12 RM.
- 5-4 Spatial distribution of the *delta* activated areas within the MG.
- 5-5 Spatial distribution of the *delta* activated areas within the Sol.
- 6-1 Representative five-colors categorized MR images from the extreme proximal end, the central region, and extreme distal end in the calf muscle.

- 6-2 Representative 3-D activation levels mapping in the triceps surae muscles.
- 6-3 Representative pre-exercise T2 images and their T2 histogram.
- 6-4 The five-colors categorized % activated volume in each triceps surae muscle.

TABLES

- 2-1 Absolute T2 and iEMG at rest, B ex, U ex, and U + 15 ex.
- 4-1 The muscle volume, activated muscle volume, and % activated volume.
- 4-2 Maximal isometric torque, normalized iEMG, and % change in T2.
- 5-1 The normalized iEMG in the MG and Sol at 25% and 75% 12 RM loads.
- 5-2 The muscle volume, activated muscle volume, and % activated volume in the MG and Sol at 25% and 75% 12 RM loads.
- 5-3 Pre- and post-exercise T2 values, and % change in T2 in the MG and Sol at 25% and 75% 12 RM loads.
- 6-1 Pre- and post-exercise T2 values, and % change in T2.
- 6-2 Standard deviation of the pre- and post-exercise T2 values.
- 6-3 Range of T2 threshold (min and max value) in each category.

ORIGINAL PAPERS

This dissertation is based on the following papers.

1. Kinugasa R & Akima H. Neuromuscular activation of triceps surae using muscle functional MRI and EMG. *Med Sci Sports Exerc* 37: 593-598, 2005.
2. Kinugasa R, Kawakami Y, Fukunaga T. Muscle activation and its distribution within human triceps surae muscles. *J Appl Physiol* 99: 1149-1156, 2005.
3. Kinugasa R, Kawakami Y, Fukunaga T. Quantitative assessment of skeletal muscle activation using muscle functional MRI. *Magn Reson Imaging* 24: 639-644, 2006.
4. Kinugasa R, Kawakami Y, Fukunaga T. Mapping activation levels of skeletal muscle in healthy volunteers: an MRI study. *J Magn Reson Imaging* 24: 1420-1425, 2006.
5. Kinugasa R, Kawakami Y, Sonobe T, Sunakawa R, Fukunaga T. Load-specific distribution of muscle activity in human medial gastrocnemius and soleus muscles. In submission.

CHAPTER 1

Introduction

Understanding the basis of such fundamental phenomena as movement and strength requires an understanding of the neuromuscular system. Because muscle accounts for about 3/4 of our bodies mass, a healthy muscular system is associated with healthy cardiovascular, pulmonary, and endocrine systems. Conversely, disorders of the neuromuscular system have dramatic adverse effects on our daily activities and independence.

The basic biological elements of the neuromuscular system that underlies movement in humans are the joint, muscle, tendon, neuron, and sensory receptor (Figure 1-1). The energy contained in the motor neuron action potential is converted into chemical energy by the release of neurotransmitter and then back to electrical energy by the generation of the muscle action potential. Through this process, motor neuron provide the ability to control the force exerted by skeletal muscle, which enables them to act across joints to rotate body segments in a coordinated fashion to produce movement. Thus, movement can be thought of as the activation of muscle by motor neurons to control the rotation of adjacent body segments.

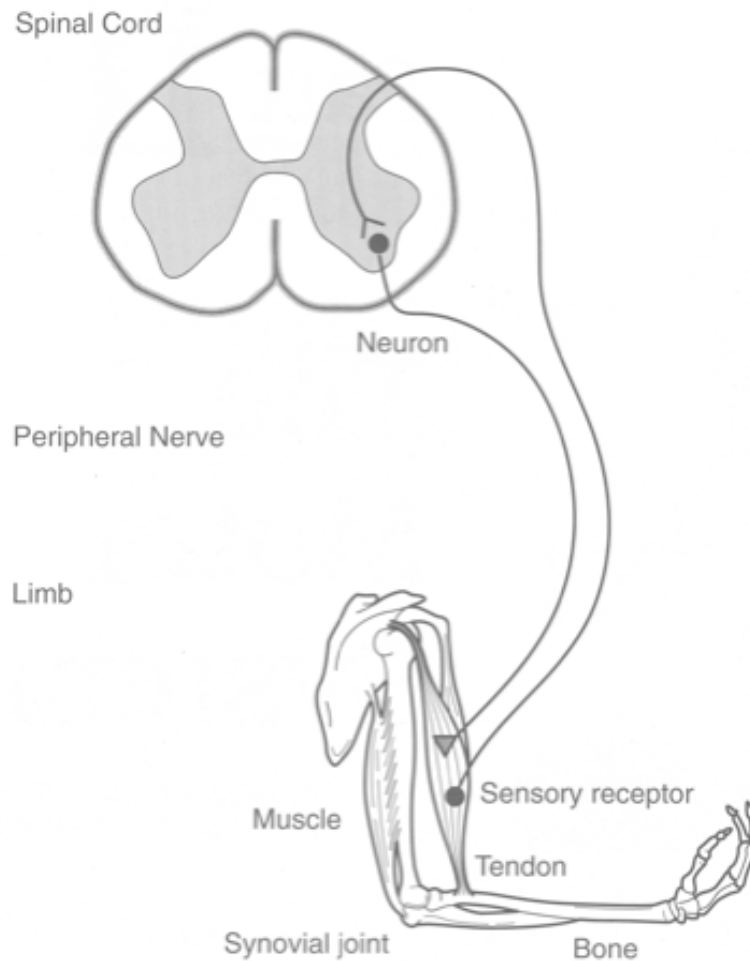


Figure 1-1. The basic biological components of the neuromuscular system (Enoka 2001).

Activation of a muscle

The force that a muscle is varied by altering in the amount of motor unit (MU) activity (Kernell 1992). This is accomplished by varying either the number of MUs activated or the rate at which motor neurons discharge action potentials. The relative contribution of MU recruitment to muscle force varies among muscles. In some muscles of the hand, for example, all the MUs are recruited by the time the force reaches about 50% of maximum. In other larger muscles, such as the biceps brachii,

Chapter 1 Introduction

deltoid, and tibialis anterior, MU recruitment continues up to 85% of the maximum force (DeLuca *et al.* 1982; Kukulka & Clamann 1981; Van Cutsem *et al.* 1997). Increases in muscle force beyond the upper limit achieved through MU recruitment is accomplished entirely through increases in motor neuron discharge rate.

In the 1960s, Henneman and colleagues (Henneman *et al.* 1965) carried out a classic study in which they measured motor neuron electrical activity as a muscle was slowly stretched causing tension to slowly increase [it is now known that increasing the passive tension applied to a muscle cause more MUs to be recruited (Zajac 1989)]. They found that, at very low forces, electrical spikes from the nerve were very small in amplitude, which is noteworthy because spike amplitude is related to the diameter of the axon). As muscle force increased, the size of the spikes also increased in an orderly fashion, indicating that at low muscle forces MUs with small axons are recruited, and as the force required is increased, increasingly larger axons are recruited.

This has become known as the “size principle,” which provides an anatomical basis for the orderly recruitment of MUs to produce increases in contraction. In addition, it was determined from other studies that small motor axons generally innervate slow MUs, while larger motor axons innervate fast MUs (Burke & Tsairis 1973; Garnett *et al.* 1979).

All of the data summarized above were obtained from studies of isolated MUs in animals, but Milner-Brown *et al.* (1973) showed that during voluntary effort in humans, slow contracting MUs are recruited at low muscle tensions, and that as the tension increases, faster MUs are recruited. It thus appears that the size principle is applicable to human as well as animal subjects.

A given muscle will contain numerous MUs, each of which is comprised of a

single motor neuron and its composite muscle fibers. Among the classic studies of MU physiology is the study by the Burke and his colleagues (Burke *et al.* 1971), who isolated single cat hindlimb MUs and characterized the electrophysiological properties of the motor neuron and the mechanical properties of the MUs. They found that MUs could generally be classified into three categories based on several physiological properties of the contracting fibers.

The muscle fibers of a single MU tend to be randomly and densely distributed within muscles, though remarkably few of the innervated fibers touch (Willison 1978). Indeed, fibers belonging to the same MU can be distributed over a surprisingly large volume: some MUs involve up to a quarter of the cross-sectional area in the tibialis anterior and up to three-quarters of the soleus in both cat and rat (Bodine-Fowler *et al.* 1990; Burke & Tsaris 1973; Edström & Kugelberg 1968; Monti *et al.* 2001).

Magnetic resonance imaging

Magnetic resonance imaging (MRI) (Figure 1-2) is a widely employed imaging technique that uses radiofrequency waves and a strong magnetic field to provide remarkably clear and detailed pictures of internal organs and tissues. In a strong magnetic field, atoms with an odd number of nucleons have the magnetic moment (also denoted as spin) of the atom nucleus aligned with the direction of the field. This principle is used in MRI. A short radiofrequency pulse is transmitted, which alters the direction of the net magnetic moment. The frequency has to match the frequency of the protons that it is processing. The pulse excites the protons to a higher energy state, which they leave as soon as the pulse is switched off. The spins return to their equilibrium state and electromagnetic radiation is emitted. This takes some time,

Chapter 1 Introduction

which is referred to as the relaxation time. The two relaxation times measured are referred to as the T1 and T2, respectively.



Figure 1-2. A 1.5-Tesla magnetic resonance scanner.

The relaxation times are different for different kinds of tissue, which gives different intensities in the image. T1 is the longitudinal relaxation time: the time it takes for the proton magnetic moment to reach its earlier equilibrium state in line with the magnetization axis of the constant external magnetic field. This relaxation depends on how the protons exchange energy with their surroundings and that is in its turn dependent on the tissue type. T1 is the time it takes the excitation to return to 63% of its original value. On the other hand, T2 is the transversal relaxation time: this depends on internal dephasing factors and the intensity is reduced. During the dephasing process the protons lose their synchronicity and start spinning at different rates. When the proton spin returns to its aligned axis, the amplitude of the signal decays exponentially to zero. T2 is the time it takes for the signal to return to 37% of its original value (Figure 1-3).

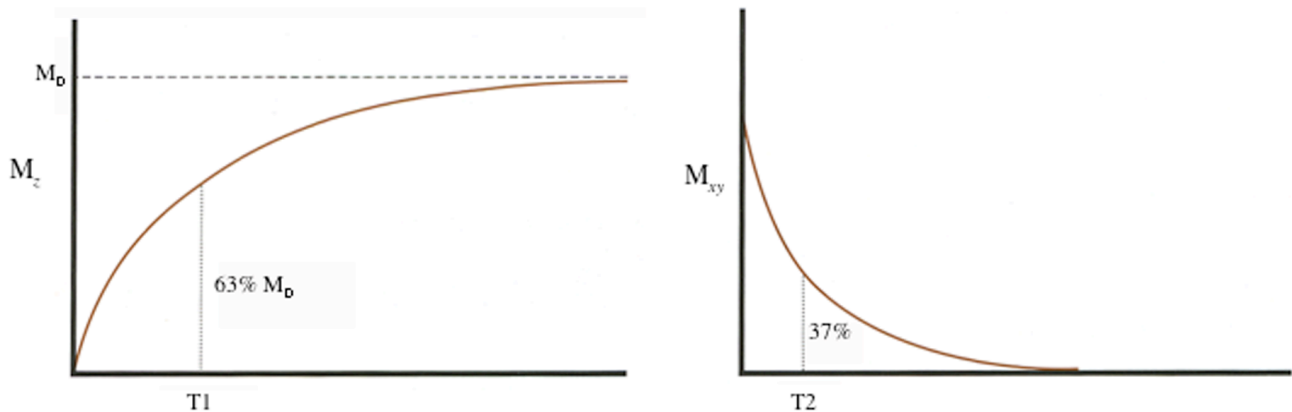


Figure 1-3. Longitudinal relaxation time (T1) recovery curve (left) and transverse relaxation time (T2) decay curve (right). Those two curves are mathematically described by an exponential curve. M_0 ; magnetization moment or vector, M_z ; longitudinal magnetization, M_{xy} ; transverse magnetization.

MRI ushered in new era of exercise physiology studies. Because MRI is completely noninvasive and does not depend on ionizing radiation, exercise scientists progressively use it for basic and applied studies of human subjects. An increase in the T2 of frog muscle was observed after a series of stimulated contractions (Bratton *et al.* 1965). Years later, similar changes in T2 were shown to occur in stimulated rabbit muscle in which blood flow had ceased due to aortic occlusion (Fleckenstein *et al.* 1992a).

The first practical application of exercise enhancement of human muscles on MRI was demonstrated that active and inactive muscles could be clearly distinguished following exercise (Fleckenstein *et al.* 1988). They have been demonstrated that flexor digitorum profundus and flexor digitorum superficialis resulted in an increase in the T2 after handgrip exercise, but flexor carpi ulnaris were not changed, suggesting MRI could be determined the muscle activation patterns. An example of the application of this technology is shown in Figure 1-4. Figure 1-4, A is an axial image across the right thigh of a healthy human subject at pre-exercise. Figure 1-4, B is an

Chapter 1 Introduction

image acquired from the same location 5 min after the subject performed four sets of 10 repetitions of a knee extension exercise. Note that the quadriceps femoris (QF) muscles at the post-exercise are “bright” compared to those at the pre-exercise and the other thigh muscles at the post-exercise. The QF muscles at the post-exercise are then showed much higher T2 than those at the pre-exercise (Figure 1-4, C) (Kinugasa *et al.* 2002). The obvious implication of these images is that the bright portions of the QF muscles were activated during the exercise, and therefore that the image acquired after the exercise can be interpreted as a “activate” image. For clarity in another technique such as brain functional MRI, this type of technique has been referred to as the muscle functional MRI (mfMRI). The exercise-induced increase in T2 is detectable after as few as two contractions (Yue *et al.* 1994) and rises to a work-rate dependent plateau within a few minutes (Jennar *et al.* 1994). Recovery of the phenomenon after the exercise takes 20 min or more (Fisher *et al.* 1990; Price *et al.* 1998), so it is quite possible to acquire functional images after performing a task outside the scanner room.

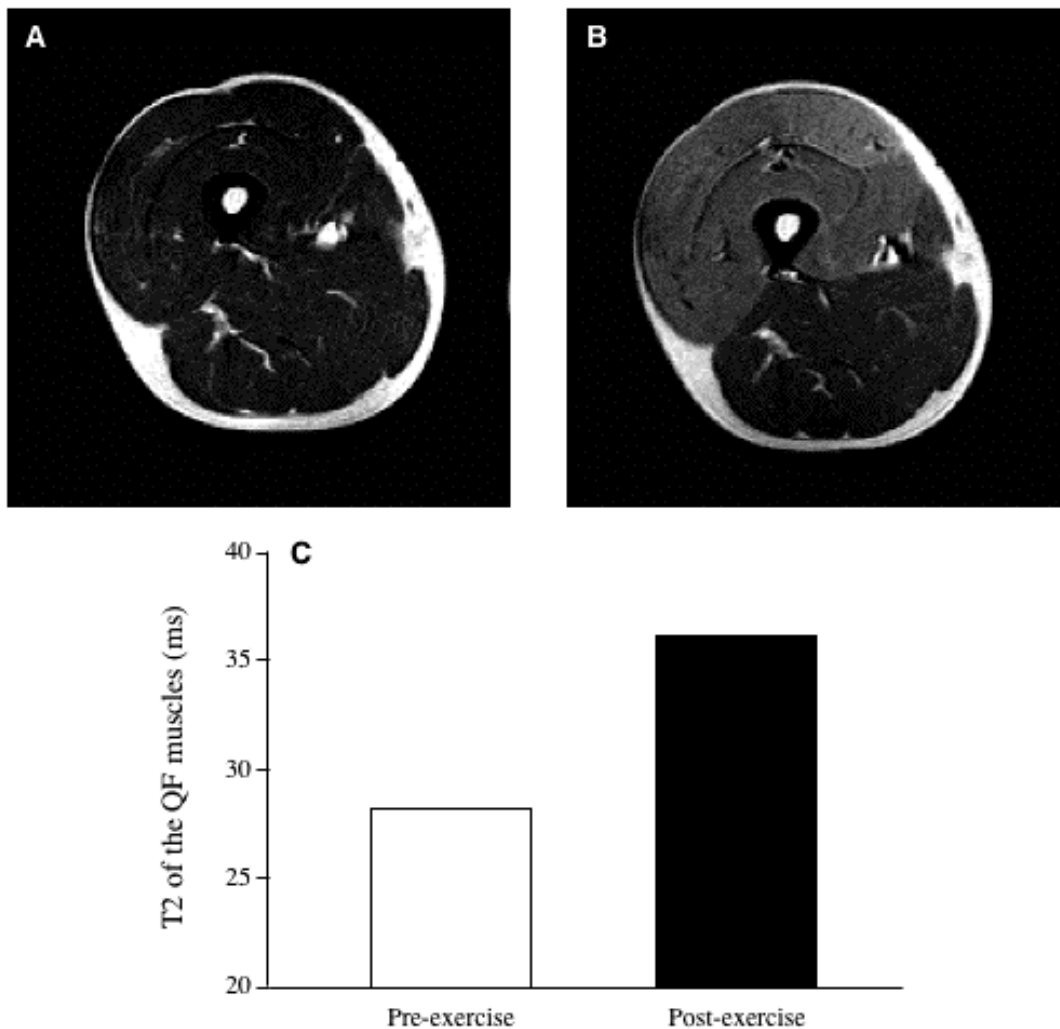


Figure 1-4. Axial magnetic resonance images across right thigh of a healthy subject at pre- (A) and post-knee extension exercise (B). The transverse relaxation time (T2) of the quadriceps femoris (QF) muscles is comparing between pre- and post-exercise (C)

Two observations underscore the usefulness of mfMRI for studying muscle activation. First, there is a positive linear relation between the T2 and intensity of a muscle contraction (Adams *et al.* 1993; Fisher *et al.* 1990). This relation has been reported for concentric and eccentric contractions (Adams *et al.* 1992) and for several different muscle groups (Yue *et al.* 1994; Akima *et al.* 2005). When a specific group of muscles moves a load and contracts concentrically, the oxygen consumption is

Chapter 1 Introduction

greater and more motor units are recruited than when the muscles contract eccentrically to move the same load (Bigland-Ritchie & Woods 1976). As a consequence, the intensities of both the T2 and the electromyography (EMG) are less during the eccentric contraction. Only one study (Adams *et al.* 1992) has shown that there is a positive correlation between the T2 and EMG activity in a single muscle within elbow flexors. However, little study has been demonstrated the relationship between the T2 and EMG activity within a synergistic muscles that are act simultaneously during contraction. Second, the MRI measurement has enough spatial resolution to identify the subvolume of finger flexor muscles (Fleckenstein *et al.* 1992b). This capability enables researchers to determine the prevalence of functional compartmentalization within a single muscle and within a group of synergist muscles (Akima *et al.* 2000; Livingston *et al.* 2001; Segal & Song 2005). It also makes it possible to determine whether a task involves coactivation of an agonist-antagonist set of muscles (Akima *et al.* 2004). However, the measurement is not reliable enough to allow the development of maps of muscle activation based on pixel-by-pixel estimates of T2 (Prior *et al.* 1999).

Triceps surae muscles

The triceps surae (TS) muscles are the main synergists for plantar flexion (Fukunaga *et al.* 1992, 1996; Murray *et al.* 1976). The muscles other than the TS muscles, i.e., flexor digitorum longus and peroneus longus, also act as plantar flexors, but contributions of these muscles to plantar flexion torque have been shown to be < 20% (Murray *et al.* 1976). The TS muscles composed of the gastrocnemius muscle medial head (MG), the gastrocnemius muscle lateral head (LG), and the soleus (Sol) muscles. The TS muscles are one of the muscle groups which is the most important

Chapter 1 Introduction

when we live, because these muscles are involved a number of movements such as walking and standing, and is a muscle group that is most affected by disuse, i.e., spaceflight and bed rest, than other muscles (Akima *et al.* 1997; LeBlanc *et al.* 2000).

Anatomically, the MG and LG have their origins on the posterior surfaces of the medial and lateral femoral epicondyles, respectively (Thompson & Floyd 1994). In contrast, the origin of the Sol is along the upper two-thirds of the posterior surfaces of the tibia and fibula. This means that the gastrocnemius muscles are two-joint muscles crossing both the knee and ankle joints, whereas the Sol is a single-joint plantar flexor. However, three muscles share a common insertion on the posterior surface of the calcaneus via the Achilles tendon. Different functional roles have been elucidated for mono-articular and bi-articular muscles during movement (Jacobs & van Ingen Schenau 1992; van Bolhuis *et al.* 1998; van Ingen Schenau *et al.* 1992, 1995). In comparing the fiber type characteristics of the three muscles, the Sol contains a higher proportion of slow-twitch fibers (70%) than the gastrocnemius muscles (50%). The MG and LG are similar with respect to fast and slow-twitch fiber populations (Edgerton *et al.* 1975; Johnson *et al.* 1973). It has been established that MU activation is affected by the size of the motor neuron (Henneman *et al.* 1965; Milner-Brown *et al.* 1973; Zajac & Faden 1985): the fast-twitch fibers have larger motor neuron than slow-twitch fibers (Burke & Tsairis 1973; Garnett *et al.* 1979). Thus, TS muscles represent an interesting experimental model.

Summary and Conclusions

Human movement reflects the activation of whole muscle groups innervated by numerous motor neurons. If all the muscles of the body are considered together as

Chapter 1 Introduction

one system, then activation, and thus movement, can be studied at several levels of resolution: the level of whole muscle groups, the level single muscles, and the levels of the three-dimensional space within a single muscle. But although the studies summarized above suggest how MUs are distributed within muscles and that they are recruited in an orderly fashion, depending upon the required force level, it is difficult to determine which muscle fibers are activated at a particular tension or where they are situated within the muscle using conventional methodology.

This prompted me to ask can muscle functional magnetic resonance imaging (mfMRI) be used to detect spatial variations in tension within a muscle? The answer depends on the spatial distribution of the recruited MUs and on the density of the innervated muscle fibers within the MU territories (Meyer & Prior 2000). The planar resolution of standard MR images (0.4 mm^2 per pixel) is relatively coarse compared with the size of single muscle fibers ($\sim 0.004\text{-}0.005 \text{ mm}^2$). Consequently, a single pixel within an image may include ~ 100 muscle fibers. In the lower extremities, a typical motor neuron innervates ~ 400 muscle fibers, or about 5% of the cells in a circular unit territory 7 mm in diameter perpendicular to the long axis of the fibers, so that a single MU territory will be spread over several dozen pixels. The remaining 95% of the fibers in that territory are innervated by 25 or so other motor neurons with overlapping territories. Considering this sparse fiber density and the overlapping arrangement of unit territories, it would seem unlikely that mfMRI could resolve the activity of a single MU within a human skeletal muscle. On the other hand, subregions of activity within a muscle can be observed using mfMRI. In addition, mfMRI enables direct acquisition of large volumetric datasets consisting of series of cross-sections that can be reassembled into three-dimensional (3-D) reconstructions. The advantage of using

Chapter 1 Introduction

such 3-D volume sets is that they enable muscles, which are geometrically and architecturally complex, to be represented with greater accuracy than can be achieved with 2-D data. The geometric relationships among synergistic muscles also can be represented more realistically in 3-D reconstructions. In addition, volumetric data can be segmented along the transverse (x -axis), longitudinal (y -axis) and vertical (z -axis) axes, enabling volumes and areas within 3-D reconstructions to be determined.

Little is known about basic mechanism of muscle activation from the standpoint of the size and distribution of the activated regions within a muscle and level of that activation. Greater understanding of such activation properties in human skeletal muscle would shed new light on the fundamental mechanisms of movement. Therefore, the aims of my research were:

1. To clarify the relationship between transverse relaxation time (T_2) in the muscle functional magnetic resonance imaging (mfMRI) and electromyographic (EMG) activity in the triceps surae (TS) muscles during calf-raise exercise at three different loads.
2. To clarify i) whether mfMRI can be used to create 3-D images of muscles; ii) whether activated volume as evaluated by mfMRI correlates the EMG activity, and iii) whether mfMRI can be used to determine the intramuscular distribution of activation.
3. To examine the volume and spatial distribution of active regions within each TS muscle during calf-raise exercises.
4. To examine the activated volumes and the spatial distributions of activation within the medial gastrocnemius and soleus muscles under two different workloads
5. To clarify whether mfMRI can be used to determine the activation levels within a

Chapter 1 Introduction

muscle and to compare activation levels among TS muscles.

CHAPTER 2

Neuromuscular activation of triceps surae using muscle functional MRI and EMG

Introduction

In recent years, muscle functional magnetic resonance imaging (mfMRI) has been used to assess patterns of muscle activation based on exercise increases the proton transverse (spin-spin) relaxation time (T₂) of skeletal muscle (Fung & Puon 1981; Meyer *et al.* 2001). Exercise-induced changes in T₂ correlate with exercise intensity (Adams *et al.* 1992, 1993; Fisher *et al.* 1990; Fleckenstein *et al.* 1993) and relate to isometric torque evoked by electromyostimulation (Adams *et al.* 1993). As such, the mfMRI technique is known to provide a noninvasive measure of the intensity of recently performed muscular activity. Additional studies have also shown that increases in T₂ depend on the metabolic capabilities and the fiber type composition of a muscle (Prior *et al.* 2001; Vandenborne *et al.* 2000; Weidman *et al.* 1991). However, it remains unknown whether mfMRI data, i.e., T₂, actually reflect neuromuscular activation of individual synergistic muscles, irrespective of fiber type composition.

Electromyography (EMG) has long been considered the gold standard for studying neuromuscular function. Measured from within a muscle or from the skin surface overlying a muscle, EMG is a record of the spatial and temporal interference pattern of electrical activity in the activated motor unit (MU) located near the detection surfaces. Despite the development of mfMRI techniques, few studies have investigated the relationship between mfMRI and EMG variables in involved muscle.

Indeed, despite the fact that the combining T2 and EMG could provide novel insight into the functioning of the neuromuscular system, only two earlier studies have used this approach (Adams *et al.* 1992; Price *et al.* 2003). Of those, Adams *et al.* (1992) showed that T2 correlate well with integrated EMG (iEMG) activity for both concentric and eccentric contractions in biceps brachii, which is composed of similar fiber types. One aim of the present study was to extend those findings to obtain a more complete understanding of the relationship between mfMRI and EMG in the muscle group.

Comprised of the gastrocnemius and soleus muscles, triceps surae (TS) is a useful subject for these experiments because the gastrocnemius muscles [i.e., the medial gastrocnemius (MG) and lateral gastrocnemius (LG)] have a mixed fiber composition and are two-joint muscles crossing both the knee and ankle joints, whereas the soleus (Sol) contains a considerably higher percentage of slow-twitch fibers and is a single-joint plantar flexor muscle (Edgerton *et al.* 1975; Johnson *et al.* 1973). It would be interesting to know whether T2 and iEMG show linear coupling with increasing exercise intensity in individual TS muscles. One attractive hypothesis is that the relation between the T2 and workload and the relation between the T2 and iEMG differ between the gastrocnemius and Sol muscles. Thus, a second aim of the present study was to test this hypothesis by comparing the activation patterns among individual TS muscles during calf-raise exercise at three different loads using mfMRI and EMG.

Methods

Subjects

Six healthy male subjects participated in the study. Their average age, height, and weight were 25 ± 2 yrs., 1.69 ± 0.05 m, and 65 ± 6 kg (means \pm SD), respectively.

The subjects were screened for medical and orthopedic conditions that would preclude them from strenuous calf-raise exercises or MR measurements. Persons who had participated in a weight-training program or had regularly performed strenuous exercise in lower limb for occupational or recreational purposes within the 2-month period prior to the study were excluded. Subjects were fully informed of the procedures to be used as well as the purpose of the study, after which written informed consent was obtained from all subjects. The experiments were carried out in accordance with the guidelines for the use of human subjects laid down by the Ethics Committee of Nippon Sport Science University.

Exercise Protocol

The calf-raise exercise was performed in a standing position and involved raising and lowering one's body bilaterally (B ex), unilaterally (U ex), and unilaterally with an additional 15% of body weight load (U+15 ex). The leg used and the order of the workload was chosen randomly. To avoid differing contributions to the force generation between gastrocnemius and Sol muscles, the knee joint angle was set at a fully extended position throughout the exercise. Each subject performed the calf-raise exercise for five sets of 10 repetitions at each workload. This exercise required the plantar-flexor muscles to contract concentrically to raise the body and eccentrically to lower it. Each subject stood on a columnar box (height, 11 cm; diameter, 29 cm), and the exercise began with the ankle joint in an anatomical position. The subject's body was raised by flexing the ankle joint to a fully plantar flexed position in 2 s and then lowered by dorsiflexing the ankle joint so that the ankle resumed its initial position in 2 s, essentially as described previously (Akima *et al.* 2003). The subjects were required

to maintain tension on the ankle between contractions. During exercises, the heel was positioned above the ground because this makes it easy to exercise. There were no rest periods between the plantar flexion and dorsiflexion of the ankle or between repetitions of the movement. During the 1 min rest interval between sets, the subjects sat on a chair. Subjects were allowed to put their hands on a wall for balance. There was also a rest interval of 30 min between the B ex and U ex, and the U+15 ex was separated by at least 1 day from the other two workloads. Before all exercise trials, I confirmed that T2 had returned to its baseline value.

Muscle functional magnetic resonance imaging

mfMRI was performed on a 0.3-Tesla MR imaging system (AIRIS, Hitachi Medical, Japan). Spin-echo images (repetition time = 1,500 ms; echo time = 25 and 80 ms; field of view = 27 cm; matrix = 256×256 ; number of excitations = 1; total scan time; 5 min 18 s) were collected using an extremity coil (40 cm). Seven 10 mm-thick axial slices were collected with a 0-mm gap between slices, and the third slice was located at 30% of the distance from the spina liliaca anterior superior (0%) to the extremities distal to the tibia (100%). The subjects lay on their back with the knee and ankle kept at 180° (full extension) and 0° (anatomical position), respectively. The calf-raise exercise was executed outside the magnet bore, after which subjects immediately moved into the magnet for mfMR imaging; 90 s elapsed between the end of the exercise to the start of scanning. Ink marks on the calf were used to ensure similar positioning over repeated MRI measurements.

The collected mfMR images were transferred to a personal computer for calculation of the T2 values using the public domain National Institutes of Health (NIH)

Image software (written by Wayne Rasband at the NIH and available via the Internet by anonymous ftp from [zippy.nimh.nih.gov](ftp://zippy.nimh.nih.gov)). A region of interest (ROI) was defined by tracing the outline of the individual TS muscles used in analyses. Each ROI was selected so that visible blood vessels, membranes, and fat were avoided. The T2 values for these regions were averaged over seven images. The extent of muscle activation was evaluated based on the determined % change in T2 [(post-exercise T2 – pre-exercise T2) / pre-exercise T2 × 100] for each muscle, as in earlier studies (Akima *et al.* 2002; Kinugasa *et al.* 2004; Weidman *et al.* 1991; Yue *et al.* 1994).

Electromyography

EMGs (Bagnoli 2.0, Delsys, Boston, MA, USA) were recorded from the midbellies of the MG, LG, Sol, and tibialis anterior (TA; reference muscle) using preamplifier surface electrodes (DE-2.1, 10 mm interelectrode distance). The earth electrodes were placed over the thighbones of both legs. The skin was cleaned with ethanol to reduce the skin-electrode impedance. The analogue EMG signals were acquired continuously throughout the calf-raise exercise, filtered using a band pass-filter set to between 15 and 500 Hz, and digitized at a sampling rate of 1 kHz using analog to digital converter (Mac Lab/16s, ADInstruments, Sydney, Australia). The digital signals were then full-wave rectified and integrated over 40 s to yield iEMGs, which were then averaged over the five sets of exercises for each subject. As T2 reflects the total amount of work during a task (Fleckenstein *et al.* 1993), I ensured that the two variables (T2 and iEMG) were equally weighted for comparison by setting the calculation period to 40 s, which corresponds to the time required to complete each set of calf-raise exercise. In addition, a cross-correlation analysis was carried out in

preliminary testing to confirm that there was no crosstalk among the EMG channels. Ink marks on the calf were used to ensure similar positioning over repeated EMG measurements.

Statistics

All data are presented as means \pm SE. T2 and EMG data were each compared over the three workloads using two-way analysis of variance with repeated measures. Correlation between two variables was assessed by determining Pearson's product-moment (r). Values of $P < 0.05$ were considered significant.

Results

Figure 2-1 shows a representative set of mfMR images obtained from a subject immediately after five sets of 10 repetitions of B ex (right calf), U ex (left calf), and U+15 ex (right calf). The white regions within image are considered to be activated regions due to exercise.

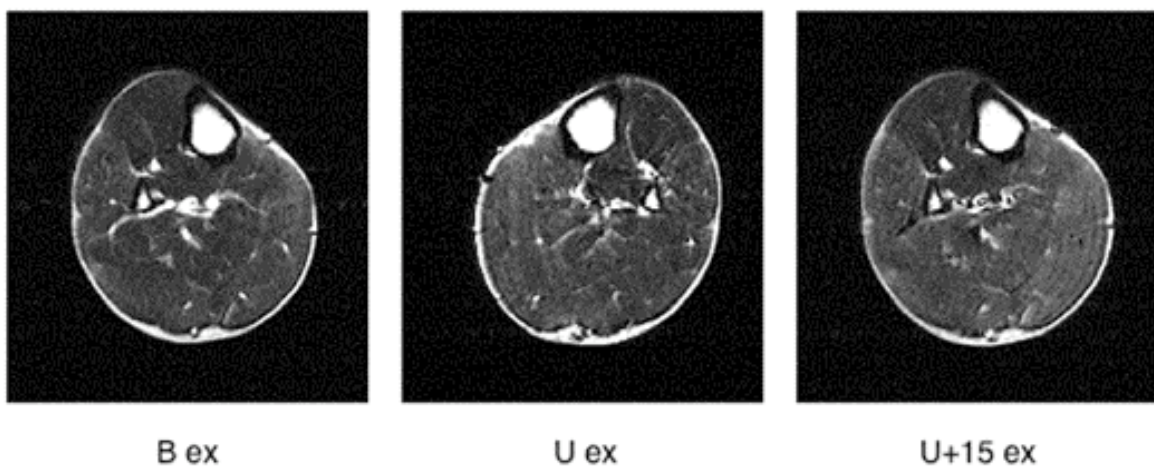


Figure 2-1. Representative post-exercise magnetic resonance images from one subject at three different workloads. Subjects performed calf-raise exercise of five sets of 10 repetitions of a calf-raise exercise, bilaterally (B ex), unilaterally (U ex), and unilaterally with a load of 15% of body weight (U+15 ex). B ex and U + 15 ex: right calf, U ex: left calf.

Chapter 2 Relationship between mfMRI and EMG

The % changes in T2 and iEMG that occurred at the three workloads are shown in Figure 2-2. I found that % change in T2 was significantly greater after U+15 ex than B ex in the all three muscles ($P < 0.05$), and was also significantly greater after U+15 ex than U ex in the MG ($P < 0.05$). In addition, the % change in T2 after U+15 ex was greater in the MG than in the LG or Sol ($P < 0.05$). Similarly, iEMG activity in the LG was significantly greater during U+15 ex than B ex ($P < 0.05$), and iEMG in the Sol was greater during both U ex ($P < 0.05$) and U+15 ex ($P < 0.05$) than during B ex. In the MG, iEMG tended to be greater during U+15 ex than B ex, but the difference did not reach the level of statistical significance ($P = 0.06$). iEMG was significantly greater in the MG than the LG or Sol during both B ex and U+15 ex ($P < 0.05$).

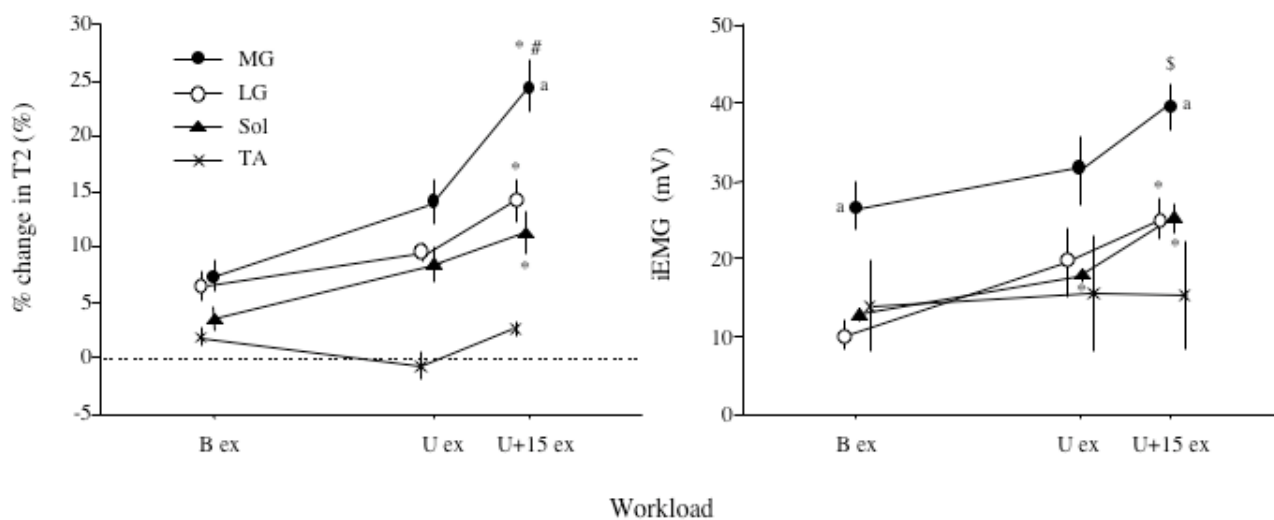


Figure 2-2. Changes in the % change in transverse relaxation time (T2) and integrated electromyography (iEMG) with the three workloads. Bar represent means \pm SE for all subjects. * $P < 0.05$ vs. B ex; # $P < 0.05$ vs. U ex; \$ $P = 0.06$ vs. B ex; $^aP < 0.05$ vs. LG and Sol. MG, medial gastrocnemius; LG, lateral gastrocnemius, Sol, soleus; TA, tibialis anterior. B ex, calf-raise exercise bilaterally; U ex, calf-raise exercise unilaterally; U + 15 ex, calf-raise exercise unilaterally with a load of 15% of body weight.

I found a significant correlation between T2 and iEMG as they varied as a function of increasing workload in the MG ($r = 0.58, P < 0.05$) and Sol ($r = 0.63, P < 0.01$), but not in the LG ($r = 0.40, P = 0.10$) (Figure 2-3). MG showed similar relationship between T2 and iEMG in all six subjects, but the LG and Sol had greater inter-subject variation than that of the MG (Figure 2-4).

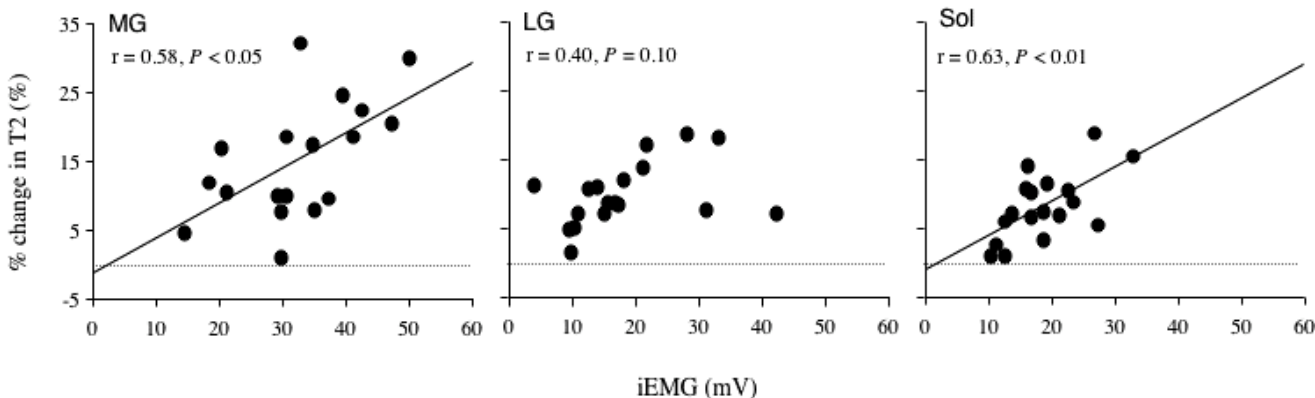


Figure 2-3. Relationship between the % change in transverse relaxation time (T2) and integrated electromyography (iEMG) in the medial gastrocnemius (MG), lateral gastrocnemius (LG), and soleus (Sol).

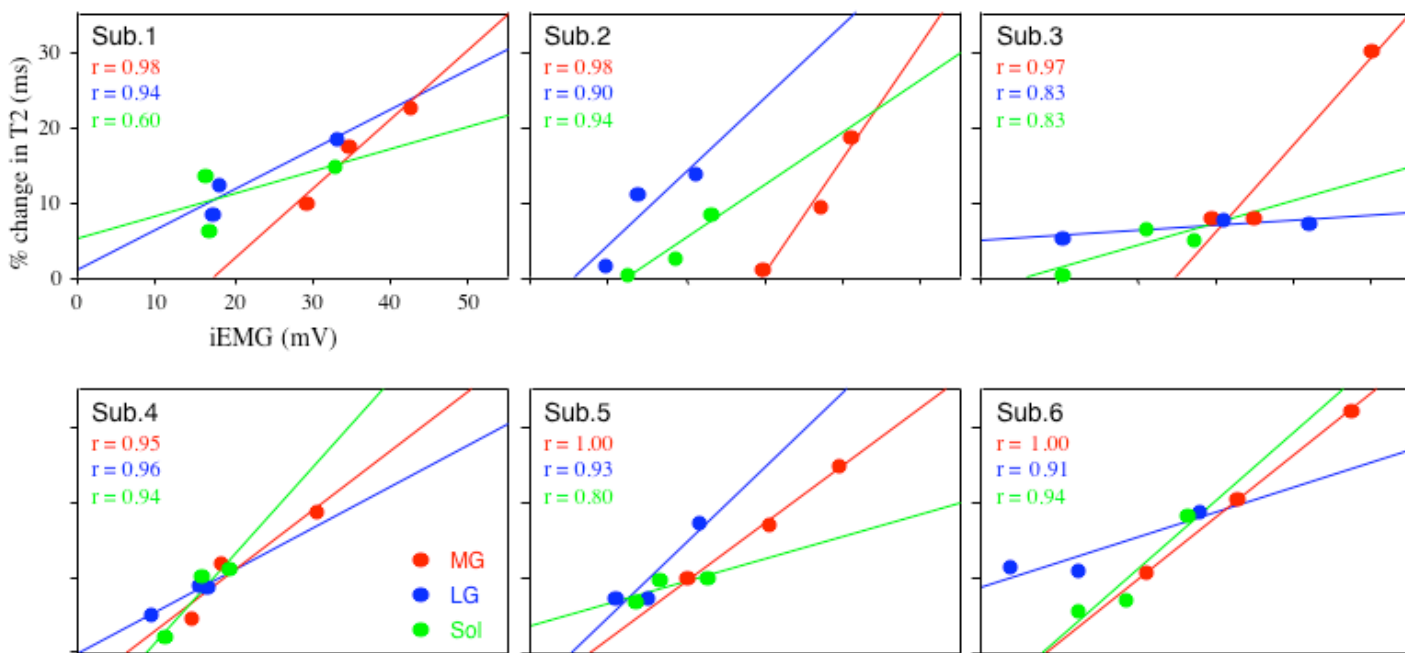


Figure 2-4. Relationship between the % change in transverse relaxation time (T2) and integrated electromyography (iEMG). Data plot of two variables in the medial gastrocnemius (MG), lateral gastrocnemius (LG), and soleus (Sol) under the three workloads in all six subjects, respectively.

Table 2-1. Absolute T2 and iEMG at rest, B ex, U ex, and U+15 ex.

	Rest	B ex	U ex	U+15 ex
T2, ms				^a
MG	32.4 ± 0.7	34.8 ± 0.8 [†]	36.9 ± 1.5 ^{† *}	40.3 ± 1.3 ^{† * #}
LG	33.1 ± 0.7	35.2 ± 0.9 [†]	36.3 ± 1.3 [†]	37.8 ± 1.6 ^{† * #}
Sol	33.0 ± 0.9	34.2 ± 1.4	35.7 ± 1.0 [†]	36.7 ± 2.0 ^{† #}
TA	31.0 ± 0.3	31.4 ± 0.9	30.8 ± 0.7	31.8 ± 0.4
Marrow	66.6 ± 0.7	66.3 ± 0.8	66.3 ± 1.6	67.2 ± 1.4
iEMG, mV		^a		^a
MG	—	26.7 ± 7.5	31.2 ± 10.9	39.4 ± 7.0 ^{\$}
LG	—	10.2 ± 4.3	19.5 ± 11.2	25.3 ± 6.4 [*]
Sol	—	12.8 ± 2.2	17.8 ± 2.0 [*]	25.3 ± 4.7 [*]
TA	—	13.9 ± 14.4	15.6 ± 18.3	15.4 ± 17.1

Values are means ± SE.

[†] $P < 0.01$ vs. rest; ^{*} $P < 0.05$ vs. B ex; [#] $P < 0.05$ vs. U ex; ^{\$} $P = 0.06$ vs. B ex;

^a $P < 0.01$ vs. LG and Sol.

T2, transverse relaxation time; iEMG, integrated electromyography;

B ex, bilateral calf-raise exercise; U ex, unilateral calf-raise exercise;

U+15 ex, unilateral calf-raise exercise with load of 15% of body weight;

MG, medial gastrocnemius; LG, lateral gastrocnemius; Sol, soleus; TA, tibialis anterior.

Finally, Table 2-1 shows the absolute values for T2 and iEMG at rest and with B ex, U ex, and U+15 ex. I found that for the MG and LG T2 measured after B ex, U ex, and U+15 ex were significantly larger than that of at rest ($P < 0.05$), and were significantly larger after U ex and U+15 ex in the Sol ($P < 0.05$). T2 measured in MG and LG after U ex and U+15 ex were also greater than values measured after B ex ($P < 0.05$), and values measured after U+15 ex was significantly greater than after U ex in all three muscles ($P < 0.05$). The peak T2 measured after U+15 ex in MG were significantly higher than the corresponding values obtained with LG or Sol ($P < 0.05$). The absolute iEMG data summarized in Table 2-1 are consistent with those in Figure

2-2.

Discussion

I began the present study with the hypotheses that the relationship between T2 and workload or iEMG may differ in the gastrocnemius and Sol muscles. The aim was to test these hypotheses by comparing the patterns of activation among individual TS muscles during calf-raise exercises at three different workloads using mfMRI and EMG. I found that in the TS muscles T2 and iEMG showed similar patterns of variation with increasing workloads (Figure 2-2). Although mfMRI signals reflect metabolic changes within muscles and do not directly measure electrical activity of a muscle (for a review, see Meyer & Prior 2000), this result nevertheless imply that mfMRI may be a useful tool with which to evaluate exercise intensity, complimenting EMG as a direct measure of muscle activity.

With increasing workload, the MG showed greater increases in T2 and iEMG than both the LG and Sol. This is consistent with an earlier finding that peak iEMG is higher in the MG than in the LG and Sol during plantar flexion contraction (Tamaki *et al.* 1997), as well as with the more recent earlier findings that increases in T2 are greater in the MG than in the LG or Sol during calf-raise exercise (Akima *et al.* 2003; Yanagisawa *et al.* 2003). It is notable regard that the Sol contains largely slow-twitch fibers, whereas the gastrocnemius muscles contain nearly equal proportions of both fibers (Edgerton *et al.* 1975; Johnson *et al.* 1973). It is well established that MU recruitment is affected by the size of the innervating motor neuron and that muscle fatigue depends primarily on the fiber type composition (Colliander *et al.* 1988; Oches *et al.* 1977). As such, one would expect the gastrocnemius and Sol muscles to exhibit

different fatigue characteristics. In fact, earlier study (Oches *et al.* 1977) has shown that, during maximal voluntary plantar flexions, the gastrocnemius muscle exhibits a greater decline in activation than does the Sol, suggesting a greater susceptibility to fatigue. Consequently, the MG likely facilitates the activation of MUs when exercise intensity is high (e.g., during unilateral task), leading to accumulation of metabolic by-products such as lactate and inorganic phosphate (Pi). Notably, individuals with McArdle's disease (deficiency of muscle phosphorylase), who cannot substantially increase metabolic flux through glycolysis and therefore do not produce lactate at high rates or develop metabolic acidosis, do not show an increase in muscle T2 during exercise. This has been interpreted as evidence of the contribution made by lactate to the change in T2, but T2 is also reportedly related to intracellular pH and the Pi-to-phosphocreatine (PCr) ratio (Fleckenstein *et al.* 1991; Prior *et al.* 2001; Vandeborne *et al.* 2000; Weidman *et al.* 1991). Thus, the greater increase in T2 observed in the MG likely reflects the greater neuromuscular activity and its resultant metabolic state. On the other hand, it is conceivable that because the Sol is less fatigable, the increases in T2 seen there at higher resistive loads could be caused by neuromuscular factors such as activation and/or recruitment of MUs rather than metabolic factors. However, the finding that there was no significant difference in the iEMG recorded over the 5 sets of exercise for each muscle (data not shown) suggests neuromuscular fatigue is not related to the differences in load-related changes in T2 among TS muscles. More likely, the workloads and exercise protocol employed in the present study are significant factors in such differences.

I found there to be a significant correlation between the T2 and iEMG in the MG and Sol, but not in the LG (Figure 2-3). To my knowledge, this is the first report

of the effects of exercise intensity on the relationship between mfMRI and EMG activity among individual synergistic muscles. Adams *et al.* (1992) showed that T2 and iEMG increase linearly as a function of load in a single biceps brachii muscle during forearm curls, but it does not address the question of how the relation between T2 and EMG may differ among synergistic muscles. The observed correlation between the T2 and iEMG in the MG and Sol, despite the differences in their anatomical and architectural properties between gastrocnemius and Sol muscles (Fukunaga *et al.* 1992; Kawakami *et al.* 1998), indicates that T2 can be related to EMG activity among synergistic muscles, even if their anatomical and metabolic characteristics differ.

It is noteworthy that I determined the T2 and iEMG during calf-raise while the subject was in a standing position (i.e., while the muscles were bearing weight with the knee fully extended). In an earlier study, Price *et al.* (2003) made similar measurements while the subjects were in a seated position (i.e., the muscles were not bearing weight, and the knee joint angles varied). They found that the T2 and EMG amplitude for the MG and LG during plantar flexion exercise were nearly equivalent across the knee joint angles. By contrast, I found that with increasing workload the MG showed a greater increase in T2 and iEMG than the LG, which is consistent with another earlier report (Yanagisawa *et al.* 2003). This discrepancy between my findings and findings of Price *et al.* (2003) may reflect the differing conditions in the lower limbs during the period the measurements were made (e.g., whether or not the muscles were bearing weight). The morphological properties of the MG may also contribute to this discrepancy, as the volume of the MG in humans is greater than that of the LG (Fukunaga *et al.* 1992). In addition, Kawakami *et al.* (1998) reported that as a result of

its architectural characteristics, the MG contains more fibers per unit volume than the LG, and would thus have greater force potential. This, too, could account for the greater load-related increases in T2 and EMG seen in the MG.

With respect to the Sol, the T2 and iEMG increased linearly with increasing workloads, and T2 was significantly greater during exercise than when the muscle was at rest. As mentioned above, the Sol is a monoarticular muscle that originates along the upper two-thirds of the posterior surface of the tibia and fibula and generally has a higher percentage of slow-twitch fibers than the gastrocnemius muscles (Edgerton *et al.* 1975; Johnson *et al.* 1973). Price *et al.* (1995, 2003) reported that T2 for the Sol did not significantly increase from baseline during non-weight-bearing plantar flexion exercise. This suggests that the Sol could be activated by weight-bearing, per se, which is consistent with the % changes in T2 and iEMG found in the present study where a “weight-bearing-exercise” was employed. In fact, the H-reflex amplitude of the Sol is higher during plantar flexion under weight-bearing conditions than under non-weight-bearing conditions (Yamashita *et al.* 1989), suggesting the excitability of the motor neurons innervating the Sol is facilitated by the weight-bearing.

In summary, I have shown that % changes in T2 parallel those in iEMG in individual TS muscles under three different workloads. Moreover, there was a significant correlation between T2 and iEMG in the MG and Sol, but not in the LG. These results suggest 1) that mfMRI signals and iEMG correlate with workload in individual TS muscles; 2) that mfMRI signals are associated with the neuromuscular activity reflected in the iEMGs in the MG and Sol, but not in the LG; and 3) that these relationships are associated with both neuromuscular and metabolic factors during exercise.

CHAPTER 3

Quantitative assessment of skeletal muscle activation using muscle functional MRI

Introduction

Magnetic resonance imaging (MRI) is being used with increasing frequency in research involving acquisition of anatomical information. One unique aspect of MRI is that exercise induces signal changes resulting primarily from increases in the proton transverse (spin-spin) relaxation time (T₂) of tissue water (Fung & Puon 1981; Meyer *et al.* 2001). Exercise is known to produce changes in the amount and distribution of water within skeletal muscle, and at the present time a shift in the water distribution is the purported mechanism for changes in T₂ (Zhu *et al.* 1992). These T₂ changes are well correlated with integrated electromyography (iEMG) (Adams *et al.* 1992; Kinugasa & Akima 2005), and increases with exercise intensity (Adams *et al.* 1992; Kinugasa & Akima 2005; Fisher *et al.* 1990), and relate to torque evoked by electrical stimulation (Adams *et al.* 1993). Moreover, T₂ and EMG activity show similar changes during exercise at different joint angles (Price *et al.* 2003). This technique, which is referred to as muscle functional MRI (mfMRI), is useful for assessing the level of muscle activation while performing a task.

Given the architectural and topographical complexity of muscle fibers (Kawakami *et al.* 2000) and motor units (MUs) (Hammond *et al.* 1989; Windhorst *et al.* 1989), and the nonuniform distribution of innervation territories of motor neurons, it would seem necessary to collect data from the entire length of a muscle in three

dimensions to fully characterize its activation. The principal advantage of mfMRI is that it overcomes some of the limitations of surface EMG. With surface EMG, for example, it is difficult to detect muscle activity over large regions or in regions deep within the muscle, and it is virtually impossible to detect the activity of an entire muscle of interest and/or limit cross-talk between muscles. By contrast, mfMRI readily enables one to study the activity in an entire muscle and to noninvasively obtain three-dimensional (3-D) images of muscles. Meyer & Prior (2000) stated that, as compared to surface EMG, the most notable feature of mfMRI is its potential for use in mapping the spatial variations in activity within a muscle, which could enable determination of the spatial distribution of activated muscle fibers during a task. The first application of mfMRI to map spatial variations in activity within a muscle was by Adams *et al.* (1993), but theirs was a two-dimensional analysis. Indeed, because most studies reported thus far have investigated muscle activity in only two dimensions, the patterns of 3-D variation in muscle activity and how those patterns relate to muscle function remain largely unknown.

The purpose of the present study, therefore, was to determine whether mfMRI can be used to obtain 3-D images useful for evaluating muscle activity, and if so, to measure the distribution of muscle activity within human skeletal muscle. I studied the activation of the medial gastrocnemius (MG) muscle, testing the following three hypotheses: 1) that mfMRI can be used to create 3-D images that enable one to distinguish active from inactive muscle; 2) that muscle activity, as evaluated by mfMRI reflects the iEMG; and 3) that mfMRI can be used to determine the spatial distribution of activity within a muscle.

Methods

Subjects

Seven healthy male subjects participated in the study: age, 24 ± 2 yrs; height, 1.70 ± 0.07 m; weight, 63 ± 4 kg (mean \pm SD). All subjects were in good health, with no orthopedic abnormalities. Subjects were fully informed of the procedures to be used as well as the purpose of the study, and written informed consent was obtained from all subjects. The experiments were carried out according to the guidelines laid down by the Ethical Committee of the University.

Magnetic resonance image acquisition and analysis

Axial MR image was collected on an 0.3-Tesla MR imaging machine (AIRIS, Hitachi Medical, Japan) using extremity coil (25-cm diameter) and a T2-weighted spin-echo sequence (repetition time, 2500 ms; echo time, 25 and 80 ms; field of view, 270 mm; 22 slices; slice thickness, 10 mm; slice gap, 0 mm; matrix 256×256 ; scan time, 5 min 30 sec). The subjects were lying supine in the magnet with the leg held steady using a bitemporal clamp while the knee joint kept at 180° (full extension). The MRI scans were carried out before the exercise and started within 1 min of the end of exercise.

Because of the limited range of the imaging coil, each subject participated in two imaging sessions separated by at least 10 days. Images were obtained from either between the proximal of the patella and midcalf (at proximally 50% of the distance between the proximal of the patella and the distal end of the tibia) or between the midcalf and the distal end of the tibia. The order of the acquired MR images was random. A permanent water-soluble marker was used on the subjects' skin as an

Chapter 3 Assessment of 3-D activation

anatomic reference point to ensure that images were collected from the same location for repeated scans. This reference point was also used to align collected MR images from the two sessions.

MR images were transferred to a personal computer. T2 images were calculated on a pixel-by-pixel basis from the 25 and 80 ms MR images, analyzed by tracing an region of interest (ROI) around the MG using a modified version of the public domain National Institutes of Health (NIH) Image program. Care was taken to exclude subcutaneous and intramuscular fat, aponeurosis and vessels from the traced regions. The T2 (mean \pm SD) was determined for the ROI in each slice. As previously described (Adams *et al.* 1993), ranges of pixels with a T2 greater than the mean + 1SD of the ROI in pre-exercise image and a T2 lower than the mean +1SD of the ROI in post-exercise image were determined. Survived pixels showing T2 are defined as active muscle (Figure 3-1). The threshold was defined for each muscle in the every slice.

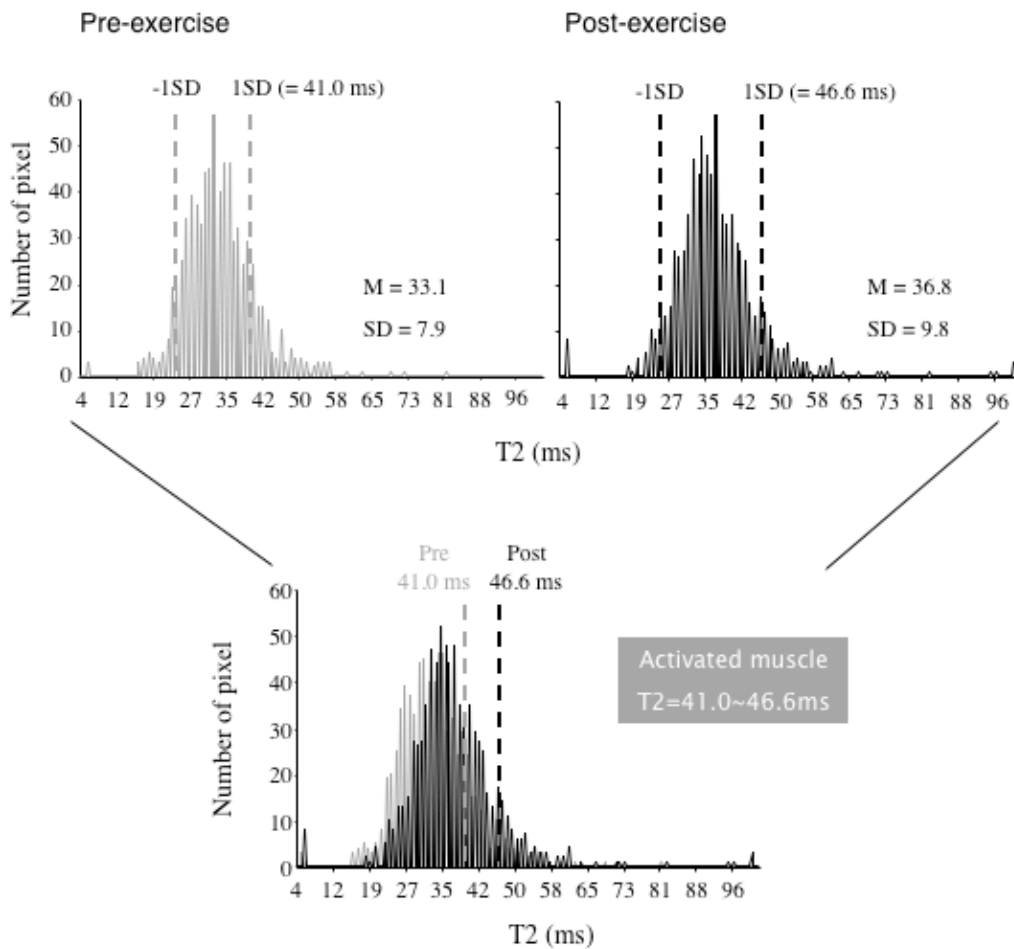


Figure 3-1. Illustration of the method for determining “active region” of a muscle. Transverse relaxation time (T2) for each pixel in magnetic resonance (MR) images at pre- (upper left) and post-exercise (upper right). In this case, mean and SD of pre-exercise T2 values is 33.1 ms and 7.9 ms, and those of post-exercise T2 values are 36.8 ms and 9.8 ms, respectively. The 1SD of mean T2 is 41.0 ms for pre-exercise and 46.6 ms for post-exercise. A range of T2 greater than the mean + 1SD of the pre-exercise MR images and T2 lower than mean + 1SD of the post-exercise MR images were considered to be activated region on MR images. Thus, the T2 within the range from 41.0 ms (from pre-exercise) to 46.6 ms (from post-exercise) are activated within a muscle in the post-exercise image.

After the contours of the individual muscle and bone in each image were defined using visualization, data analysis, and geometry reconstruction software package (Amira 3.0, Mercury Computer Systems, San Diego, CA, USA), the activated area within a muscle was defined using the aforementioned threshold method and displayed in red. All contours were reviewed by superimposing them on the

corresponding image slice and, if necessary, corrected using simple manual point and check operations within the platform. The colors and transparency of the surfaces can be edited to allow the user to display one surface inside another. The surface of the muscle, bone, and activated area were then 3-D reconstructed using a surface rendering algorithm (Figure 3-2), from which their volumes were determined.

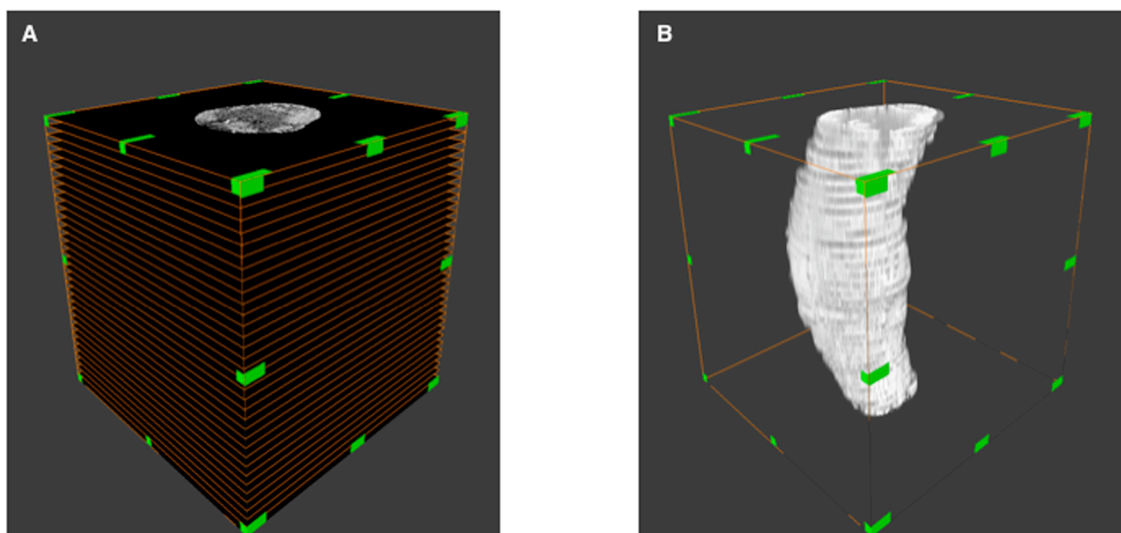


Figure 3-2. Representative accumulated magnetic resonance (MR) images (A) and three-dimensional reconstructed MR images (B) in the calf muscle.

The surface rendering equation (*I*) is expressed as follows:

$$L_0(x, \vec{\omega}) = Le(x, \vec{\omega}) + \int_{\Omega} f_r(x, \vec{\omega}', \vec{\omega}) L_i(x, \vec{\omega}') (\vec{\omega}' \cdot \vec{n}') d\vec{\omega}' \text{ -----}(I)$$

$L_0(x, \vec{\omega})$ is light outward at a particular position x and in direction $\vec{\omega}$.

$Le(x, \vec{\omega})$ is light emitted from the same position and direction.

$\int_{\Omega} \dots d\vec{\omega}'$ is an infinitesimal sum over a hemisphere of inward directions.

$f_r(x, \vec{\omega}', \vec{\omega})$ is the proportion of light reflected at the position (from inward direction to outward direction).

$L_i(x, \vec{\omega}')$ is light inward from the position and direction $\vec{\omega}'$.

$(\vec{\omega}' \cdot \vec{n}')$ is the attenuation of inward light due to incident angle.

To determine the 3-D distribution of activated regions, the first step was to segment the transverse (x), longitudinal (y), and vertical (z)-axes of each voxel in the 3-D images. The anatomical and activated area of a muscle was then calculated for every 0.5 cm along the x - and y -axes and for every 1.0 cm along the z -axis. To reduce the level of noise within the images, 3-D image was smoothed using a Gaussian filter (radius of 2 pixels), which redrew the images and averaged the pixel values according to a Gaussian function (Wang *et al.* 2004). This filter did not affect the volume measurement.

To validate the volume determination reconstructed from the x -, y - and z -axes, I carried out mfMRI using a known volume filled with water ($n = 5$). The water region was reconstructed in 3-D using Amira and oriented with respect to a cutting plane through each pixel along the x -, y - and z -axes. The volume was then calculated by multiplying the sum of the pixels in each plane. The error in the volume measurements was calculated using the following equation:

$$[\text{error} (\%) = (\text{measured volume} - \text{actual volume}) \times 100 / \text{actual volume}].$$

The validity of mfMRI for estimated activated volume was tested by comparing with conventional EMG measurements, looking at the effects of workload. Subjects ($n = 6$) performed seven sets of 10 unilateral plantar flexion exercises at three different workloads: 25%, 50%, and 75% of their 12 repetition maximum (RM) and 1 RM test. Activated volume of a muscle and iEMG were collected from the MG. In addition, the interday reproducibility of the T2 ($n = 5$) and volume ($n = 8$) measurements was tested on separate days.

Exercise Protocol

Subjects performed calf-raise exercises for 5 sets of 10 repetitions. Exercise leg was randomly chosen. The subject's own body weight with additional 15% of body-weight load was raised by flexing the ankle joint to a fully plantar flexed position in 2 s and then lowered by dorsiflexing the ankle joint so that the ankle resumed its initial position in 2 s, as described earlier studies (Kinugasa & Akima 2005; Akima *et al.* 2003). There were no rest periods between the plantar flexion and dorsiflexion of the ankle or between repetitions of the movement. During the 1-min rest interval between sets, the subjects were seated in a chair. The knee remained in full extension throughout the exercise and they were allowed to put their hands on the wall to provide balance but not support. The exercise was performed outside the magnet bore, after which, subjects immediately moved into the magnet for imaging.

Electromyography

EMG (Bagnoli 2.0, Delsys, Boston, MA, USA) was recorded from the midbellies of MG using preamplified surface electrodes (DE-2.1, interelectrode distance 10 mm). After careful abrasion of the skin, the electrodes were placed at the same locations in each session with use of permanent spot marks. The reference electrode was placed over the patella. The EMG signals were acquired continuously throughout the plantar flexion exercises with a band-pass filter between 15 and 500 Hz and were analog-to-digital converted (Mac Lab/16s, ADInstruments, Sydney, Australia) at a sampling rate of 1 kHz. The EMG was full-wave rectified and integrated for the duration of the exercise (30 s) to give iEMG. A calculation period of 30 s was

employed because it corresponded to the time required to complete each set of exercise. The iEMGs were then averaged over seven sets and normalized to the peak iEMG obtained during the 1 RM test.

Statistics

Descriptive statistics are means \pm SE. Statistical significance of the relationship between activated volume and iEMG was studied by regression analysis, and Pearson product-moment correlations (r) was calculated. Accuracy of reconstructed volume determination, reproducibility of T2 and volume measurements was tested by regression analyses and Student's t test. Difference in activated area between different regions was tested by one-way analysis of variance. The probability level accepted for statistical significance was set at $P < 0.05$.

Results

The correlation coefficients between the first and second measurements were $r = 0.89$ ($P < 0.05$) for rest T2, $r = 0.86$ ($P < 0.05$) for after exercise T2, and $r = 0.97$ ($P < 0.01$) for volume. The respective errors were calculated to be 0.7% for rest T2, 0.1% for after exercise T2, and 1.0% for volume. There were no significant differences in the T2 and volume between mean values of the two measurements.

The reconstructed volume determined from segments along the x -, y - and z -axes was found to be in good agreement with the actual volumes ($r = 1.00$, $P < 0.05$) (Figure 3-3). The errors ranged from -2.0% to -4.9% , and there were no significant differences between the reconstructed and actual volumes.

Chapter 3 Assessment of 3-D activation

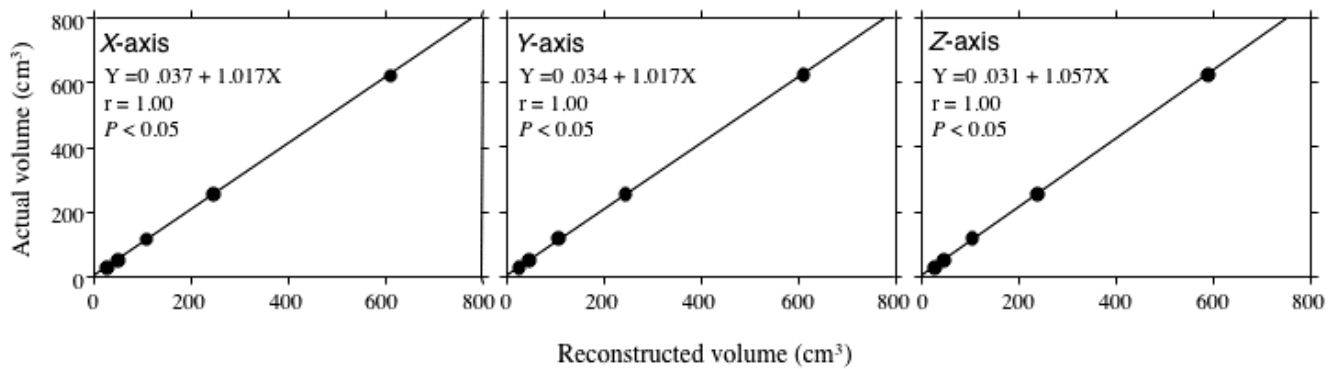


Figure 3-3. The relationship between actual volume and reconstructed volume, from which estimated by magnetic resonance images. The water portion was reconstructed in three-dimensionally using Amira and oriented with respect to a cutting plane through each pixel along the transversely (*X*-axis), longitudinally (*Y*-axis), and vertically (*Z*-axis). The volume was then calculated by multiplying the sum of the pixels in each plane.

The % activated volume determined by mfMRI, which is expressed relative to the anatomical volume, was significantly correlated with both normalized iEMG or workload with correlation coefficients of 0.84 ($P < 0.05$) and 0.85 ($P < 0.05$), respectively (Figure 3-4). Inter-subject variation was a small scale for relationship between % activated volume and normalized iEMG under three workloads (Figure 3-5).

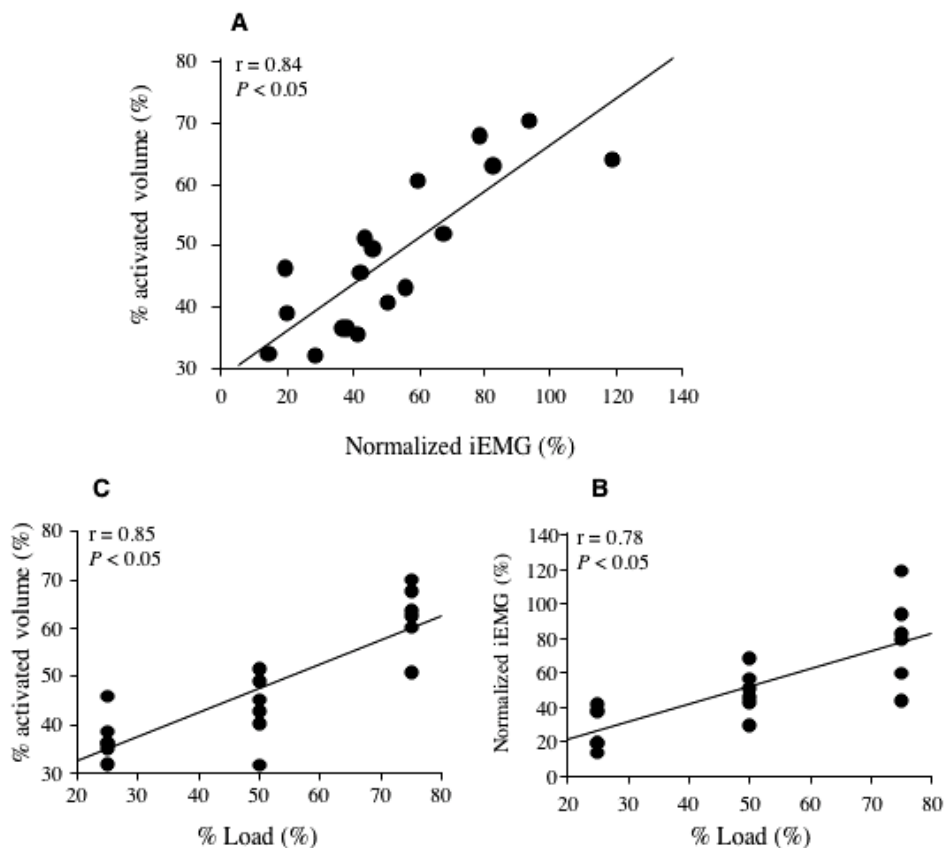


Figure 3-4. The relationship between % activated volume and normalized integrated electromyography (iEMG) (A), and between % activated volume and % load (B), and between normalized iEMG and % load (C). The normalized iEMG was express as a percentage of the corresponding value obtained during seven sets of 10 repetitions with a load equal to their 12 repetitions maximum.

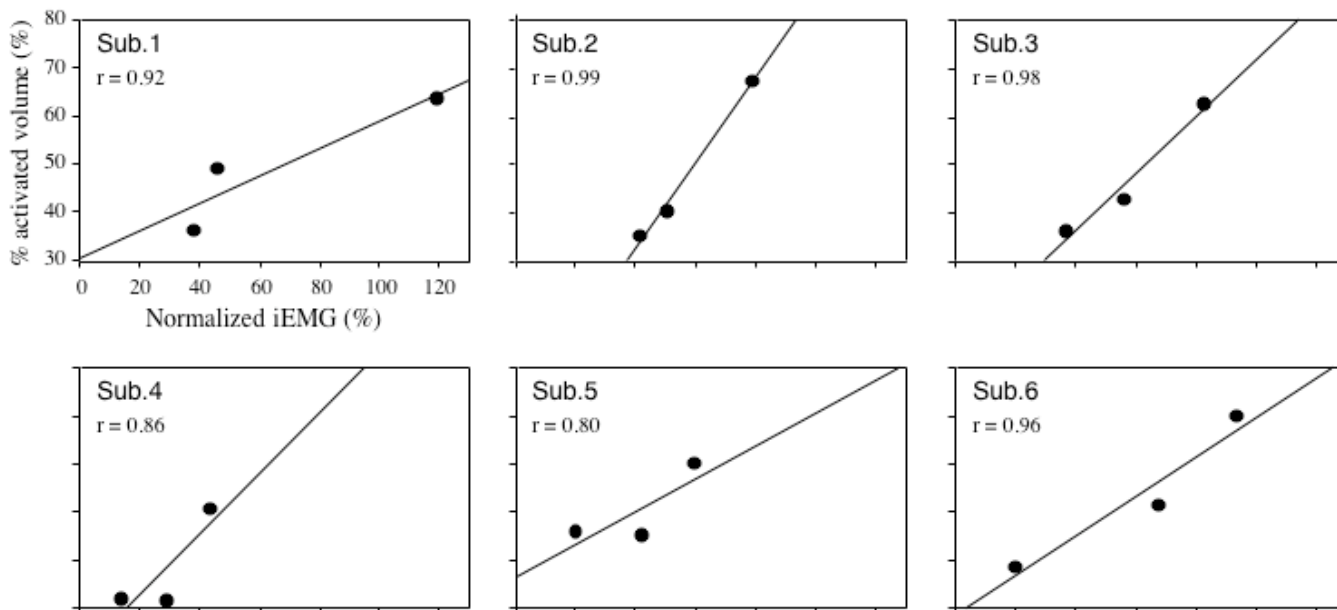


Figure 3-5. The relationship between % activated volume and normalized integrated electromyography (iEMG) in all six subjects.

Figure 3-6 presents axial MR images that were acquired before (A) and immediately after exercise (B) and 3-D activation mapping (C) of the MG from one subject. Following exercise, the muscles that were activated appear hyperintense on these T2-weighted images (B). The red regions indicate the muscle portions, which are activated due to exercise (C).

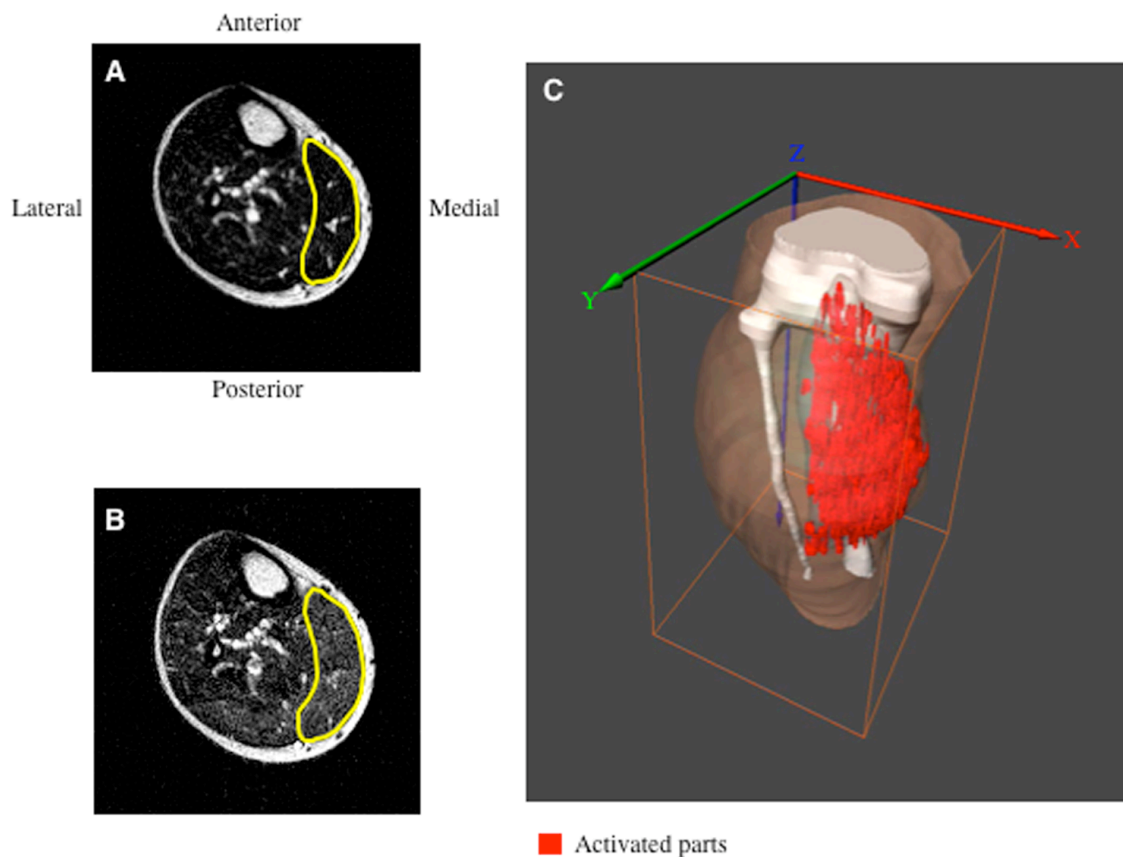


Figure 3-6. Representative transverse relaxation time-weighted magnetic resonance (MR) images at pre- (A) and post-exercise (B), and three-dimensional (3-D) activation mapping (C) of the medial gastrocnemius (MG) from one subject. The axial MR images (A and B) were located in the mid-belly of the calf muscle. Yellow line indicated contour of the MG. In 3-D activation mapping (C), semitransparent color represents the contour of the MG and the red regions indicate activated parts. The red, green, and blue lines indicate the transverse (X), longitudinal (Y), and vertical (Z)-axes respectively.

At the exercise level used in the present study, the % activated volume in the MG was $62.8 \pm 4.5\%$. The % activated area expressed relative to the anatomical

cross-sectional areas along the x -, y - and z -axes of the MG are shown in Figure 3-7. The % activated area was significantly larger in the medial than in the lateral region, in the anterior than in the posterior region and in the distal than in the proximal region ($P < 0.05$). Collectively then, this finding indicate that the intramuscular distribution of muscle activity within the exercised MG can vary along the x -, y - and z -axes, resulting in a three-dimensionally nonuniform distribution of muscle activity.

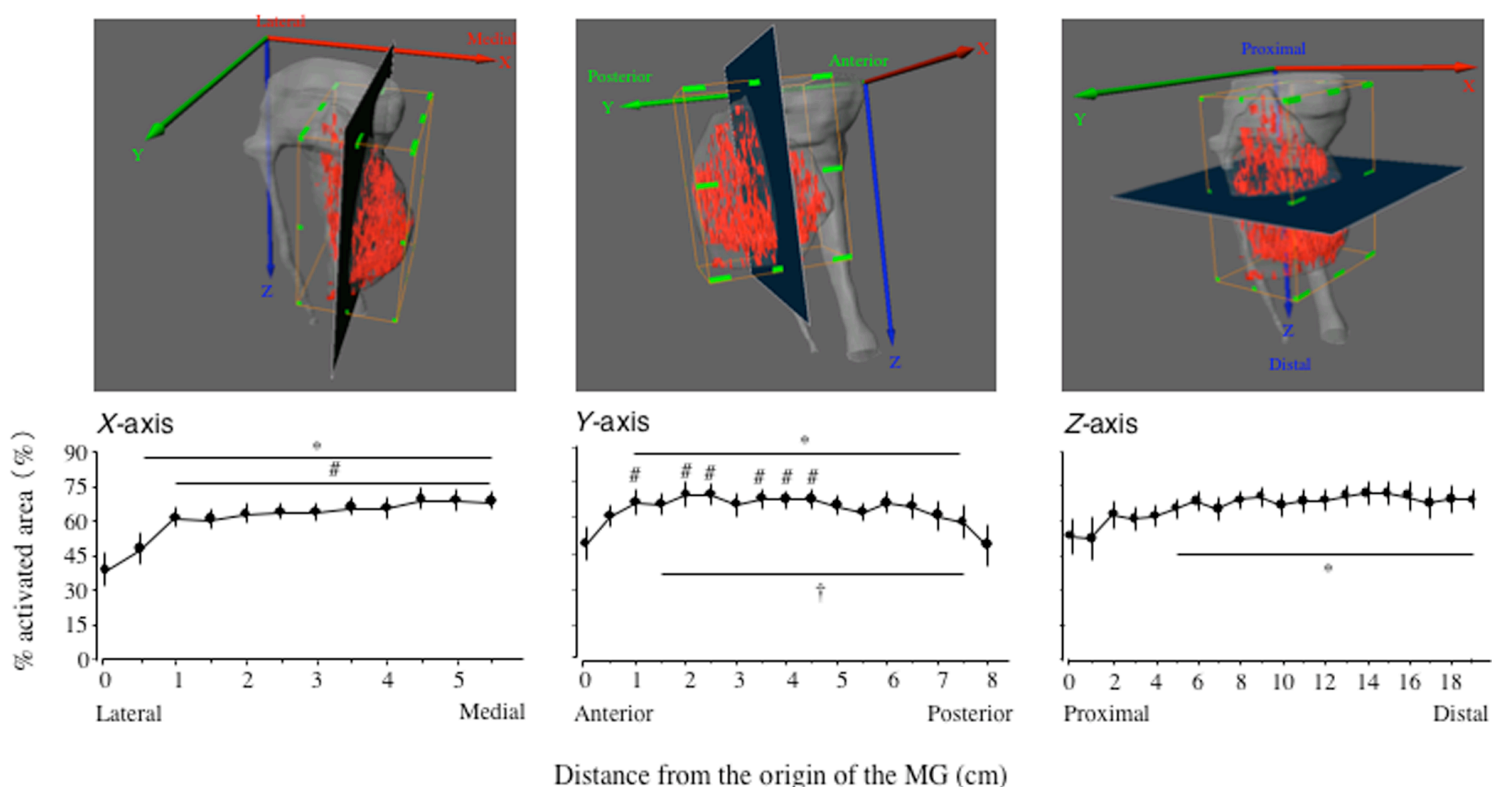


Figure 3-7. The % activated area (bottom), which is expressed relative to the anatomical cross-sectional area, along the transversely (X -axis), longitudinally (Y -axis), and vertically (Z -axis) of the medial gastrocnemius (MG). Distance 0 was identified for each subject by the lateral, anterior, and proximal edges of the MG, respectively. The upper example images correspond to the respective cutting plane through each pixel along the X , Y , and Z -axes, respectively. The red, green, and blue lines indicate the X , Y , and Z -axes, respectively. Bar represent means \pm SE for all subjects. *Significantly different from the 1st value $P < 0.05$; #Significantly different from the 2nd value $P < 0.05$; †Significantly different from the 17th value $P < 0.05$.

Discussion

Chapter 3 Assessment of 3-D activation

When implementing a new measuring technique, it is important to confirm its accuracy, reproducibility, and validity. The results of the present study demonstrate mfMRI is both highly accurate and highly reproducible. The measurement error of reconstructed volumes was less than 5%, which is remarkably low given that the imaging protocol included two imaging sessions, and should be tolerable when making measurements of tissue volume. In addition, measurements made using this technique were found to be highly reproducible, as there was a strong correlation between the first and second measurements of T2 and volume. It is also noteworthy that there was a significant correlation between the workload-related changes in % activated volume measured using mfMRI and normalized iEMG. This means that because it is the activity of individual MUs that induces the activation of muscles or muscle groups, regions of muscle activity measured with mfMRI can be considered to represent regions of neural evoked activation. Taken together, these findings indicate that the mfMRI technique described here is sufficiently accurate, reproducible, and valid for use in determining “active muscle” as a measure of an amount of muscle activation.

The novel finding in the present study was that there is a substantial variation in the muscle activation within the MG. Activation was greatest in the medial, anterior and distal regions along the transverse, longitudinal and vertical axes, respectively, and was distributed in a parabolic fashion longitudinally, but in a more linear fashion transversely and vertically. Apparently, the medial, anterior and distal portions of the MG are the most susceptible to contraction and may thus generate more force and work than other regions of the muscle do.

As implied above, one possible interpretation of these nonuniform patterns of muscle activity relates to the innervation pattern of nerve fiber. Wolf & Kim (1997)

showed that patterns of nerve ramification are variable. The human MG has one primary nerve that divides into two secondary branches and then into highly variable numbers of tertiary and quaternary branches. Patterns of nerve ramification previously have been mapped in three dimensions within a volume using 3-D computer modeling (Loh *et al.* 2003), but I did not map the pattern of innervation of the MG. An alternative explanation for the nonuniform pattern of muscle activity is that MUs are arranged topographically within some muscles (Hammond *et al.* 1989; Windhorst *et al.* 1989) and are activated in the order of their size (Henneman *et al.* 1965; Henneman & Mendell 1981). This would enable contraction to be evoked in discrete regions of a muscle (Nichols 1994). In either case, it is conceivable that submaximal contractions, involving incomplete activation of all MUs, would activate only some areas of the muscle.

It should be noted that mfMRI does not directly measure muscle electrical activity; instead, it is a reflection of muscle cell metabolism and fluid shift. The underlying cause of the T2 increase in the exercising muscle is not fully understood. But given that mfMRI is based on signals from hydrogen atoms and that the primary source of hydrogen in the human body is water, it seems likely that the exercise-induced increase in T2 seen in skeletal muscle involves movement of water into the muscle. On the other hand, the simple movement of water into the muscle does not fully explain the observed T2 change, as increase in muscle area similar in magnitude to those observed after exercise, but achieved through venous occlusion, are not associated with increases in muscle T2 (Fisher *et al.* 1990). Moreover, changes in osmotically active metabolites, such as lactate and phosphate, have been shown to directly correlate with the degree of T2 alteration (Fleckenstein *et al.* 1991; Weidman *et al.* 1991). It is

therefore thought that increases in T2 are the result of osmotically driven shifts in muscle water, which increase the volume of the intracellular space and intracellular acidification caused by metabolic by-products (Damon *et al.* 2002; Polak *et al.* 1988). This suggests that although increases in iEMG are indicative of increases in the firing rate and/or recruitment of MUs (Moritani & deVries 1978), exercise-induced changes in T2 are indicative of the metabolic activity associated with force generation. Still, alteration of EMG variables is also reportedly related to accumulation of muscle lactate, intracellular acidosis, muscle conduction velocity, force output and mechanical changes (for a review, see Bendahan *et al.* 2004). It thus appears likely that metabolic events related to muscle activation and energy demands of the activated myocytes are responsible for the increases in T2 observed in mfMR images obtained after exercise.

There are nevertheless several limitations to the present study. First, the active muscle was estimate based on thresholded T2 values. Given the strong correlation they observed between the number of pixels showing an increase in T2 and the observed force output. Adams *et al.* (1993) concluded that T2 greater than the mean \pm 1SD from the values in corresponding pre-exercise images could be considered indicative of active muscle. To measure the area of nonmuscle tissues within muscle, they were defined as the areas with resting T2 greater than 35 ms subtracted from the postexercise images. Although several studies have used this threshold method to the map the location and level of muscle activity (Adams *et al.* 1992; Akima *et al.* 1999; Kinugasa *et al.* 2003; Ploutz *et al.* 1994; Ploutz-Snyder *et al.* 1995; Prior *et al.* 1999), it is somewhat equivocal because resting T2 are affected by the scan parameters (for a review, see Meyer & Prior 2000), as well as by the fiber type (Bonny *et al.* 1998) and the intramuscular fat (Hatakenaka *et al.* 2001; Reid *et al.* 2001). For example, there is

a difference in the resting T2 between my published data (Kinugasa *et al.* 2005b) and Akima's data (Akima *et al.* 1999), even though the muscles and the physical characteristics of the subjects were similar. For that reason, to accurately quantify the active and non-active muscle areas, ranges of pixels with T2 greater than the mean + 1 SD of the entire ROI in the pre-exercise image and lower than the mean + 1 SD of the entire ROI in the post-exercise image were defined as a active muscle in the present study. The first threshold was consistent with earlier studies (Adams *et al.* 1993, Akima *et al.* 1999; Ploutz *et al.* 1994; Ploutz-Snyder *et al.* 1995; Prior *et al.* 1999), while the second should account for excluded areas of nonmuscle tissues, given that this threshold value is about the same as that obtained with bone marrow, and that intramuscular fat has a greater T2 than marrow. In this way, I was able to accurately exclude areas of nonmuscle tissue from areas of activated muscle. In an earlier report, Prior *et al.* (1999) suggested that T2 could not be used to reliably map active muscle on a pixel-by-pixel basis in normal subject. Nevertheless, in view of this finding that there is a highly significant correlation between activated area and iEMG or workload, I was conclude that muscle activation estimated using mfMRI are representative of the actual amount of muscle activation. Second, mfMRI was not performed in real time during exercise; images were acquired within 7 min after the subjects finished their exercise. An exercise-induced shift in T2 is detectable after as few as two contractions (Yue *et al.* 1994) and then increases to a work-rate-dependent plateau within a few minutes (Jenner *et al.* 1994). Recovery after exercise takes 20 min or more (Fisher *et al.* 1990), which should have enabled us to acquire functional images following exercise performed outside the scanner room (Meyer & Prior 2000). Third, because of the limited range of the imaging coil, mfMRI was carried out in two imaging sessions

separated by at least 10 days. This necessitated two exercise periods, introducing the possibility that the response would differ between the first and second periods. On the other hand, the high degree of reproducibility in the volume and T2 measurements suggests that this source of error is minimal. Forth, the present study was performed using a 0.3-Tesla scanner, but the 1.5-Tesla scanner is the one most widely used. This is likely not a problem, however, as it was previously shown that resting T2 is not significantly affected by different magnetic fields (Adams *et al.* 1993). Finally, measurements of mfMRI and EMG were not made simultaneously. As described above, the measurements of active muscle area and iEMG can be made in the same subject and at the same position, but the two measurements cannot be made simultaneously. Despite these limitations, the present findings clearly document the feasibility of using mfMRI to noninvasively and quantitatively map regions of human muscle activation in three dimensions.

In summary, there was a significant correlation between % activated volume and normalized iEMG. The % activated area was significantly larger in the medial than in the lateral region, in the anterior than in the posterior region, and in the distal than in the proximal region. Thus, mfMRI can be used to determine the amount of muscle activity and its intramuscular variations within a human skeletal muscle. The present method has many potential applications in the field of exercise physiology and biomechanics in humans.

CHAPTER 4

Muscle activation and its distribution within human triceps surae muscles

Introduction

Muscle force is a function of the amount of activation of the muscle fibers, which are arranged in three dimensions (Kawakami *et al.* 2000; Scott *et al.* 1993) and are distributed across neighboring muscles (Bruke 1981; Hammond *et al.* 1989; Trotter 1993). Because motor units (MUs) are activated in the order of their size (Henneman *et al.* 1965), it is conceivable that submaximal contractions, involving incomplete activation of all MUs, would affect only part of the volume of the activated muscle. One should therefore be able to characterize muscle activation with respect to its distribution in three-dimensional (3-D) space.

Muscle functional magnetic resonance imaging (mfMRI) has been frequently used to examine the intensity and/or pattern of muscle activation. This method relies on an exercise-induced increase in the proton transverse (spin-spin) relaxation time (T₂) in MR images of muscle. Exercise-induced changes in T₂ correlate with integrated electromyographic (iEMG) activity (Adams *et al.* 1992, Kinugasa & Akima 2005), force induced by electrical stimulation (Adams *et al.* 1993), and workload (Adams *et al.* 1992, Kinugasa & Akima 2005). This has enabled investigators to use a threshold method to map activity in functionally related regions of muscles, though mainly only one or a few axial MR images were examined (Adams *et al.* 1992; Akima *et al.* 2000; Kinugasa *et al.* 2003; Ploutz *et al.* 1994; Ploutz-Snyder *et al.* 1995; Prior *et al.* 1999).

But to date there have been very few reports on the activation of a whole muscle (Livingston *et al.* 2001; Prior *et al.* 1999), and no reports in which whole-muscle activation was examined in three dimensions within a muscle in group of synergistic muscle. Such information on the 3-D distribution of muscle activation would further understanding of the physiological characteristics of human skeletal muscle and could suggest new approaches to physical rehabilitation.

3-D imaging, such as computed tomography, MRI, and ultrasonography, was developed to extract improved qualitative and quantitative information about an object or object system from images obtained with multiple modalities. For instance, 3-D MRI has been shown to be more accurate than two-dimensional (2-D) imaging for the quantification of tissue volumes (Rusinek & Chandra 1993), and segmentation of volume images at selected sections can be used to identify and delineate objects. Moreover, because 3-D MRI has the ability to provide maximum-intensity projections, which can be useful for evaluating complex 3-D structures, the visualization of small muscle regions without the use of paramagnetic contrast material may be possible.

The combination of 3-D technology and mfMRI should have clear advantages over conventional 2-D MRI and provide insight into the functional and anatomic properties of skeletal muscle. Bearing that in mind, the aims in the present study were to use mfMRI to quantify the volumes of activated muscles and examine the distributions of activated area along the lengths of those muscles. My focus was on the triceps surae (TS) muscles, and I hypothesized that because TS muscles have different architectural and functional characteristics (Kawakami *et al.* 1998), the spatial characteristics of their activation would also differ.

Methods

Subjects

Seven healthy men participated in this study. Physical characteristics of the subjects are as follows; age 24 ± 2 yrs; height 1.70 ± 0.07 cm; weight 63 ± 4 kg (means \pm SD). All subjects were in good health with no orthopedic abnormalities and no neurological or motor disorders prior to testing. Each provided written informed consent after the procedures and purposes of the study as well as the benefits and risks of participating in the study were explained. This study was approved by the ethical committee of the university for research involving human subjects.

Experiment 1

Protocol

The lower leg length was measured, and the one-fourths and three-fourths distances from the origin of the patella to the lateral malleolus were marked on the subject's skin with a pen. Because of the limited range of the imaging coil, mfMR images were not available over the entire length of the TS muscles. To resolve this problem, MR imaging was carried out at two sessions, i.e., upper and lower parts of the lower leg based on these marks, and these two sessions were separated by at least two days, and the order of testing was randomized. Subjects were positioned supine with the lower leg within a MR device, and then consecutive axial MR images were collected. Thereafter, subjects performed repetitive calf-raise exercises. The exercise was executed outside the magnet bore, after which subjects immediately moved into the magnet for imaging.

Exercise

Each subject stood on a columnar box (height, 11 cm; diameter, 29 cm) and performed a calf-raise exercise that involved raising and lowering one's body unilaterally for five sets of 10 repetitions. As described previously (Akima *et al.* 2003; Kinugasa & Akima 2005), the subject's body was raised by flexing the ankle joint concentrically to a fully plantar flexed position in 2 s, and then lowered by dorsiflexing the ankle joint eccentrically so that the ankle resumed its initial position in 2 s (Figure 4-1). During the exercise, the heel was positioned above the ground to facilitate exercise, and the knee joint angle was set at a fully extended position throughout the exercise. There was no rest period between the raising and lowering of one's body. Use of a chair permitted subjects to take a 1-min rest interval between sets. Subjects were allowed to put their hands on a wall for balance. All subjects were familiarized with the calf-raise exercise prior participating in the study and were supervised by an investigator to ensure that the exercise was performed correctly.

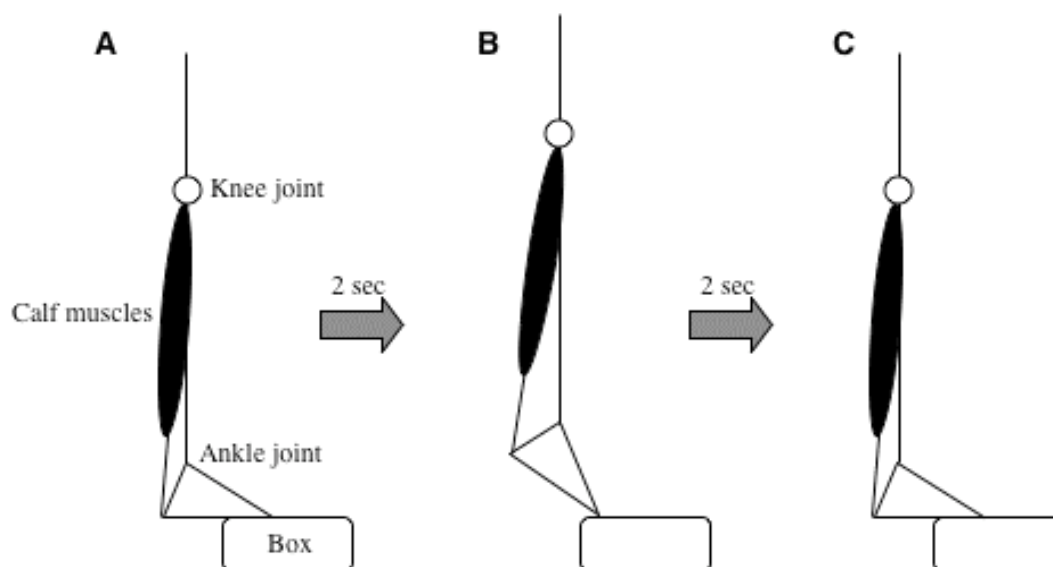


Figure 4-1. Schematic illustration of calf-raise exercise. Exercise was performed in a standing position (A) and involved raising and lowering one's body unilaterally for five sets of 10 repetitions. The subject's body was raised by flexing the ankle joint concentrically to a fully plantar flexed position in 2 s (B), and then lowered by dorsiflexing the ankle joint eccentrically (C) so that the ankle resumed its initial position in 2 s.

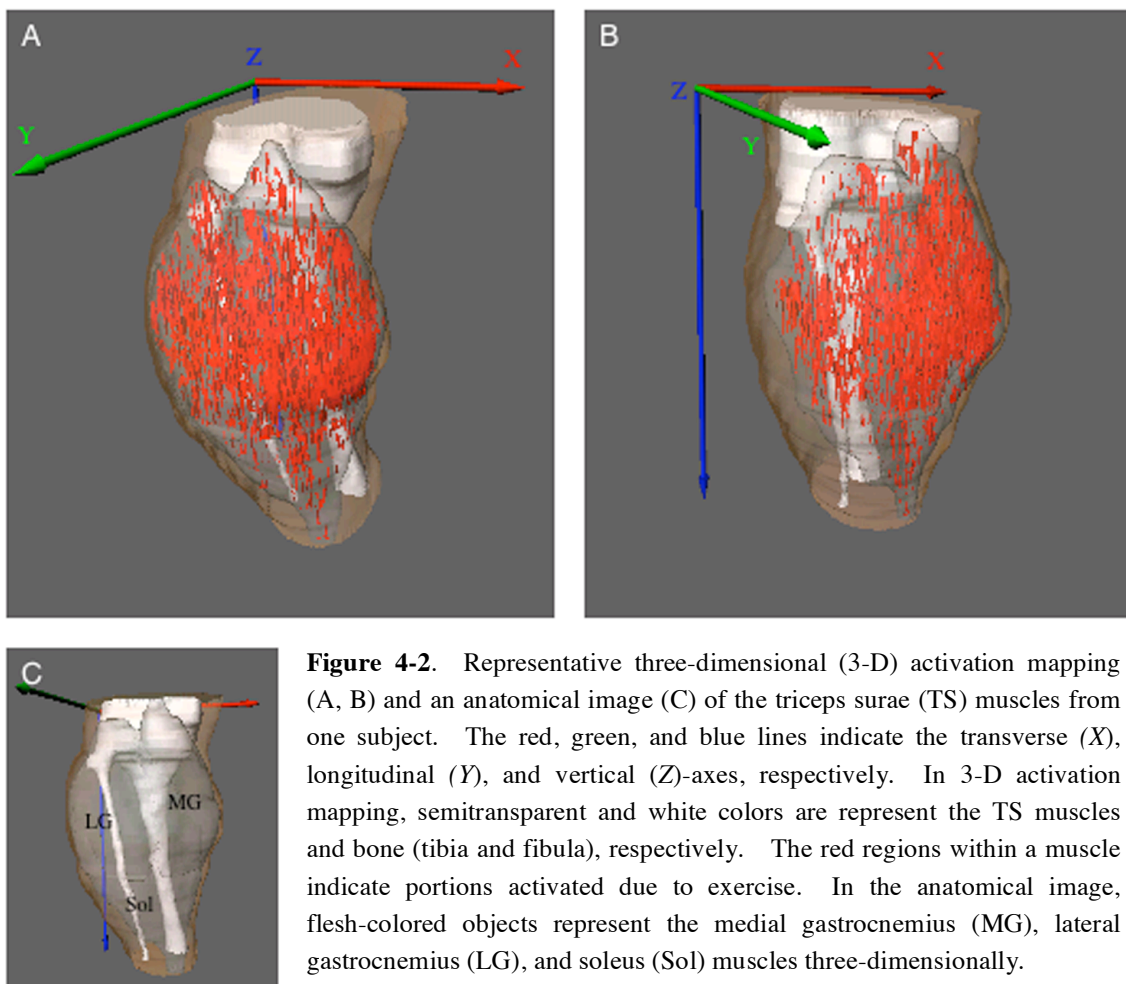
mfMR imaging and analysis

MRI scans were carried out before and within 1 min after completion of the exercise using a 0.3-Tesla MR imaging system (AIRIS, Hitachi Medical, Japan). A T2-weighted spin-echo sequence (repetition time = 2500 ms, echo time = 25, 80 ms, 256×256 matrix, scan time = 5 min 30 sec) was used to collect 22 MR images using an extremity body coil; the images were 10 mm thick and 0 mm apart and provided a 27 cm field of view. The subjects lay on their back with the knee and ankle kept at 180° (full extension) and 0° (anatomical position), respectively.

The MR images were transferred to a personal computer using fixed software on the MR system. Mean muscle T2 values (\pm SD) were calculated from reconstructed 2-D T2 images on a pixel-by-pixel basis from the two magnitude images with the assumption of a single-exponential decay using a modified version of the public domain National Institutes of Health (NIH) Image program. The T2 images analyzed extended from one obtained just inferior to the origin of the medial gastrocnemius (MG) (first image) through one that included the distal end of the soleus (Sol) (last image). A region of interest (ROI) in each image was defined by manually tracing around the individual muscles and then subcutaneous and intramuscular fat, tendon, aponeuroses, and vessels were excluded by tracing. The active muscle regions were defined by the ranges of pixels with T2 values greater than the mean + 1SD of the entire ROI in each pre-exercise image and lower than the mean + 1SD of the entire ROI in each post-exercise image, as referred by earlier studies (Adams *et al.* 1993; Kinugasa *et al.* 2006).

The 3-D visualization was performed on visualization, data analysis, and

geometry reconstruction software package (Amira 3.0, Mercury Computer Systems, San Diego, CA, USA). After the contours of the individual muscle in each image were defined, the active area within a muscle was defined using the aforementioned threshold method and displayed in red. The surfaces of the muscle and its activated regions were then reconstructed (Figure 4-2) with a surfacing algorithm. The areas were calculated for every 1.0 cm along the vertical (z)-axis. A Gauss filter was used to remove image noise (Wang *et al.* 2004).



Reconstructed 3-D images were segmented into eight portions to quantify the volume of different regions of active muscle using a semiautomated segmentation technique. The first step in this method is to divide the 3-D images of each muscle

into eight regions so as to orientate the cutting plane with respect to the center of the transverse (x), longitudinal (y), and z -axis, respectively. The volumes of these muscle regions were quantified for every four of the eight regions, enabling comparison of lateral and medial regions, anterior and posterior regions, and proximal and distal regions (Figure 4-3).

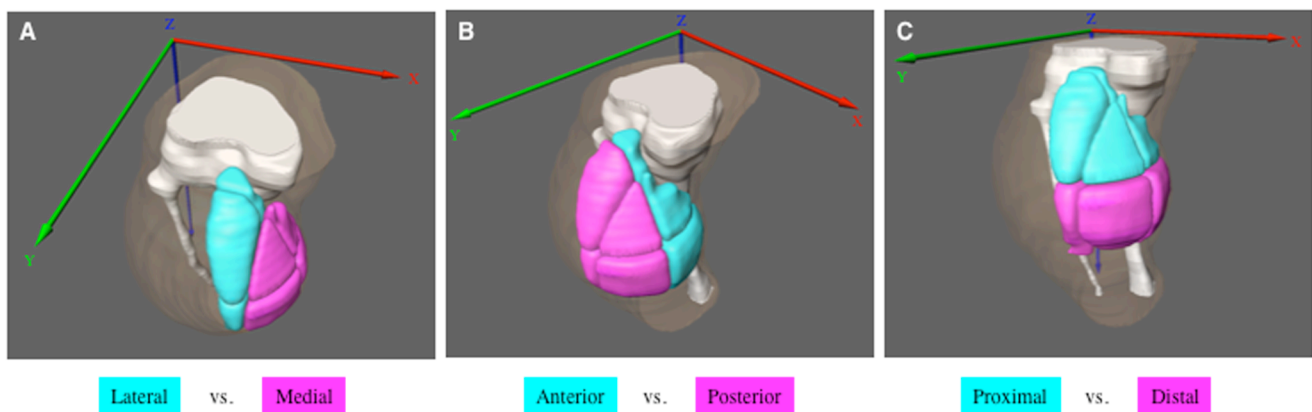


Figure 4-3. Examples of representative segments along three planes, which are divided into eight regions, in the medial gastrocnemius muscle. The muscle is classified into every four of the eight regions [lateral and medial regions (A); anterior and posterior regions (B); proximal and distal regions (C)]. The red, green, and blue lines indicate the transverse (X), longitudinal (Y), and vertical (Z)-axes, respectively.

Experiment 2

Protocol

Based on the results of Experiment 1, all subjects further participated in an EMG study. A maximal voluntary contraction (MVC) test was performed after familiarization session, from which the torque and EMG were determined. After a sufficient rest period (~10 min) after completion of the MVC measurement, subjects performed five sets of 10 repetitions of the calf-raise exercises, during which the EMG activity was measured.

Electromyography

Using preamplified surface electrodes (DE-2.1; interelectrode distance 10 mm), EMGs (Bagnoli 2.0, Delsys, Boston, MA, USA) were recorded from the proximal and distal parts of the MG, and the midbellies of the lateral gastrocnemius (LG) and Sol muscles during the MVC and calf-raise exercises. The Sol electrode was placed as described by McLean & Goudy (2004), centered at a location two-thirds the distance from the calcaneus to the head of the fibula, which corresponds to the length of the Sol. Care was taken to ensure that this site was located between the Achilles tendon and the inferior border of the LG and a preliminary cross-correlation analysis revealed negligible cross-talk among EMG channels. After carefully cleaning the skin, the electrodes were placed at locations previously marked with a permanent marker. The permanent marks enabled us to place the electrodes at the same spot in each session. Reference electrodes were placed over the patella of both legs. The EMG signals were amplified ($\times 1,000$), and band-pass filtered (15-500 Hz).

Torque

Maximal isometric plantar flexion torque was measured on an electrical dynamometer (System 3, Biodex, Shirley, NY, USA). Subjects were placed in a comfortable, upright, seated position (hip at 90° flexion) on the dynamometer chair and were secured using thigh, pelvic, and torso straps so as to minimize extraneous body movements. The ankle joint was set at 90° (anatomical position), with the knee joint at full extension and the foot securely strapped to a footplate connected to the lever arm of the dynamometer. After a warm-up and sub-maximal contractions, the subjects were required to exert maximal plantar flexor force for 2-3 s. The task was repeated twice

per subject with at least 5 min between trials. During the measurement of isometric torque, each subject was required to fold the arms across the chest and was given verbal encouragement in an attempt to achieve a maximal voluntary effort level. All procedures and verbal encouragement were administered by the same investigator for all subjects.

Data analysis

The EMG and torque signals were stored on a personal computer after analog-to-digital conversion (Mac Lab/16s, ADInstruments, Sydney, Australia) at a sampling frequency of 1 kHz. For the MVC trials, the torque was quantified as the peak value. The EMG signals were full-wave rectified and then determined as the integral value (i.e., iEMG) over the duration of contraction (i.e., 40 s). A calculation period of 40 s was employed because it corresponded to the time required to complete each set of calf-raise exercises. The iEMGs recorded during calf-raise exercise were then averaged over 5 sets. Each iEMG recorded during MVC and calf-raise exercise was divided by the respective duration, and average iEMG during calf-raise exercise was expressed as a percentage of the corresponding values (% iEMG) obtained during the MVC.

Statistical analysis

Means (\pm SE) were calculated for all variables. Statistical significance of the relationship between active muscle area and EMG or workload was studied by regression analysis, and Pearson product-moment correlations (r) were calculated. Differences in muscle measures (volume and CSA of anatomical and activated muscle),

normalized iEMG, and % change in T2 between different muscles and regions were tested by one-way analysis of variance. Statistical significance of the relationship between volume of actual muscle and activated muscle was checked by the regression analysis. Statistical significance was accepted at $P < 0.05$.

Results

Table 2 shows the muscle volume, activated muscle volume, and the relative values for individual TS muscles. The Sol was found to have to the largest muscle volume ($430.2 \pm 12.2 \text{ cm}^3$), followed by the MG ($247.0 \pm 16.8 \text{ cm}^3$) and LG ($130.3 \pm 6.5 \text{ cm}^3$) ($P < 0.05$), and these values were similar those obtained in earlier study (Fukunaga *et al.* 1992). During calf-raise exercise, the % activated volume varied among muscles. Those most activated muscle were the MG ($45.7 \pm 2.3\%$), followed by the LG ($34.9 \pm 1.6\%$) and Sol ($34.9 \pm 1.3\%$). There was a significantly difference between MG and LG or Sol ($P < 0.05$). The absolute activated volume of muscle was linearly related to the muscle volume ($r = 0.94$, $P < 0.05$).

Table 4-1. The muscle volume, activated muscle volume and % activated muscle volume.

	MG	LG	Sol
Muscle volume, cm^3	247.0 ± 16.8	130.3 ± 6.5	$430.2 \pm 12.2^*$
Activated muscle volume, cm^3	112.2 ± 7.5	45.6 ± 3.6	$149.6 \pm 5.5^*$
% activated muscle volume, %	$45.7 \pm 2.3^\#$	34.9 ± 1.6	34.9 ± 1.3

Values are means \pm SE.

* $P < 0.05$ vs. MG and LG; # $P < 0.05$ vs. LG and Sol.

MG, medial gastrocnemius; LG, lateral gastrocnemius; Sol, soleus.

The anatomical and activated CSA along the length of each TS muscle are shown in Figure 4-4. The location of the largest activated CSA was observed in the mid-belly of each muscle, and thus individual TS muscles had similar locations for the

Chapter 4 Muscle activation in the TS muscles

largest anatomical and activated CSA. Figure 4-5 shows the % activated CSA along the length of each muscle, which is expressed relative to the anatomical CSA. The distal region of the MG had larger % activated CSA than the proximal region ($P < 0.05$). In contrast, there was no regional difference in the LG and Sol.

Chapter 4 Muscle activation in the TS muscles

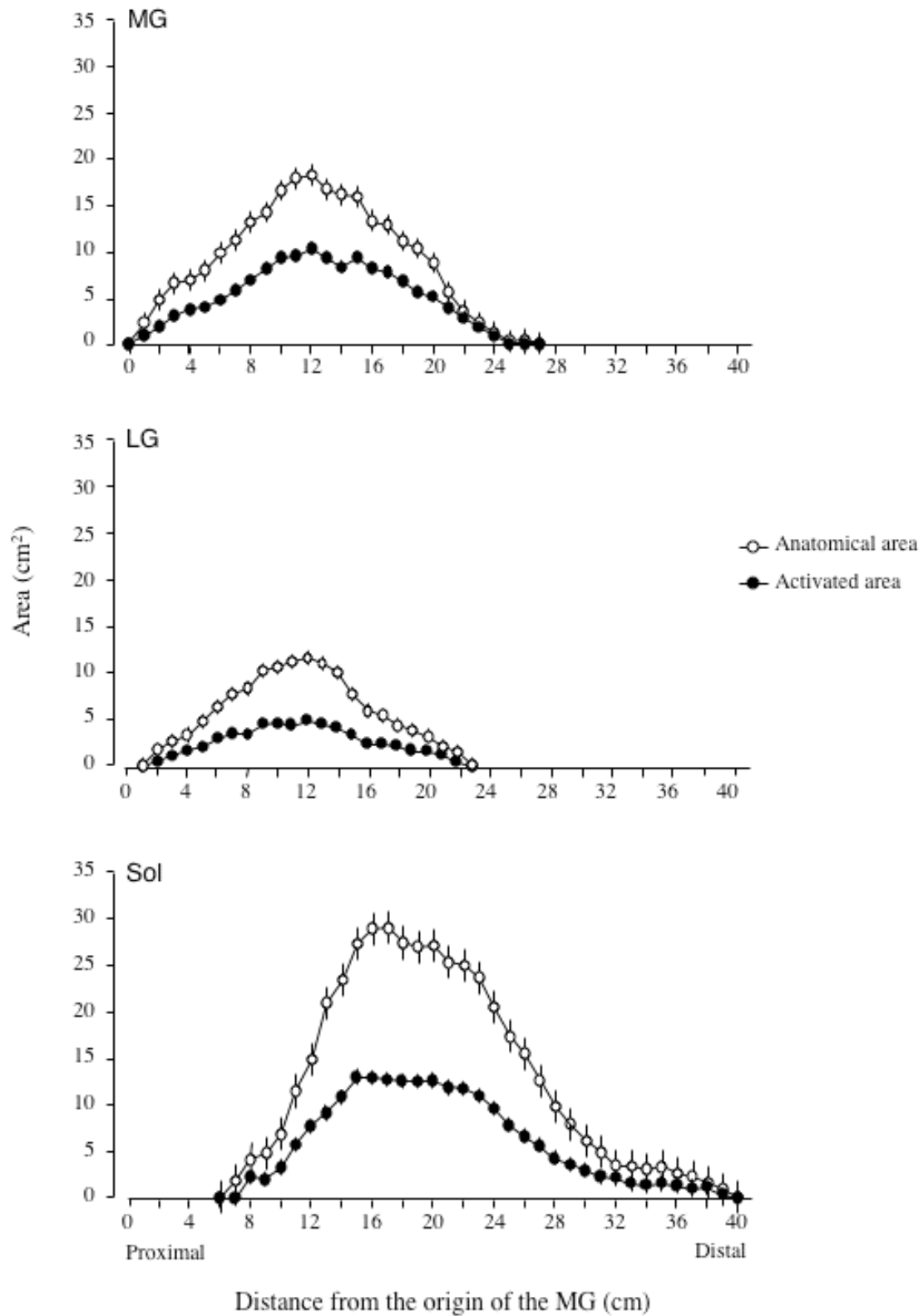


Figure 4-4. Anatomical (white symbol) and activated areas (black symbol) along the length of the medial gastrocnemius (MG), lateral gastrocnemius (LG), and soleus (Sol) muscles. Activated regions that were determined by the transverse relaxation time (T₂) on magnetic resonance images. The *abscissa* shows the distance from the origin of the MG muscle. Bars represent means \pm SE for all subjects.

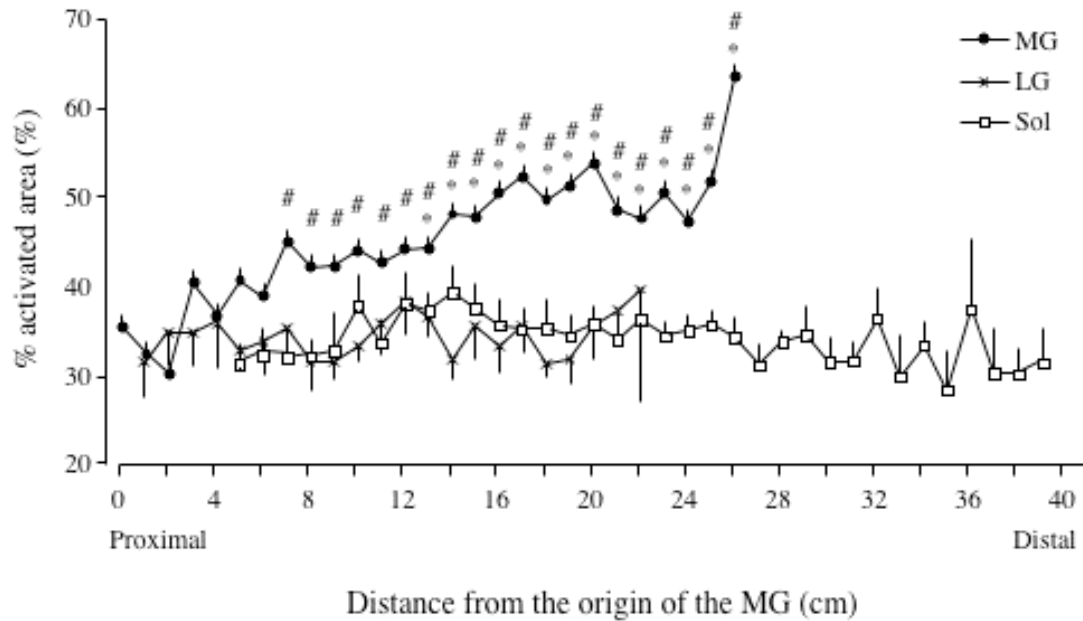


Figure 4-5. The % activated area along the length of the medial gastrocnemius (MG), lateral gastrocnemius (LG), and soleus (Sol) muscles. The % activated area is expressed relative to the anatomical cross sectional area. Distance 0 was identified for each subject by the proximal edge of the MG muscle. Bars represent means \pm SE for all subjects. *Significantly different from the 2nd value; #Significantly different from the 3rd value.

The % activated volume in every region for each TS muscle is shown in Figure 4-6. In the MG, there was a significant difference in % activated volume between distal and proximal regions ($P < 0.05$). However, the LG, Sol, and another region of the MG did not show such partial differences.

Chapter 4 Muscle activation in the TS muscles

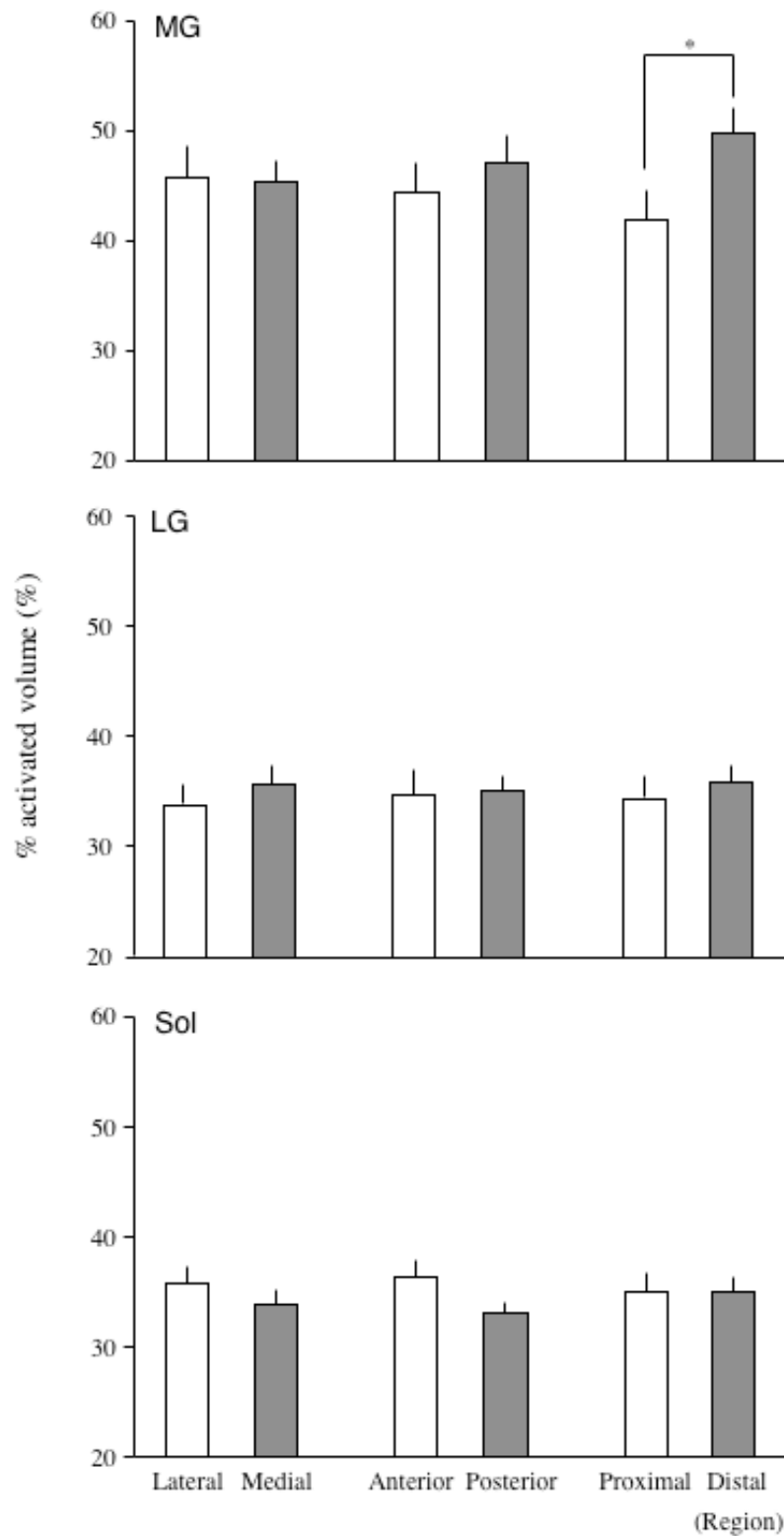


Figure 4-6. The % activated volume of lateral and medial regions, anterior and posterior regions, and proximal and distal regions in the medial gastrocnemius (MG), lateral gastrocnemius (LG), and soleus (Sol) muscles. The % activated volume is expressed relative to the whole muscle volume. The % activated volume is compared with lateral and medial regions, anterior and posterior regions, and proximal and distal regions, respectively. Bars represent means \pm SE for all subjects. *Significant difference.

Chapter 4 Muscle activation in the TS muscles

Table 4-2 shows the maximal isometric torque, normalized iEMG, and % change in T2 in the individual TS muscles. The normalized iEMG in the distal parts of the MG was greater than the LG, Sol as well as proximal parts of the MG ($P < 0.05$). MG had the largest % change in T2 among TS muscles ($P < 0.05$).

Table 4-2. Maximal isometric torque, normalized iEMG and % change in T2.

Isometric torque, Nm	150.5 ± 9.0
Normalized iEMG, %	
MG proximal parts	64.1 ± 3.0
MG distal parts	88.0 ± 11.0*
LG	57.4 ± 9.7
Sol	48.9 ± 5.7
% change in T2, %	
MG	13.5 ± 1.3#
LG	8.1 ± 1.3
Sol	4.6 ± 1.6

Values are means ± SE.

* $P < 0.05$ vs. MG in proximal parts, LG, and Sol for iEMG.

$P < 0.05$ vs. LG and Sol for T2.

iEMG, integrated electromyography; T2, transverse relaxation time;

MG, medial gastrocnemius; LG, lateral gastrocnemius; Sol, soleus.

Discussion

The major finding of this study was that the relative areas of activated muscle accounted for approximately 46% of the total MG and 35% of the total LG and SOL, respectively. From a muscle architecture perspective, the MG has characterized by shorter fascicle lengths and larger fascicle angles than the LG (Kawakami *et al.* 1998), and thus contains more fibers within a given volume (Fukunaga *et al.* 1992). Consequently, the MG has a greater force-producing capacity than the LG and Sol. Those results are corroborated by data reported for ankle plantar flexor exercise, in

which the MG showed higher iEMG (Kinugasa & Akima 2005; Price *et al.* 2003; Signorile *et al.* 2002; Tamaki *et al.* 1997) and T2 values (Akima *et al.* 2003; Kinugasa & Akima 2005; Price *et al.* 2003; Yanagisawa *et al.* 2003) than the LG and Sol at several workloads setting. I therefore conclude that the relative areas of activation differ among TS muscles during the present exercise protocol.

The Sol showed the largest absolute activated area among the TS muscles. Although earlier study (Signorile *et al.* 2002) have reported that the Sol is certainly active during planar flexion with the knee fully extended, minimal activation was observed using a resistance setting that yielded 50 repetitions. The normalized iEMG and % change in T2 obtained in the present study are consistent with those earlier ones (Kinugasa & Akima 2005, Kinugasa *et al.* 2006). Moreover, another calculations indicate that the Sol made up 53% of the total volume of the TS muscles, followed by the MG (31%) and LG (16%). Total muscle volume strongly correlated with the volume of activated muscle in the present study, and thus the larger activated volume seen in the Sol is likely related to the overall size of the muscle.

I found that, in the MG, % activated area in the distal region of the muscle was larger than that in the proximal region. This region-specific difference was consistent with the present EMG data, suggesting muscle activation is distributed unevenly along the length of the MG. The functional consequence of this heterogeneity is that the force generated by a unit will be spread over a larger tissue area. This may minimize mechanical stress in focal regions within the muscle (Lieber 2002).

The activation heterogeneity is reflected by the architecture of the MG muscle (Kawakami *et al.* 2000); the fiber pennation angles in the distal part are significantly smaller than in the proximal part. That there is a significant negative

correlation between the specific tension and the fiber pennation angle (Ichinose *et al.* 1998) means that the distal region of the human MG has a greater force-generating capacity.

The existence of compartmentalization within muscle has been demonstrated in the MG of the rat (De Ruyter *et al.* 1996; Hutchison *et al.* 1989), where there is a load-related activation differential between the proximal and distal compartments. On the other hand, direct dissection of cadaver specimens revealed no neuromuscular compartmentalization in the human MG (Wolf & Kim 1997). It is known that neuromuscular compartmentalization is dependent on the innervation ratio and muscle architecture (Segel *et al.* 1991). However, muscles in embalmed cadavers change their morphological characteristics due to factors such as shrinkage (Friedrich & Brand 1990), which makes it difficult to acquire precise information about muscle architecture. Furthermore, the fact that non-uniform architecture along the length of a muscle can play a key role in creating different regions of muscle activation (Wolf *et al.* 1993) is consistent with the idea that human MG possesses neuromuscular compartmentalization, as has been shown for the LG (Segel *et al.* 1991).

MUs located in the distal region of the rat MG have a greater fiber CSA than those in the proximal region (De Ruyter *et al.* 1995). If these differences exist in the human MG, activated areas would differ along the length of the muscle. Indeed, heterogeneity in the distribution of fiber CSA has important implications for the mechanical and functional properties of different regions of a skeletal muscle. Unfortunately, the distribution of fiber CSA in the human MG is not yet known; thus a more detailed study is warranted. Still, this finding suggests that the differences in activation between the distal and proximal regions of the MG are likely related to the

differences in muscle architecture and neuromuscular compartmentalization and/or fiber distribution.

Region-related differences in activation were not observed in the LG or Sol. English and co-authors (Segal *et al.* 1991; Wolf *et al.* 1993) reported that the LG, which contains three anatomically distinct heads, exhibits functional partitioning. However, when Wolf *et al.* (1993) recorded task-oriented EMG activity from the LG, they found no statistically significant differences in EMG activity between the proximal-distal and medial-lateral regions when the subject performed a standing unilateral plantar flexion with non-weight-bearing. My findings are consistent with those and suggest task-dependent nonuniform activation might occur in the LG. To my knowledge, however, no regional variations in Sol activation have yet been found. Further studies would be necessary to clarify the activation difference in the Sol.

So why does the distal region of the muscle show greater activation than the proximal region in the MG, but not in the LG or Sol? One possibility is that, because the MG acts as an agonist muscle among plantar flexors, greater activation in the distal region is effective to force transmission to the ankle joint. Zuurbier *et al.* (1994) found that the largest extension of the MG aponeurosis occurred in the most distal part of the muscle during contraction in humans, which suggests the greatest agonistic action of a muscle might be located in the region nearest a joint. On the other hand, Muramatsu *et al.* (2001) reported that the aponeurosis of the human MG is not heterogeneously stretched along the muscle length during contraction. To resolve this discrepancy, additional studies will need to be carried out under conditions in which the knee joint is flexed.

There is a main limitation to the noninvasive measurement of muscle

activation using mfMRI. Because exercise-induced increases in T2 depend on muscle fiber type (Prior *et al.* 2001), differences in T2 values among TS muscles cannot be directly interpreted as a difference in muscle activation. The gastrocnemii muscle, for example, contains a considerably higher percentage of fast-twitch fibers than does the predominantly slow-twitch fibers Sol (Edgerton *et al.* 1975, Johnson *et al.* 1973). The T2 increase is greatest in a muscle characterized by high percentage of fast-twitch fibers that low oxidative capacity and high glycolytic capacity (Reid *et al.* 2001). Fortunately, fiber types and their distributions in human muscles do not dramatically compare with those in the corresponding muscles of rodents and other quadrupeds (Saltin & Gollnick 1983), Therefore, Prior *et al.* (2001) have concluded that semiquantitative comparisons among muscles can be justified irrespective of fiber type. In fact, human TS muscles have frequently been used in studies in which mfMRI was used to measure muscle activation (Akima *et al.* 2003; Kinugasa & Akima 2005; Price *et al.* 2003; Yanagisawa *et al.* 2003).

In conclusion, my data show that the MG had the largest % activated areas (45.7%), followed by the LG (34.9%) and Sol (34.9%) after unilateral calf-raise exercise. There was a nonuniform distributed pattern of muscle activation in the MG, but not in the LG and Sol. These results suggest that the size of the activated region and its distribution would be different among TS muscles, thus indicating that individual TS muscles play different functional roles during contraction.

CHAPTER 5

Load-specific distribution of muscle activity in human medial gastrocnemius and soleus muscles

Introduction

Skeletal muscle tissue is composed of activatable muscle fibers and a passive matrix of tendinous tissues. The force exerted by a skeletal muscle depends on the force generating capacity of muscle and its degree of activation by the central nervous system. Earlier studies (Akima *et al.* 2000; Kinugasa *et al.* 2005a, 2006; Livingston *et al.* 2001; Prior *et al.* 1999; Segal & Song 2005; Wolf *et al.* 1993) revealed the activation of muscle fibers is differed among the sites. This means that the activation is distributed non-uniformly within a muscle. However, the location of activated fibers within a muscle according to increasing force level remains unknown. This is in part because the distribution of muscle activation is difficult to map, the activation is typically studied at a particular position within a muscle.

Magnetic resonance imaging (MRI) is frequently used for clinical diagnostic applications because of the detailed visualization of soft tissue that it provides. Recent developments in MR imaging have enabled the acquisition of physiological, or functional measurements, in addition to the more traditional anatomic information. Of particular interest to the study of neuromuscular physiology is the observation that exercise induces contrast shift in proton transverse (spin-spin) relaxation time (T₂) of skeletal muscle (Fung & Puon 1981; Meyer *et al.* 2001). This T₂ contrast shift is correlated with integrated electromyographic (iEMG) activity (Adams *et al.* 1992;

Kinugasa & Akima 2005), increase with exercise intensity (Adams *et al.* 1992; Kinugasa & Akima 2005) and related to isometric torque (Adams *et al.* 1993). The MRI can be quantified to provide a noninvasive measure of the intensity of recently performed muscular activity, the absolute and relative area or volume of activated muscle and three-dimensional (3-D) distribution patterns of muscle activation (Kinugasa *et al.* 2005a, 2006).

The triceps surae muscles are comprised of the gastrocnemius and soleus (Sol) muscles, which are the main synergists for plantar flexion (Fukunaga *et al.* 1992, 1996; Murray *et al.* 1976). The gastrocnemius has a mixed fiber composition and thus contains a considerably higher percentage of fast-twitch fibers than the Sol (Edgerton *et al.* 1975). Earlier study (Burke & Tsairis 1973) has shown that fibers of a single motor unit (MU) occupy a specific region of the muscle. An additional distinction between the two muscles is that unlike the Sol, the gastrocnemius crosses the knee joint; consequently, gastrocnemius activities are essential for stability of knee joint extended position (Lan & Crago 1992). It is conceivable, therefore, that these two muscles would not be identical the location of activated fibers across force level. However, the different muscles in fiber type may hold across synergistic motor pool is largely unknown. Medial and lateral gastrocnemius muscles are both mixed muscle fibers composed of similar MU populations (Burke *et al.* 1973) and they presumably act similarly during locomotion and jumping. In addition, in the lateral gastrocnemius, T2 was not correlated with iEMG (Kinugasa & Akima 2005). Thus, the MG and Sol are two muscles that are suitable for comparison. I hypothesized that the activation will be increase in both the two muscles as exercise load is increase, the type of activated fibers and their spatial distribution may differ between the two muscles. This hypothesis was

tested by comparing the spatial distribution of the activation within the medial gastrocnemius (MG) and Sol under two different workloads of plantar flexion exercise.

Methods

Six healthy male [average age, 25 ± 2 yrs; average height, 1.73 ± 0.08 m; average weight, 69 ± 10 kg (means \pm SD)] volunteered to participate in this study. None of the subjects had any known neurological disorder or cardiovascular disease, and all were naive to the experimental protocol and procedures. They have never done specific resistance training of plantar flexor muscles, and had not engaged in any exercises during the experiment. The dominant leg as determined by the preferred leg to kick a ball was used to experiment (3 right leg; 3 left leg). Before participation in the study, all subjects gave informed consent, and the Human Subjects Committee at the University approved the protocol. The experiments were carried out according to the Declaration of Helsinki.

MRI

Subjects lay supine with their dominant calf relaxed and in knee joint at 180° on the 0.3-Tesla MRI equipment (AIRIS, Hitachi Medical, Tokyo, Japan). The foot was firmly secured to the specially designed foot plate with straps, and the trunk and thigh were also secured to the bed by straps. T2-weighted (repetition time = 2500 ms, echo time = 25, 80 ms, 250 mm field of view, 22 slices, 10 mm slice thickness, 0 mm gap, 256×256 acquisition matrix, total acquisition time 5min 30 sec) spin-echo images were acquired before the exercise and within 1 minute of the end of exercise. Scan was carried out two sessions separated by at least 7 days, because of the limitation of

imaging range that was enable to scan up to 320 mm. Images were acquired either from the head of the patella to the center of distance the head of the patella and lateral malleolus, or from there to the lateral malleolus via a standard 25-cm-diameter extremity coil. The order of acquired two imaging sessions was randomly assigned. The total number of cross-sectional images ranged from 35 to 40, depending on the lower extremity lengths of the subjects. A water-soluble marker was used on the subjects skin as an anatomic reference point to ensure images were collected from the same location for repeated scans. This reference point was also used to align collected MR images from the two sessions.

T2 images were calculated on a pixel-by-pixel basis from the 25 and 80 ms images, and analyzed by tracing a region of interest (ROI) around the MG and Sol using a modified version of the public domain National Institutes of Health (NIH) Image program. Care was taken to exclude intramuscular fat, aponeurosis, and vascular structures from the traced regions. The contours of the MG and Sol in each slice was saved, and enabled us to reference at the same region on later analysis with use of 3-D software. The T2 value (mean \pm SD) and the total number of pixels were determined for the ROI in each slice. Active muscle areas were estimated by the threshold method, as described by Kinugasa *et al.* (2005a); pixels showing T2 greater than the mean + 1SD of ROI in the pre-exercise image and a T2 lower than the mean + 1SD of ROI in the post-exercise image. The survived pixels showing T2 are defined as active muscle, and indicated by color red for the MG and orange for the Sol. This method is modified from first reported study (Adams *et al.* 1993), the differences in method of T2 threshold between the present study and earlier study have been described in detail at my recent earlier study (Kinugasa *et al.* 2005a).

To 3-D reconstructed thresholded images, the first step is to defined the contours of the MG and Sol in each slice by manual tracing and the active muscle areas based on aforementioned threshold using visualization, data analysis, and geometry reconstruction software package (Amira 4.1, Mercury Computer Systems, San Diego, CA, USA). Thresholded images were then 3-D reconstructed, from which muscle volume and its activated volume were determined for the MG and Sol. In addition, 3-D image was segmented transverse (x), longitudinal (y), and vertical (z)-axes of each voxel. The activated areas were then determined for every 0.5-cm along x - and y - axes and for every 1.0-cm along z -axis.

Plantar flexion exercise

Subjects performed unilateral isotonic exercise with ankle flexor muscles using plate-loaded plantar flexion machine (ATLAS fitness factory, Tokyo, Japan). Each subject was seated in an adjustable chair with the knee joint angle fully extended and the hip joint angle flexed at 80° (full extension = 0°). The foot was firmly secured to the foot plate with straps, and the trunk and thigh were also secured to the chair by straps. The position of the foot and the foot plate was adjusted so that the center of rotation of the ankle joint was aligned with the center of rotation of the equipment. The exercise began with the ankle in an 5° of dorsiflexion, and then the weight was raised by plantarflexing the ankle flexors concentrically to the ankle in an 40° of plantar flexed position in 2 s, and lowered by dorsiflexing the ankle flexors eccentrically so that the ankle resumed its initial position in 1 s. There was no rest between the raising and lowering of a weight or between repetitions of exercise. A digital metronome controlled the exercise. A week before the experiment, all subjects were familiarized

with this exercise, and then maximal load of 1 repetition maximum (RM) and 12 RM that could be lifted with this exercise was determined for each subject.

1 RM test was conducted after a standardized warm-up and practice trials at submaximal intensities. The test was repeated two times per subject with at least 3 min between trials. Subjects were given strong verbal encouragement during this test. Thereafter, subjects performed seven sets of 10 repetitions with a load equal to 25% or 75% of the previously determined 12 RM with a rest period of 60 seconds between the sets. These two loads were separated by at least 7 days, and the order of testing for the two loads randomized across subjects. Before all exercise trials, I confirmed that T2 had returned to its baseline value. An investigator supervised all the sessions, and subjects completed all the required sets of exercise. There were no systematic changes with respect to the 1 RM test and 12 RM isotonic exercises between the two imaging sessions.

EMG

The surface EMG was recorded during the 1 RM test and 12 RM isotonic exercises. The technique for recording EMG is the same as that repeatedly used in our laboratory (Kinugasa & Akima 2005; Kinugasa *et al.* 2005a, 2006). The surface EMG was recorded from the MG and Sol with an active parallel-bar bipolar electrodes (1 by 10 mm in size and located 10 mm apart). The electrodes were attached over the muscle belly for the MG and centered at a location two-thirds the distance from the calcaneus to the head of the fibula for the Sol (McLean & Goudy 2004). Care was taken to ensure that this site was located between the Achilles tendon and the inferior border of the MG. Preliminary test revealed negligible cross-talk among EMG

channels. After careful abrasion of the skin, the electrodes were placed at the same locations in each session with use of permanent spot marks. The reference electrode was placed over the patella. The EMG signal was amplified ($\times 1,000$) and band-pass filtered (15-500 Hz) with Bagnoli EMG system (Delsys, Boston, MA, USA) before being recorded directly to a personal computer by using analog/digital convertor (PowerLab/16sp, ADInstruments, Sydney, Australia) with sampling frequency of 1 kHz and displayed on computer. There were no systematic changes of EMG measurements between the two imaging sessions and between 1 RM test and 12 RM isotonic exercises. The EMG was full-wave rectified and integrated for the duration of the exercise (30 seconds) to give iEMG. A calculation period of 30 seconds was employed because it corresponded to the time required to complete each set of exercise. The iEMGs were then averaged over seven sets and normalized to the peak iEMG obtained during the 1 RM test.

Statistical analysis

All values are expressed as means \pm SE throughout the text, figures, and tables. A two-way ANOVA was used to compare the muscle volume, activated volume and percentage activated volume as well as T2 at rest and after exercise, % change T2, and iEMG between loads (25% 12 RM vs. 75% 12 RM) and between muscles (MG vs. Sol). Separate one-way analysis of variance with repeated measures was used to compare the activated areas across sites on three axes between loads. When significant effects were found, Tukey-Kramer post hoc tests were performed to determine the location of the effect. The significance level for all comparisons was set at $P < 0.05$.

Results

The normalized iEMGs for the MG and Sol were both significantly greater ($P < 0.05$) at 75% 12 RM than at 25% 12 RM (Table 5-1). In addition, at 75% 12 RM, the normalized iEMG for the MG tended to be greater than that for the Sol, but the difference did not reach statistical significance. At 25% 12 RM, there was no significant difference in the normalized iEMGs for the MG and Sol.

Table 5-1. The normalized iEMG in the MG and Sol at 25% and 75% 12 RM loads.

	MG		Sol	
	25% 12 RM	75% 12 RM	25% 12 RM	75% 12 RM
Normalized iEMG, %	26.8 ± 3.4	73.0 ± 5.5*	25.9 ± 1.9	63.5 ± 3.9*

Values are means ± SE.

* $P < 0.05$ for 25% 12 RM vs. 75% 12 RM.

iEMG, integrated electromyography; RM, repetition maximum; MG, medial gastrocnemius; Sol, soleus.

Table 5-2. The muscle volume, activated volume, and % activated volume in the MG and Sol at 25% and 75% RM loads.

	MG	Sol
Muscle volume, cm ³	224.0 ± 20.5	407.4 ± 27.3#
Activated muscle volume, cm ³		
25% 12 RM	82.0 ± 9.4	162.3 ± 11.8#
75% 12 RM	122.9 ± 12.7*	176.6 ± 15.3#
% activated muscle volume, %		
25% 12 RM	36.3 ± 1.5	39.9 ± 1.3
75% 12 RM	54.6 ± 2.3*#	43.1 ± 1.2

Values are means ± SE.

* $P < 0.05$ for 25% 12 RM vs. 75% 12 RM. # $P < 0.05$ for MG vs. Sol.

RM, repetition maximum; MG, medial gastrocnemius; Sol, soleus.

I found that the volume of the Sol (407.4 ± 27.3 cm³) was greater than that of the MG (224.0 ± 20.5 cm³) ($P < 0.05$) (Table 5-2), which is comparable to earlier

studies (Fukunaga *et al.* 1996; Kinugasa *et al.* 2005a). When the subjects performed repetitive plantar flexion exercises with a load of 25% 12 RM, both the MG and Sol were nonuniformly activated throughout their entire length (Figure 5-1, A). Upon increasing the load to 75% 12 RM, the activation within the MG increased throughout its length, but there was little change in the activation within the Sol (Figure 5-1, B). Whereas the % activated volume of the MG increased from $36.3 \pm 1.5\%$ at 25% 12 RM to $54.6 \pm 2.3\%$ at 75% 12 RM ($P < 0.05$) (Table 5-2), the % activated volume of the Sol was about the same for both loads ($39.9 \pm 1.3\%$ vs. $43.1 \pm 1.2\%$; $P > 0.05$). In addition, the % activated volume was larger ($P < 0.05$) in the MG than in the Sol at 75% 12 RM, but not at 25% 12 RM. Taken together, these results confirm that there is a significant load \times muscle interaction affecting activation ($P < 0.05$).

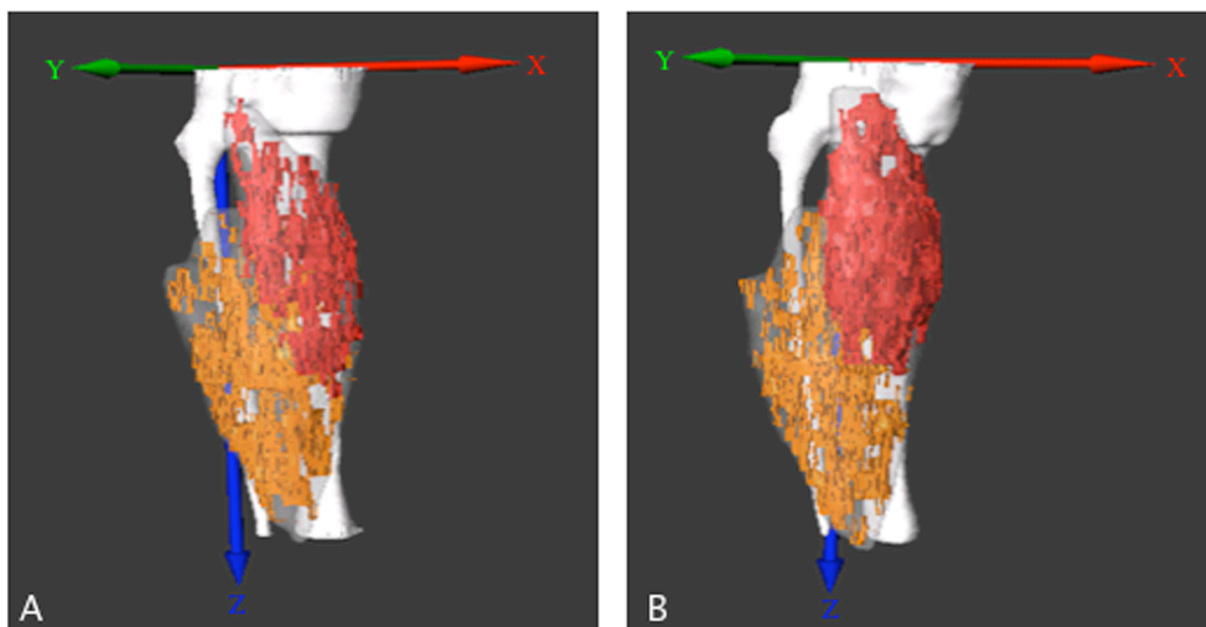


Figure 5-1. Representative three-dimensional (3-D) activation mapping in the medial gastrocnemius (MG) and solues (Sol) in one subject after exercise with loads of 25% 12 repetition maximum (RM) (A) and 75% 12 RM (B). Red and orange colors correspond to the activated regions in the MG and Sol, respectively. The red, green, and blue lines indicate the transverse (X), longitudinal (Y), and vertical (Z)-axes, respectively. Semitransparent and white objects depict the contours of the muscles and bones, respectively.

In Figure 5-2, A, the absolute areas of the MG activated by 25% and 75% 12 RM along the length of the X-axis is compared. The results show that the areas of activation in the mid-portions (4-7th segments) of the muscle are significantly larger ($P < 0.05$) at 75% 12 RM than at 25% 12 RM. Along the Y-axis, significantly larger activated areas were observed from the 4th to the 14th segments at 75% 12 RM ($P < 0.05$) (Figure 5-2, B). Activated areas along the length of the Z-axis were highly variable, ranging from 0.7 to 11.1 cm² at 75% 12 RM and from 0.4 to 6.6 cm² at 25% 12 RM (Figure 5-2, C). Nevertheless, the activated areas extending from the 3rd to the 13th segments were significantly larger ($P < 0.05$) at 75% 12 RM than at 25% 12 RM. By contrast, there were no significant differences in the activated areas at 25% 12 RM and 75% 12 RM along any of the axes of Sol (Figure 5-3, A-C).

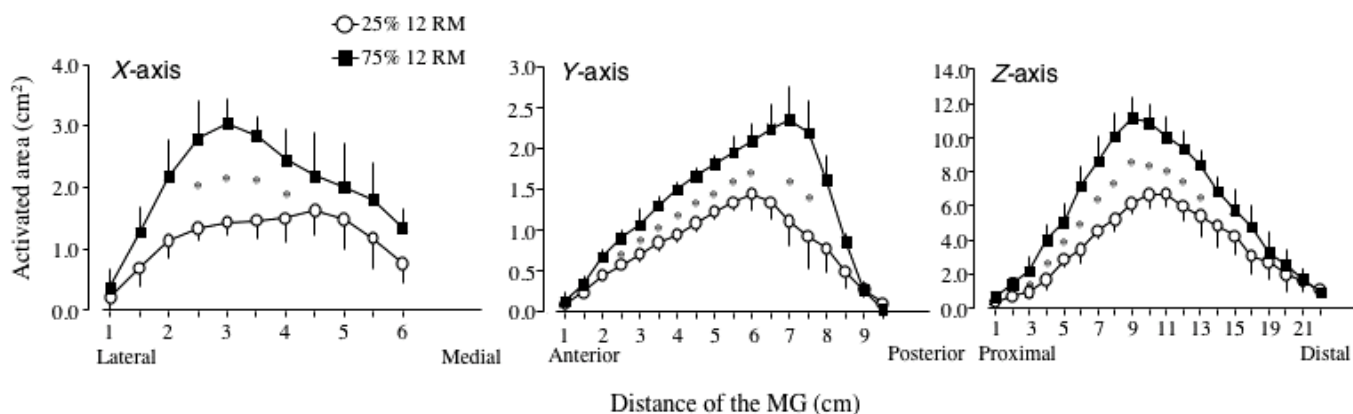


Figure 5-2. Series of activated areas of the medial gastrocnemius (MG) along the transverse (X, A), longitudinal (Y, B), and vertical (Z, C)-axes at 25% 12 repetition maximum (RM) (open symbols) and 75% 12 RM (solid symbols). The *abscissa* shows the distance from the origin of the MG calibrated in 0.5-cm intervals for the *x*- and *y*-axes and 1.0-cm intervals for the *z*-axis; the first value was identical to the origin of the MG. Values are means \pm SE. * $P < 0.05$ for exercise load (25% 12 RM vs. 75% 12 RM).

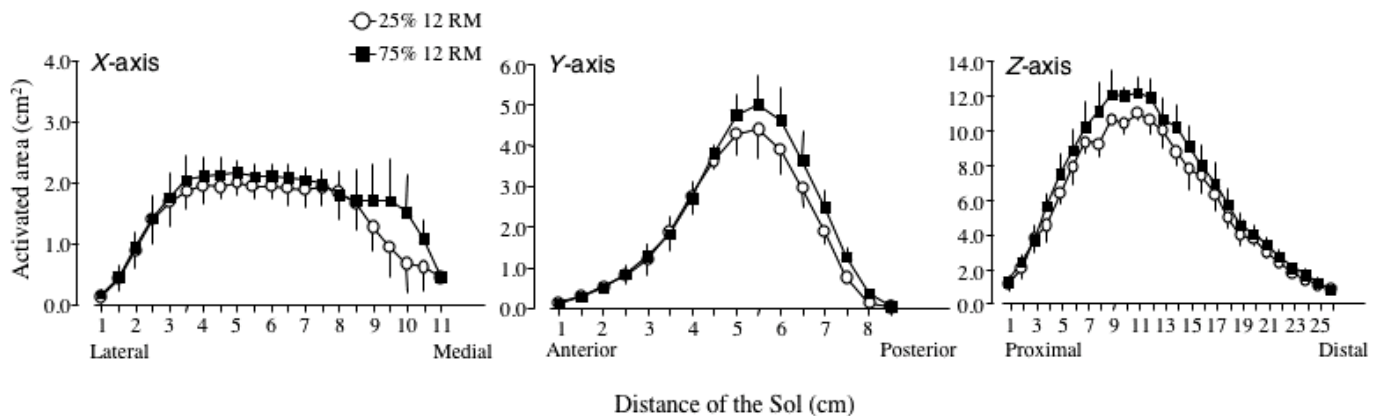


Figure 5-3. Series of activated areas of the soleus (Sol) along the transverse (*X*, *A*), longitudinal (*Y*, *B*), and vertical (*Z*, *C*)-axes at 25% 12 repetition maximum (RM) (open symbols) and 75% 12 RM (solid symbols). All conventions are the same as in Figure 5-2.

Shown in Figure 5-4 and 5-5 are spatial distributions of the *delta* activated areas, which depict the differences in the absolute magnitudes of the activated areas at loads of 25% 12 RM and 75% 12 RM in the MG. The two regions of the MG that showed the largest *delta* activated areas were the lateral-central and medial-distal portions of the *X-Z* plane (Figure 5-4, *A*). Comparison of the *delta* activated areas showed them to be smaller in the *Y-Z* plane (Figure 5-4, *B*) than in the *X-Z* plane, excluding the medial/distal portions; there it appeared that the *delta*-activated areas had a negative value in both planes, suggesting the activated area was larger at 25% 12 RM than at 75% 12 RM. The Sol clearly showed a smaller *delta* activated area than the MG along the entire length of the muscle in both planes (Figure 5-5, *A*, *B*).

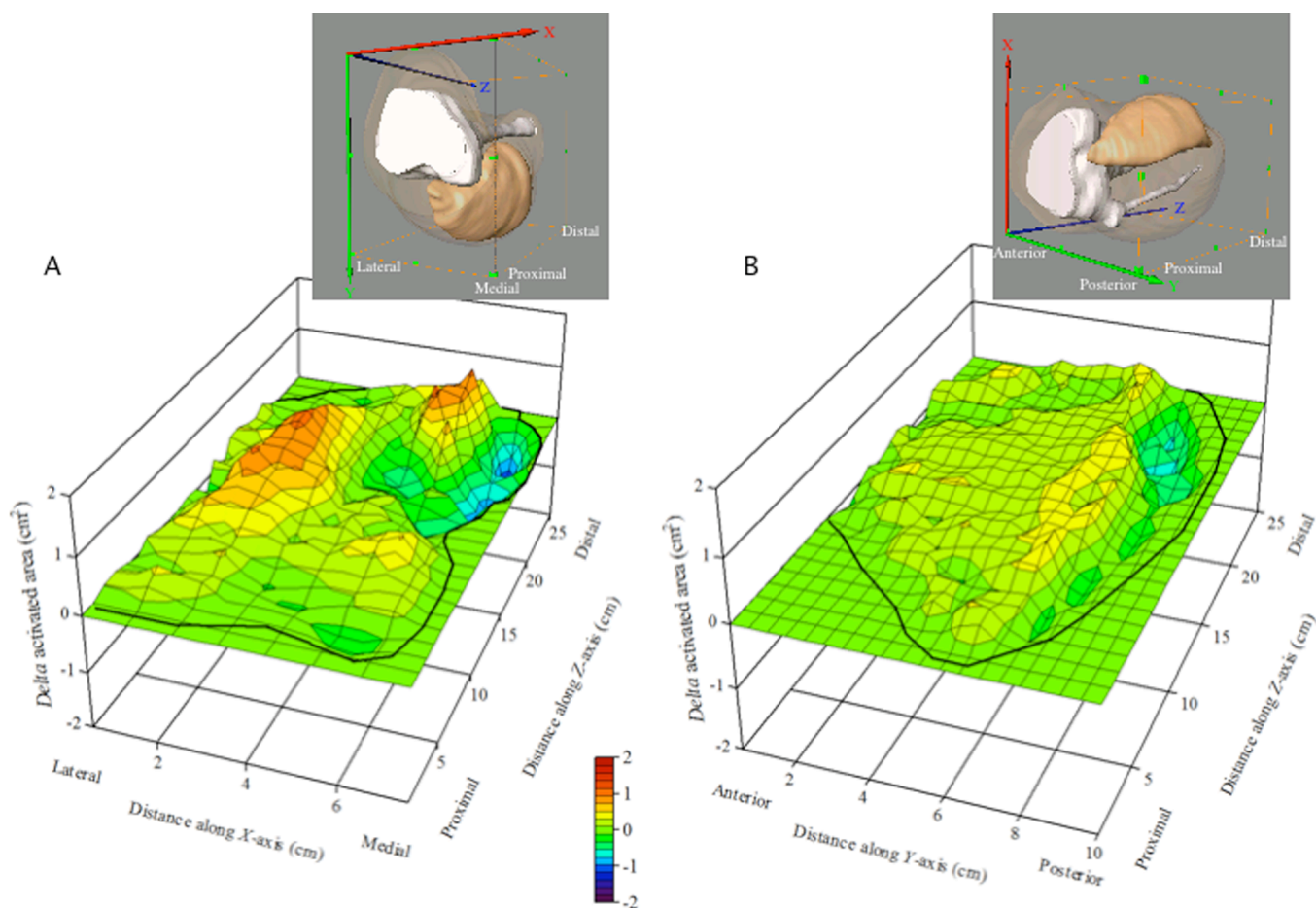


Figure 5-4. Spatial distribution of the *delta* activated areas within the medial gastrocnemius (MG). The average values of the *delta* activated areas of the MG, which are the differences in the absolute magnitudes of the activated areas at loads of 25% 12 repetition maximum (RM) and 75% 12 RM, are shown by the heights of surfaces over the transverse (*X*)-vertical (*Z*) (A) and longitudinal (*Y*)-vertical (*Z*) planes (B). Positive values on the color scale mean that the activated area is larger at 75% 12 RM than at 25% 12 RM, while negative values mean that activated area is larger at 25% 12 RM than at 75% 12 RM. The color scale, from sky blue to red, represents the variations in the activated area from low to high. The black line indicates the contour of the MG. The right bottom images correspond to the respective surface plots and show the projected contour of the MG from a similar direction.

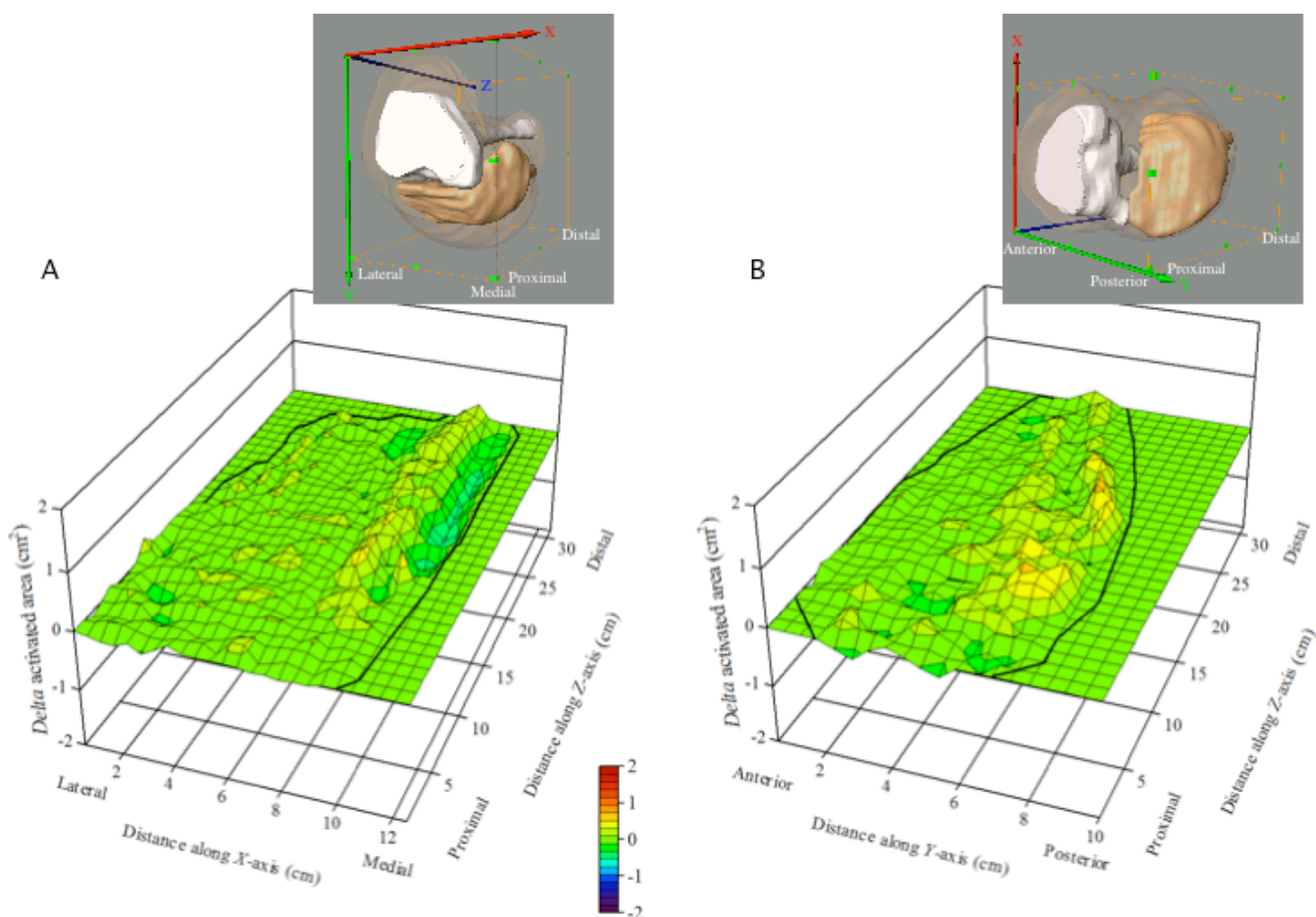


Figure 5-5. Spatial distribution of the *delta* activated areas within the soleus (Sol). Surface plots of the average values of the *delta* activated areas in the transverse (X)-vertical (Z) (A) and longitudinal (Y)-vertical (Z) planes (B) in the Sol. All conventions are the same as in Figure 5-4.

Finally, there were no significant differences in T2 between muscles at rest and under load (Table 5-3). After exercise, T2 and the % change in T2 were both significantly ($P < 0.05$) greater at 75% 12 RM than at 25% 12 RM in the MG, but not in the Sol. Although the two values were similar for the MG and Sol at 25% 12 RM ($P > 0.05$), after exercise the MG showed a significantly greater T2 and % change in T2 than Sol at 75% 12 RM ($P < 0.05$, respectively). As was seen with the activated area, there was a significant muscle \times load interaction affecting post-exercise T2 and the % change in T2 ($P < 0.05$).

Table 5-3. Pre- and Post-exercise T2, and % change in T2 in the MG and Sol at 25% and 75% 12 RM loads.

	MG		Sol	
	25% 12 RM	75% 12 RM	25% 12 RM	75% 12 RM
Pre-exercise T2, ms	31.5 ± 0.1	31.5 ± 0.1	32.3 ± 0.2	31.9 ± 0.4
Post-exercise T2, ms	35.9 ± 0.6	41.0 ± 0.3*#	37.7 ± 0.6	38.7 ± 0.4
% change in T2, %	14.0 ± 1.5	30.2 ± 1.1*#	16.7 ± 1.8	21.5 ± 1.3

Values are means ± SE.

* $P < 0.05$ for 25% 12 RM vs. 75% 12 RM. # $P < 0.05$ for MG vs. Sol.

T2, transverse relaxation time; RM, repetition maximum;

MG, medial gastrocnemius; Sol, soleus;

Discussion

The main findings of the present study are that whereas iEMGs increased in both the MG and Sol in response to increasing loads, increasing the load caused a significant increase in the % activated volume in the MG, but no such increase was seen in the Sol. A similar increase in EMG was observed in these two muscles during plantar flexion (Akasaka *et al.* 1997; Gravel *et al.* 1987; Hof & van den Berg 1977; Kinugasa & Akima 2005; Moritani *et al.* 1991). It thus appears that although the increase in force generated in response to an increase in exercise load was obtained through activation of both the MG and Sol, the species of activated fibers may differed in the two muscles. Consistent with that idea, the EMG power spectrum for the Sol was reduced (Bilodeau *et al.* 1994) or unchanged (Akasaka *et al.* 1997) with increasing load, while that of the MG was increased significantly. This suggests that in the Sol the increase in EMG seen in the present study was mostly due to the activation of slow-twitch fibers, which was different from the MG, because of the EMG power spectrum reflects activation of fast-twitch fibers (Gerdle *et al.* 1991; Moritani & Muro 1987). In fact, in the MG >30% of the maximal force could be generated by additional

recruitment of only type FF MUs, which are composed of fast-twitch fibers (Garnett *et al.* 1979).

It is noteworthy that the methods currently used to map activation of muscle do not reflect neural activity, per se, but instead reflect water shifts and vascular phenomena. Exercise-induced increases in T2 are caused by uptake of fluid into an intracellular space, which is osmotically driven by the accumulation of metabolic osmolites such as Pi [from net phosphocreatine (PCr) hydrolysis] and lactate. Earlier studies (Dudley & Terjung 1985; Meyer *et al.* 1986) have shown that when the MG and Sol are stimulated at the same rate, net PCr hydrolysis and lactate accumulation are much higher in the MG than in the Sol. In fact, the increase in T2 observed in rat muscles during stimulation was greatest in white gastrocnemius and then progressively smaller in mixed gastrocnemius, red gastrocnemius and Sol (Prior *et al.* 2001). A similar effect on human muscle T2 also has been observed in the triceps surae muscles (Kinugasa & Adams 2005; Price *et al.* 1995, 2003). Given that increases in T2 depend on the fiber type and thus changes in the T2 in Sol were too small to be detected in the present study, I suggest that most of the MRI data in the present study collected reflect activation of fast-twitch fibers. Taken together with the present EMG findings, this suggests that at the two workloads used, activation of the MG progressively changed from slow to fast-twitch fibers as the force level was increased, whereas in the Sol it was always slow-twitch fibers that were activated.

This paper introduces a novel method for *in vivo* determination of the spatial distribution of activated fibers within skeletal muscle based on exercise-induced changes in T2. This method enabled us to characterize the difference in the distributions of activated fibers in the MG and Sol. That difference could be due in

part to a difference in the dispersion of the fibers. Although the distribution of fibers within a given MU territory is relatively uniform (Armstrong *et al.* 1988; Burke & Tsairis 1973; Tötösy de Zepetnek *et al.* 1992), the fibers in small MUs, which are composed of slow-twitch fibers, tend to be more scattered relative to one another than the fibers in larger MUs, which are composed of fast-twitch fibers (Rafuse & Gordon 1996). Another possibility is that there is a difference in the distribution of MU territories throughout the muscles. The area encompassed by the MU territory is reflected by the ratio of the unit fiber number to unit fiber density (Fuglevand *et al.* 1997). The density of MU fibers ranges from ~10 unit fibres/mm² of muscle for small MUs to ~40 unit fibres/mm² of muscle for large units (Armstrong *et al.* 1988; Kanda & Hashizume 1992). The sequence in which MUs are recruited also may affect the distribution of activated fibers. MUs are normally recruited in an orderly sequence, proceeding from small MUs to larger ones (Henneman *et al.* 1965; Milner-Brown *et al.* 1973; Zajac & Faden 1985). Thus the respective distributions of activated fibers in the MG and Sol likely reflect the fiber dispersion, the distribution of MU territories, and the recruitment order.

The *delta* activated area is used to evaluate changes in the area of activation that occur with increases in force output. I observed two obvious clusters of activation within the MG: the lateral-central and medial-distal regions (Figure 5-4). One interpretation of these findings is that different neuromuscular compartments can be activated independently of one another — i.e., a single muscle can consist of several distinct regions that serve different physiological functions. Such compartmentalization has been observed in the rat MG (Burke & Tsairis 1973; DeRuiter *et al.* 1996). On the other hand, a report based on human cadaver specimens

concluded that the MG is architecturally homogeneous and thus has no neuromuscular compartmentalization (Wolf & Kim 1997). However, the results of that study might not be directly applicable to living humans. The morphological characteristics of muscles in embalmed cadavers change due to factors such as postmortem shrinkage (Friederich & Brand 1990), which makes it difficult to acquire precise information about muscle architecture. Indeed, ultrasonography, which has proved sufficiently accurate and reproducible to measure the architectural parameters (e.g., fascicle length and pennation angle) of human muscles *in vivo*, revealed that the pennation angle of the fibers within the MG varied among site (Kawakami *et al.* 2000). An architectural basis for the differences in MG regional activity is consistent with the idea that the human MG possesses neuromuscular compartments, as has been shown for the tibialis anterior (Wolf & Kim 1997). Further study will be necessary to clarify the degree to which the MG is structurally and functionally compartmentalized *in vivo*.

It also is not clear why the MG shows activation mainly in two regions (the central and distal portions) when force output is increased, but I suggest two possibilities. First, greater activation in the central portion may be related to the anatomical characteristics of the MG. The MG crosses the knee joint in a way that enables it to be able to apply torque to the knee joint, which is essential for stabilizing the knee joint in an extended position (Lan & Crago 1992). In general, the mid-belly of a muscle can generate substantially more force than other regions (Akima *et al.* 1995) because the force exerted by muscles is closely correlated with their size (Ikai & Fukunaga 1968). Therefore, greater activation in the central portion would enable contribute to the stability of the knee joint and production of large amounts of force, respectively. Second, greater activation in the distal portion is effective for force

transmission to the tendon. In a pinnate muscle such as the MG the net force of the muscle fibers that act in the direction of the line of pull varies with the cosine of the angle of pennation. Consequently, a smaller fiber pennation angle is advantageous for transmission of force from the muscle fiber to the tendon, and the distal portion of the human MG has the smallest fiber pennation angle (Kawakami *et al.* 2000). Thus the functional roles the two obvious clusters of the activation observed in the MG most likely differ.

I found that the % activated volume of the Sol did not change with increasing force, which is consistent with the findings of Price *et al.* (1995, 2003), who showed that in the Sol, T2 of did not significantly increase from baseline during nonweight-bearing plantar flexion. On the other hand, the present results contradict those of my earlier study (Kinugasa & Akima 2005) in which I reported that T2 increased linearly in the Sol as exercise load was increased during weight-bearing plantar flexion. This discrepancy could reflect the differing conditions in the lower limbs during the period the measurements were made (e.g., whether or not the muscles were bearing weight). The excitability of the motoenurons in the Sol is enhanced by the weight-bearing (Yamashita & Moritani 1989). Thus body posture — i.e., whether subjects were sitting or lying prone — would be expected influence the activation of the Sol.

In summary, the findings demonstrate that iEMGs increase linearly in both the MG and Sol as exercise load is increased. But whereas increasing the load caused a significant increase in the % activated volume in the MG, no such increase was seen in the Sol. This suggests that although muscle activation increased for both the MG and Sol with the present protocol, the differences in species (slow or fast) of activated fibers

and their spatial distribution between the two muscles would be characterized by the exercise intensity.

CHAPTER 6

Mapping activation levels of skeletal muscle in healthy volunteers: an MRI study

Introduction

The ability to comprehensively assess skeletal muscle function *in vivo* would be of significant scientific and clinical benefit. The force generated by a muscle is graded depending upon the activation of individual motor units (MUs), which are the elements that make up the neuromuscular system. Muscle force is thus determined by which MUs are activated and their level of activation. In the years since its introduction in 1988, muscle functional magnetic resonance imaging (mfMRI) has been well received as a noninvasive modality for studying muscle function. mfMRI is primarily based on the contrast derived from the proton transverse (spin-spin) relaxation time (T2) (Fung & Puon 1981; Meyer *et al.* 2001). Because T2 is sensitive to several metabolic and hemodynamic processes that accompany muscle activation, investigators have been able to use mfMRI to i) identify regional variations in activation during muscle contraction (Adams *et al.* 1993; Kinugasa *et al.* 2005a, 2006; Wadfield *et al.* 2000), ii) differences in the patterns of muscle activation in novice and elite rowers (Green *et al.* 2000), and iii) differences in the pattern of activation during uphill and horizontal running (Sloniger *et al.* 1997). But although mfMRI is able to provide important quantitative information about muscle activation (i.e., amount of activated area), it does not provide direct qualitative information about activation level of a muscle. It is anticipated that determination of the activation level can enhance utility

of mfMRI. Evidence suggests that the magnitudes of the exercise-induced changes in T2 are directly related to the force level (Adams *et al.* 1993; Fisher *et al.* 1990), as well as to the EMG activity (Adams *et al.* 1992; Kinugasa & Akima 2005) and intensity of exercise (Adams *et al.* 1992, 1993; Akima *et al.* 2005; Conley *et al.* 1995, 1997; Ploutz *et al.* 1994; Ploutz-Snyder *et al.* 1995). However, no attempt has yet been made to use mfMRI to examine this point.

MUs are classified into three main types: S (slow-twitch), FR and FF (fast-twitch). Type S MUs produce the least force, while type FF MUs produced the most (Bodine *et al.* 1987; Garnett *et al.* 1979). This makes it conceivable that T2 is indirectly related to activation of exercising muscle fibers. Bearing that in mind, I have endeavored to refine my technique, which now enables us to classify muscle activation to several levels. The purpose of the present study was to use the mfMRI technique to assess the activation levels within and among triceps surae (TS) muscles during exercise. TS muscles are the principal ankle joint plantar flexors and represent an interesting experimental model because they are composed of three muscles – the soleus (Sol), medial gastrocnemius (MG) and lateral gastrocnemius (LG) – having different fiber and MU compositions. I therefore hypothesized that the 1) mfMRI can be used to determinate the volumes of activated regions showing a different level of activation and 2) activation level would vary within and among the TS muscles.

Methods

Subjects

Seven healthy males [age, 24 ± 2 yrs; height, 1.70 ± 0.07 m; weight, 63 ± 4 kg (means \pm SD)] volunteered to participate in the present study. None of the subjects

had any known neurological disorder or cardiovascular disease, and all were naive to the experimental procedures. The subjects all were physically fit but had not engaged in specific resistance exercise of the plantar flexor muscles before the experiment. The dominant leg (i.e., the preferred leg used to kick a ball) was used for the experiment. This study was approved by the Human Subjects Committee at Musashino University, and all subjects gave informed consent before participating in the study.

Exercise Protocol

Subjects performed a unilateral heel-raise exercise while in a standing position. For each heel-rise, the subject transferred his full body weight to his toes over a period of 2 s, while the contralateral limb was not in contact with the ground. Once on his toes, the subject lowered his heel back to the ground so that the ankle resumed its initial position over a period of 2 s. The exercise consisted of five sets of 10 repetitions. There were no rest periods between the raising and lowering of the body or between repetitions, but each set was separated by a 1-min rest period. The knee remained fully extended (180°) throughout the exercise, and the subjects' fingertips were allowed to touch an adjacent wall to provide balance but not support.

Muscle Functional MRI

Imaging was performed using a 0.3-Tesla MRI scanner (AIRIS, Hitachi Medical, Japan). Subjects were positioned supine within the magnet: an extremity coil was positioned at the calf, and with the knee joint was at 180° . The tested calf was stabilized with a bitemporal clamp. The length of the calf was measured, after which the one-fourth and three-fourths distances from the origin of the patella to the lateral

Chapter 6 Mapping activation level

malleolus were marked on the subject's skin with a pen. As for this point, it is imaged the same location by synchronizing it with a laser as a reference line in scan setting. The ink marks therefore enabled similar positioning of the calf over repeated scans. Subjects were imaged before and immediately after the exercise on a given day. Twenty-two 10-mm-thick transaxial slices were collected with a 0-mm gap between slices using a T2-weighted spin echo sequence (TR 2500 ms; TE 25 and 80 ms). The field of view was 27 cm, and the data were collected with a 256×256 matrix. The total collection time was 5 min 30 s.

The exercise was performed outside the magnetic bore, after which the subjects moved quickly into the magnet. The time interval between completion of the exercise and initiation of imaging was ~60 s. Because of the limited range of the imaging area, scans were carried out at two separate sessions. Images were acquired either from the head of the patella to the center of distance between the head of the patella and lateral malleolus, or from that point to the lateral malleolus. The interval between the first and second MR collections was ≥ 7 days, which was the time deemed necessary to ensure that T2 recovered to the resting level. The order of the two sessions was randomly assigned.

All MR images were transferred to a personal computer, where they analyzed using the public domain National Institutes of Health (NIH) Image software package. T2 images were computed on a pixel-by-pixel basis from two magnitude images with the assumption of a single-exponential decay. Regions of interest (ROIs) were established for the MG, LG and Sol muscles by tracing around the image of the muscle group. Care was taken to exclude intramuscular fat, aponeurosis and vascular structures from the traced regions. The pre-exercise and post-exercise T2 images were

Chapter 6 Mapping activation level

analyzed, and the mean and SD of the T2 for the ROI was determined for each slice. In other words, T2 is the mean T2 over ROI, not a voxel to voxel T2 change in the present study. Pixel showing T2 values greater than the mean + 1SD of the ROI in the pre-exercise image and lower than the mean + 1SD in the post-exercise image were identify. The lower limit was set to exclude inactive muscle and nonmuscle tissue (e.g., aponeurosis and vessels), which exhibit a constitutively “low” T2; the upper limit was set to exclude intramuscular fat, which exhibits a constitutively “high” T2. T2 values within the range defined by the two thresholds were considered to be the active muscle area, and were previously shown to correlates significantly with both EMG activity and workload (Kinugasa *et al.* 2005a). In addition, T2 values falling within the accepted range in the post-exercise images were divided into five categories. Because the exercise-induced shift in T2 is related to the force level (Adams *et al.* 1993; Fisher *et al.* 1990), these categorization was considered to be indices of the activation level of the exercised muscle fibers and are indicated by color, from red (highest activation level) to yellow, green, sky blue, and blue (lowest activation level) (Figure 6-1).

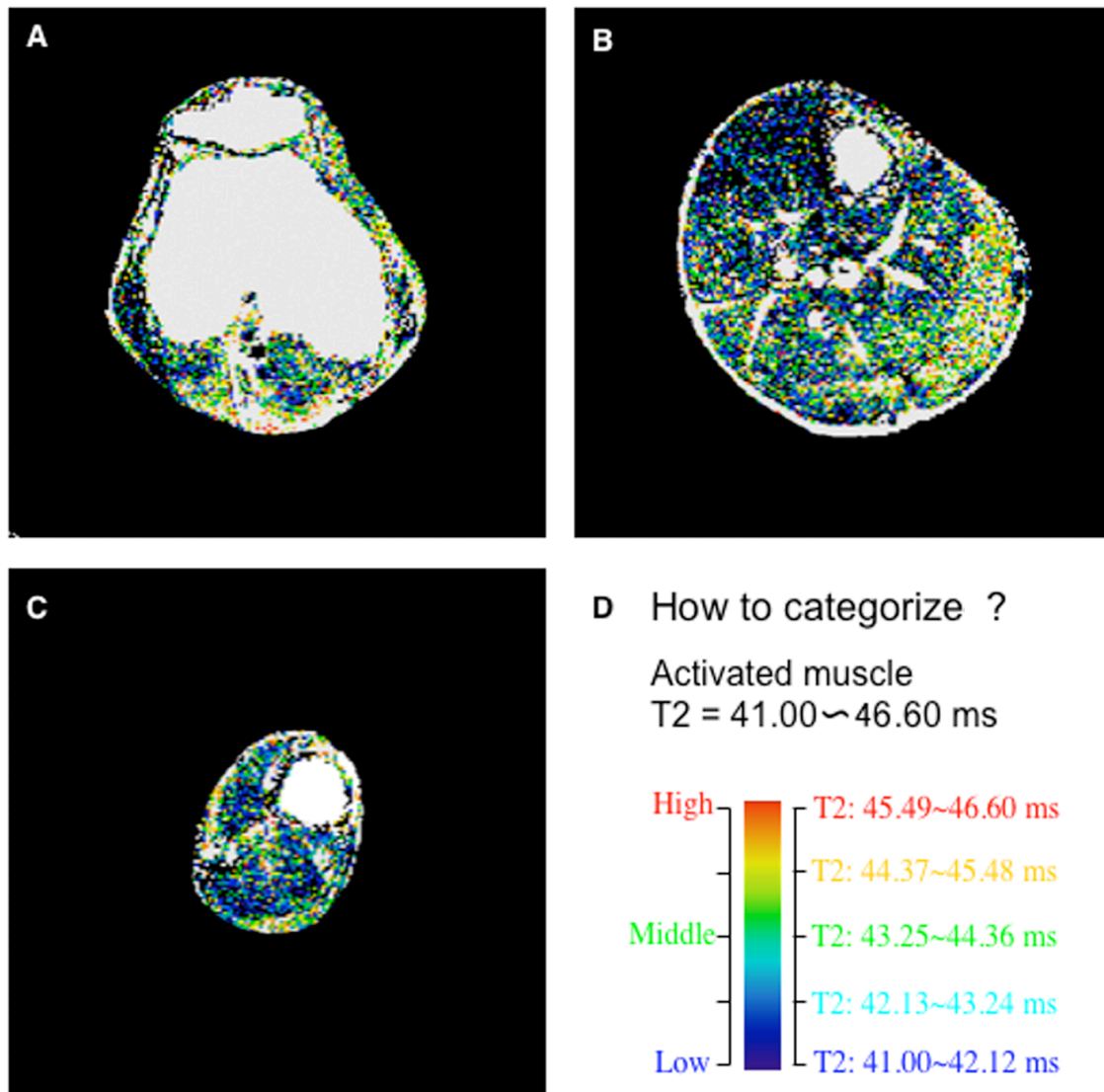


Figure 6-1. Representative magnetic resonance images, which are categorized into five colors based on their transverse relaxation time, from the extreme proximal end (A), the central region (B) and extreme distal end (C) of the triceps surae muscles from one subject. Each color are represented the levels of muscle activation (D). The red is the highest level of activation and then progressively lower in yellow, green, sky blue, and blue (lowest level of activation).

To construct three-dimensional (3-D) MR images of the muscles, the first step was to define the contours of the individual muscles in each slice by manually tracing them. The active muscle areas were then defined based on the aforementioned threshold method using visualization, data analysis and a geometry reconstruction

software package (Amira 3.1, Mercury Computer Systems, San Diego, CA, USA). Total muscle volume and the activated volume at each color map were then determined from the 3-D images, after which the activated volume was expressed relative to the total anatomical volume (% activated volume).

Statistics

All data are presented as means \pm SE. Two-way analysis of variance (ANOVA) was used to analyze differences in the % activated volume among the muscles and levels. One-way ANOVA was used to analyze differences in % changes in T2 [(post-exercise T2 – pre-exercise T2) / pre-exercise T2 \times 100] among the muscles. When significant effects were found, post hoc Tukey-Kramer tests were performed to determine the location of the effect. Values of $P < 0.05$ were considered significant.

Results

Figure 6-2 shows a 3-D image in which the distribution of muscle activation levels is illustrated using a five-color map. The MG had a great areas of painted five-colors than that of other two muscles. Each activation level was nonuniformly distributed along the length of the TS muscles.

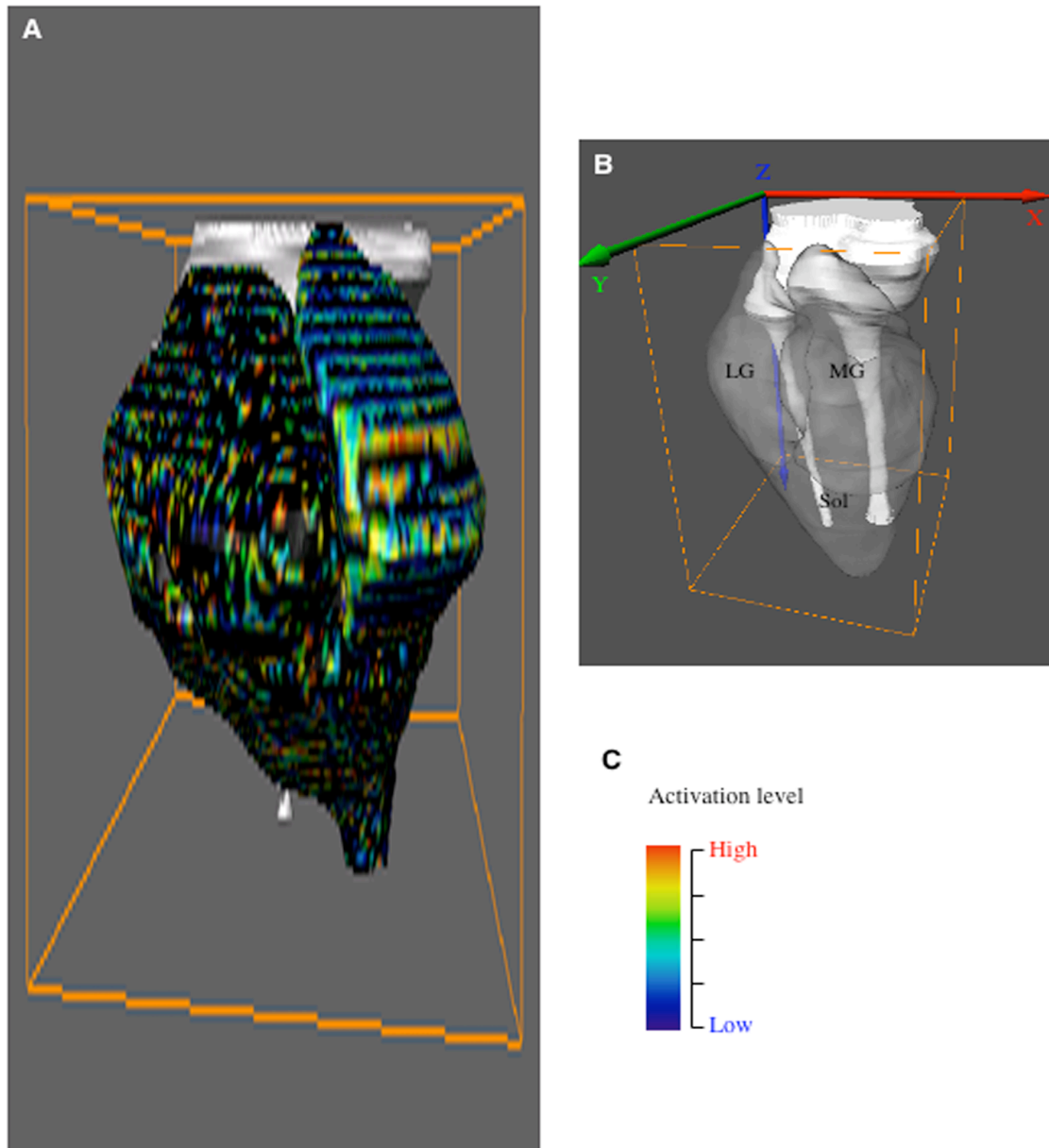


Figure 6-2. Representative three-dimensional activation level mapping (A) from one subject and the anatomical structures (B) of the triceps surae muscles. Activated parts are indicated by colors, which are related to the level of activation in panel C. Regions shown in black represent non-activated parts; the objects shown white are bones (tibia and fibula). The red, green, and blue lines indicate the transverse (*X*), longitudinal (*Y*), and vertical (*Z*)-axes, respectively. MG, medial gastrocnemius; LG, lateral gastrocnemius; Sol, soleus.

There were no significant differences in the pre- and post-exercise T2 values among the TS muscles (Table 6-1). The % change in T2 was greatest in the MG ($13.3 \pm 1.3\%$), followed by the LG ($7.8 \pm 1.2\%$) and Sol ($6.3 \pm 2.1\%$). MG had a greater %

Chapter 6 Mapping activation level

change in T2 than the Sol ($P < 0.05$), but none of the other differences were significant. The magnitudes of the changes were comparable to those obtained previously (Kinugasa & Akima 2005, Kinugasa *et al.* 2005a). Standard deviation of the post-exercise T2 values was greater in each TS muscle than those of the pre-exercise T2 values (Table 6-2). There was no significant difference in the T2 histogram at the pre-exercise T2 images between first and second measurements (Figure 6-3).

Table 6-1. Pre- and post-exercise T2 values, and % change in T2.

	MG	LG	Sol
Pre-exercise T2, ms	31.7 ± 0.3	31.6 ± 0.3	32.5 ± 0.1
Post-exercise T2, ms	39.2 ± 0.9	37.3 ± 1.0	38.8 ± 0.6
% change in T2, %	13.3 ± 1.3*	7.8 ± 1.2	6.3 ± 2.1

Values are means ± SE.

* $P < 0.05$ for MG vs. Sol.

T2, transverse relaxation time; MG, medial gastrocnemius;

LG, lateral gastrocnemius; Sol, soleus.

Table 6-2. Standard deviation of the pre- and post-exercise T2 values

	MG		LG		Sol	
	Pre-	Post-	Pre-	Post-	Pre-	Post-
Standard deviation, ms	0.7	2.5	0.9	2.6	0.3	1.6

T2, transverse relaxation time; MG, medial gastrocnemius;

LG, lateral gastrocnemius; Sol, soleus.

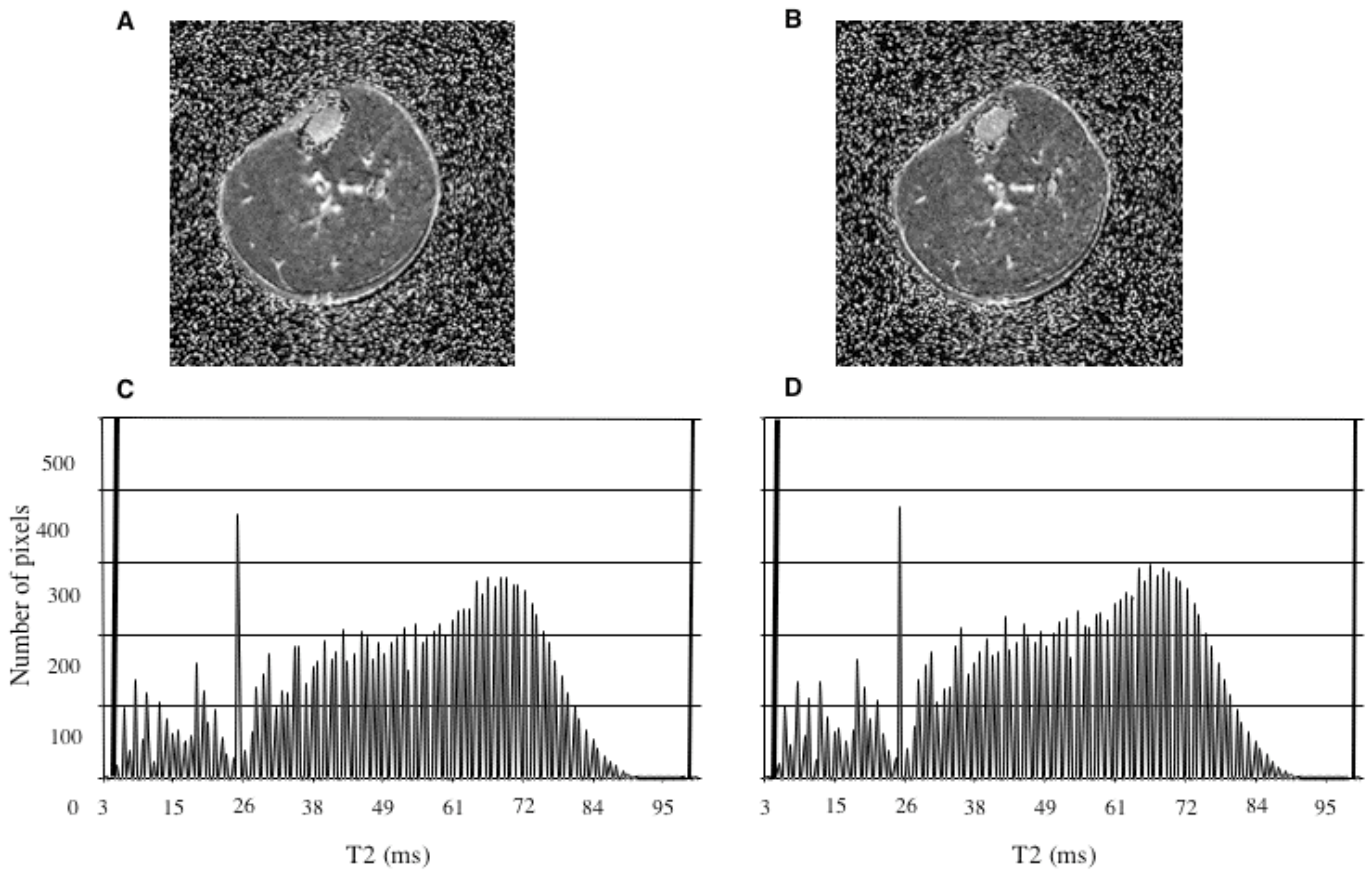


Figure 6-3. Representative pre-exercise transverse relaxation time (T2) images and their T2 histogram at first (A, C) and second (B, D) measurements, respectively. Pre-exercise T2 values histogram for each pixel in T2 images plotted against number of pixels. Region of interest was set for whole image. A and B correspond to C and D, respectively.

Range of T2 threshold in each category is shown in Table 6-3. Minimum and maximum values of T2 threshold in each category were larger in each TS muscles from blue to sky blue, green, yellow, and red, respectively ($P < 0.05$).

Chapter 6 Mapping activation level

Table 6-3. Range of T2 threshold (min and max value) in each category.

	MG		LG		Sol	
	max	min	max	min	max	min
T2, ms						
Red	53.7 ± 1.2 ^a	50.3 ± 0.9 ^a	53.1 ± 1.4 ^a	49.8 ± 1.2 ^a	56.5 ± 0.8 ^a	52.6 ± 0.6 ^a
Yellow	49.9 ± 0.9	46.9 ± 0.8	49.4 ± 1.2	46.5 ± 0.9	52.3 ± 0.6	48.8 ± 0.6
Green	46.5 ± 0.8	43.4 ± 0.5	46.1 ± 0.9	43.2 ± 0.7	48.4 ± 0.4	45.0 ± 0.3
Sky blue	43.1 ± 0.6	40.0 ± 0.3	42.9 ± 0.6	40.0 ± 0.5	44.6 ± 0.4	41.2 ± 0.1
Blue	39.6 ± 0.3	36.6 ± 0.3	39.6 ± 0.5	36.7 ± 0.3	40.8 ± 0.2	37.4 ± 0.2

Values are means ± SE.

^a $P < 0.05$ for Red > Yellow > Green > Sky blue > Blue.

T2, transverse relaxation time; MG, medial gastrocnemius; LG, lateral gastrocnemius; Sol, soleus.

At the exercise load used in the present study, the largest % activated volume showed a low level of activation (sky blue and blue regions) (Figure 6-4). In each muscle, the % activated volumes showing moderate (green region) and low levels of activation were larger than those showing a high level of activation (red and yellow regions) ($P < 0.05$). Still, the MG had a larger % activated volume showing a high level of activation ($4.9 \pm 0.6\%$ for the red region and $7.1 \pm 0.9\%$ for the yellow region) than the Sol ($3.6 \pm 0.4\%$ for red region and $5.2 \pm 0.6\%$ for yellow region) ($P < 0.05$, respectively). The % activated volume showing a low level of activation tended to be larger in the MG than the LG, though the difference did not reach statistical significance ($P = 0.07$). On the other hand, the Sol had a significantly larger % activated volume showing a low level of activation ($12.3 \pm 1.0\%$ for the sky blue region and $15.5 \pm 0.7\%$ for the blue region) than the LG ($11.9 \pm 1.2\%$ for the sky blue region and $13.4 \pm 0.9\%$ for the blue region) ($P < 0.05$, respectively).

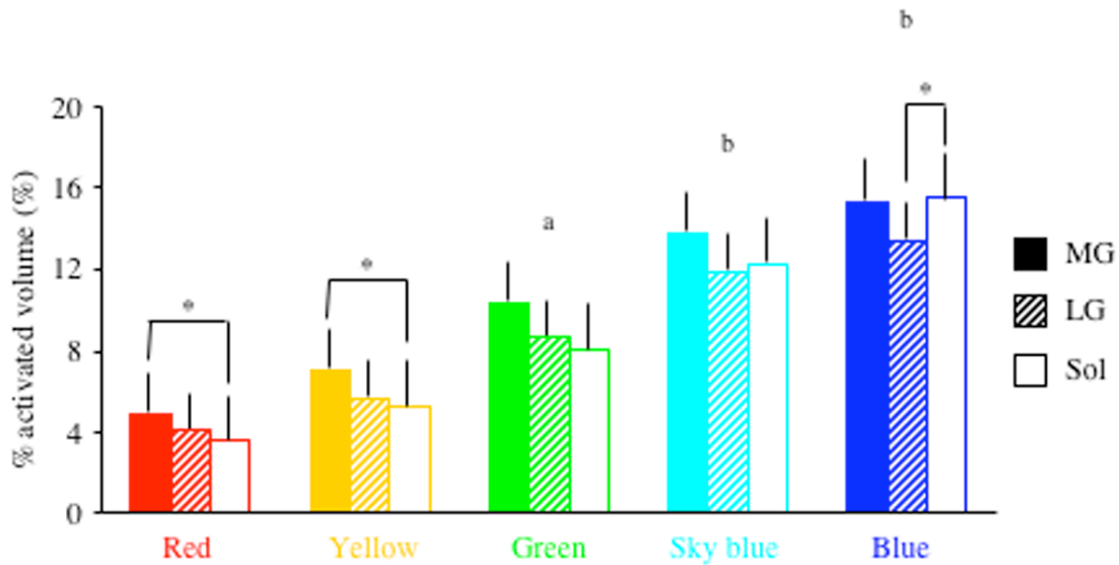


Figure 6-4. The % activated volumes, which are categorized into five colors based on their transverse relaxation time, of the medial gastrocnemius (MG), lateral gastrocnemius (LG) and soleus (Sol). Bars represent means \pm SE for all subjects. * $P < 0.05$; ^a $P < 0.05$ vs. the red and yellow regions; ^b $P < 0.05$ vs. the red, yellow and green regions.

Discussion

I hypothesized that the 1) mfMRI can be used to determinate the volumes of activated regions showing a different level of activation and 2) activation level would vary within and among the TS muscles. The force generated by a muscle is depending upon the activation of individual MUs. In general, MUs are classified into three types basis of their physiological properties. Type S (slow-twitch) MUs produce least force with low activation level and the type FF (fast-twitch) the greatest (Garnett *et al.* 1979). This idea consistent with the findings of earlier study (Prior *et al.* 2001) that increase in T2 observed in rat muscles was greatest in white gastrocnemius (mainly composed of type FF MUs) and then progressively smaller in mixed gastrocnemius, red gastrocnemius and Sol (mainly composed of type S MUs) because the exercise-induced change in T2 directly related to the force level (Adams *et al.* 1993; Fisher *et al.* 1990).

Chapter 6 Mapping activation level

It is known that mfMRI valid for use in determining active regions within a muscle (Kinugasa *et al.* 2006), which are defined by T2 threshold method. These findings suggest that if the difference in the T2 including range of threshold among the various levels, mfMRI can be used to determine the activation level of a muscle. In the present study, despite of there was a highly reproducibility of the pre-exercise T2 values (Figure 6-3 and see Kinugasa *et al.* 2006), the variability of the post-exercise T2 values has to be greater in each TS muscles (Table 6-2). If the whole muscle group were activated in the same manner, it would be expected that variability be maintained at the same degree at after the exercise. Moreover, there were significant differences in the range of T2 threshold among category (Table 6-3). This means that each category has different T2 values. Thus, mfMRI is a feasible means to determine *in vivo* activation level of skeletal muscle.

I found that the % activated volume showing a high level of activation (red and yellow regions) was larger in the MG than in the Sol, which likely reflects the fact that the MG contains a higher percentage of fast-twitch fibers than the Sol (Edgerton *et al.* 1975; Johnson *et al.* 1973). Because muscle activation reaches higher levels in fast-twitch MUs (Garnett *et al.* 1979), the MG would be expected to show a larger amount of high-level activation than the Sol. Conversely, the Sol contained a larger % activated volume showing a low level of activation than the LG. Again, this likely reflects the muscles' composition, as slow-twitch fibers and MUs are more predominant in the Sol than the LG (Edgerton *et al.* 1975; Johnson *et al.* 1973). It has been reported that the MG and LG has 50–70% fast-twitch fiber, whereas the Sol muscle has 80–100% slow-twitch fiber in humans. Thus, the activation level within the exercised muscle appears to be influenced mainly by the fiber types from which the muscles are

composed.

I had expected the unilateral heel-raise exercise to present the TS with high workloads, but that does not appear to have been the case. In a similar exercise model used in an earlier study (Kinugasa *et al.* 2005a), normalized EMG activity ranged between 49% and 88% of the values obtained during maximal voluntary contraction of the individual TS muscles. Nonetheless, here I found that, for each muscle, the % activated volume showing a low or moderate level of activation was larger than showing a high level of activation. Apparently, the present exercise is primarily associated with the low and moderate levels of TS muscle activation.

I also found that the five colors map varied within each muscle at the exercise load used (Fig. 1), indicating the activation level is not constant throughout the muscle. This variation likely reflects the placement of the muscle fibers and the innervation territories of the motor neurons. Within a muscle, the fibers are arranged into 3-D structures (Kawakami *et al.* 2000; Lemos *et al.* 2000), such that the distribution of each class of muscle fiber is heterogeneous (Chanaud *et al.* 1991). Because each alpha motor neuron innervates muscle fibers of only a single histological type, their innervation territories are distributed nonuniformly. In that regard, human TS muscles represent an interesting experimental model because they are composed of the Sol and gastrocnemius muscles, which differ in their fiber and MU compositions (Edgerton *et al.* 1975; Johnson *et al.* 1973). However, this is purely speculative at the moment, and I cannot entirely rule out the possibility that the territory of a single MU is spread over several voxels, so that different fibers and/or MUs could comprise the tissue volume represented by a single voxel.

Finally, it should be noted that some current limitations of mfMRI warrant

Chapter 6 Mapping activation level

mentioning. In the present study, the activation level is classified into five different groups. Certain disadvantages arise due to that categorized activation level depends on the size of T2 threshold. For example, difference of the range of T2 threshold would be influence the mean \pm SD of the T2 values in each group. This suggests that the red region within one muscle group has different activation from the red region within another muscle group. Mathematically, also, the thresholded images actually could be resolved to five different levels. However, five levels were selected from relatively small changes in T2 in the present study. There may definitely be a lot of overlapping regions. Future studies may focus on the categorization of various levels across the muscle groups and existence of overlapping.

In summary, the activation level was mainly in the moderate to low range in each TS muscle at the present protocol. The highest activation level was greater in the MG than in the Sol. On the other hand, Sol had the lowest activation level compared with other TS muscles. mfMRI can be used to determine *in vivo* activation level of skeletal muscle.

CHAPTER 7

Conclusion

The goal of this dissertation was to explore the activation properties of synergistic triceps surae (TS) muscles at a single workload and when workload was increasing. To achieve this goal, I developed a three-dimensional (3-D) muscle functional magnetic resonance imaging (mfMRI) method that enabled the development and analysis of reconstructions of the TS muscles such that the distributions of activation within the muscles could be mapped.

Using this approach, I was able to show that at a given load the medial gastrocnemius (MG) had greater % activated volume and a higher level of activation than the lateral gastrocnemius (LG) or soleus (Sol). Moreover, the activated regions of the MG were distributed heterogeneously over the entire length of the muscle. Thus, the size and location of the activated regions and the level of their activation varied among synergistic muscles, and those variations likely reflect their functional significance for force production.

The % activated volume was larger in the distal region of the MG than that in the proximal region, which may mean that the anatomical structure of the distal region is especially well suited to produce large amounts of force. In a pinnate muscle, the net force of the muscle fibers that act in the direction of the line of pull varies with the cosine of the angle of pennation, so that a smaller fiber pennation angle is advantageous for transmission of force from the muscle fiber to the tendon. And in the human MG

Chapter 7 Conclusion

the region close to ankle joint has the smallest fiber pennation angle (Kawakami *et al.* 2000). The distal region of muscle may thus generate more force and more work than other regions of the muscle do. Although speculative, this idea is generally supported by earlier findings that muscle injuries tend to occur near the acting joint (Shellock *et al.* 1991; Weishaupt *et al.* 2001).

When the required force level was increased the MG still showed nonuniform activation, and the distribution of activated regions within the muscle varied, depending upon the required force level. I used the *delta* activated area to evaluate differences in the absolute magnitudes of the activated areas of the MG at two loads. I observed two obvious clusters of *delta* activated areas, the lateral-central and medial-distal regions, which suggests that although the MG had the largest % activated volume and showed the highest level of activation, it was not necessary to activate all of the fibers throughout the muscle to achieve the required level force. Instead, muscle fibers were selectively activated at certain sites as the force required was increased.

I found that not only the sites of activation, but also the species of activated muscle fibers vary, depending upon the force level. Whereas increasing the load caused a significant increase in the % activated volume in the MG, no such increase was seen in the Sol. On the other hand, iEMGs increased in both the MG and Sol in response to increasing loads, which was consistent with the results of earlier studies (Akasaka *et al.* 1997; Gravel *et al.* 1987; Moritani *et al.* 1991), though a pronounced increase in the EMG power spectrum with increasing force is observed in the MG but not in the Sol (Akasaka *et al.* 1997; Bilodeau *et al.* 1994). A shift in the mean or median frequencies is indicative of progressive recruitment of MUs with type FT fibers (Bernardi *et al.* 1996, 1999). In addition, the sensitivity of mfMRI also was influenced

Chapter 7 Conclusion

by the proportion of FT fibers. In humans, FT fibers account for about 25% of muscle fibers in the Sol and 50% in the MG (Edgerton *et al.* 1975), which suggests that although the increase in force generated in response to an increase in workload was achieved by activation of both the MG and Sol, the species of activated fibers likely differed in the two muscles. In other words, the fibers newly activated shifted from ST fibers to FT fibers with increasing force level in the MG, but activation of ST fibers continued throughout the exercise protocol in the Sol.

In this dissertation, I confirmed that mfMRI is a useful tool for quantitatively assessing such activation properties as size of the activated muscle volume, the distribution of activated regions within muscles, and the level of that activation at various spatial resolutions. However, as this is the first completed 3-D mfMR image-based model of human muscle activation, several problems remain to be solved before it can be applied to other fields.

mfMRI do not reflect neural activity, *per se*, but reflect several of the metabolic and hemodynamic processes accompanying muscle activation. During intense exercise, the intracellular milieu shows increased tissue water content and acidity; as a result of one or both of these changes, the T2 of muscle water increases (Damon *et al.* 2002; Fung & Puon 1981; Meyer *et al.* 2001; Ploutz-Snyder *et al.* 1997; Prior *et al.* 2001). mfMRI technique was relied on those phenomenon. Because the subjects might differ in metabolic capacity, it would not be appropriate to conclude that the fractional activation of muscle cells was greater in one subject than the other. Similarly, it would difficult to conclude from mfMRI measurements that activation had decreased in a subject after an exercise-training program, because the training might

Chapter 7 Conclusion

also alter the metabolic profile and vascular dynamics in the muscle. The use of mfMRI, electrical stimulation, and biochemical analysis to compare the T2, electrical activity, and metabolic profile between muscles of different subject is less established. Future studies should focus on the relationship among T2, electrical activity, and metabolic capacity at various stimulation protocols, e.g., alternation of intensity, frequency, and duration.

Another problem was that the present mfMRI technique was not performed in real time during exercise; images were acquired within 7 min after the subjects finished their exercise. An exercise-induced shift in T2 is detectable after as few as two contractions (Yue *et al.* 1994) and then increases to a work-rate-dependent plateau within a few minutes (Jenner *et al.* 1994). Recovery after exercise takes 20 min or more (Fisher *et al.* 1990), which have enabled us to acquire functional images following exercise performed outside the scanner room. Echo-planar imaging (EPI) is a data acquisition strategy used in MR imaging permitting very rapid data acquisition, in about 40 to 100 ms. Future studies should use real time imaging such as EPI technique for determination of activation properties after a verification of its accuracy, reproducibility, and validity.

mfMRI techniques have proven to be extremely robust and sensitive methods for noninvasive detection and mapping of human muscle activation. Nevertheless, limitations in temporal and spatial resolution as well as interpretation remain because metabolic and hemodynamic changes accompanying muscle activation are relatively sluggish and variable, and therefore imprecise measures of neuronal activity. A hope among MR imagers would be to possess a technique that would allow direct mapping of muscle activity with spatial resolution on the order of a fascicle and temporal resolution

Chapter 7 Conclusion

on the order of an action potential or at least a post synaptic potential.

The emergence of a technique that is able to more directly map neuronal activity at the spatial and temporal resolution with which it takes place would certainly lead to another acceleration of insights into human muscle functional organization and clinical applications. Bodurka & Bandettini (2002) demonstrated by modulation of the temporal position and duration of the stimuli-evoked transient magnetic field changes as small as 2×10^{-10} T (200 pT) and lasting for 40 ms can be detected. New MRI approaches using direct imaging of neural firing may provide fruitful alternatives to traditional mfMRI.

CHAPTER 8

Bibliography

- Adams GR, Duvoisin MR, Dudley GA. Magnetic resonance imaging and electromyography as indexes of muscle function. *J Appl Physiol* 73: 1578-1583, 1992.
- Adams GR, Harris RT, Woodard D, Dudley GA. Mapping of electrical muscle stimulation using MRI. *J Appl Physiol* 74: 532-537, 1993.
- Akasaka K, Onishi H, Momose K, Ihashi K, Yagi R, Handa Y, Hoshimiya N. EMG power spectrum and integrated EMG of ankle plantarflexors during stepwise and ramp contractions. *Tohoku J Exp Med* 182: 207-216, 1997.
- Akima H, Foley JM, Prior BM, Dudley GA, Meyer RA. Vastus lateralis fatigue alters recruitment of musculus quadriceps femoris in humans. *J Appl Physiol* 92: 679-684, 2002.
- Akima H, Ito M, Yoshikawa H, Fukunaga T. Recruitment plasticity of neuromuscular compartments in exercised tibialis anterior using echo-planar magnetic resonance imaging in humans. *Neurosci Lett* 296: 133-136, 2000.
- Akima H, Kinugasa R, Kuno S. Recruitment of the thigh muscles during sprint cycling by muscle functional magnetic resonance imaging. *Int J Sports Med* 26: 245-252, 2005.
- Akima H, Kuno S, Suzuki Y, Gunji A, Fukunaga T. Effects of 20 days of bed rest on physiological cross-sectional area of human thigh and leg muscles evaluated by magnetic resonance imaging. *J Gravit Physiol* 4: S15-21, 1997.

Chapter 8 Bibliography

- Akima H, Kuno S, Takahashi H, Shimojo H, Katsuta S. Effect of the different levels of cross-sectional areas in four heads of quadriceps femoris and muscle fiber composition on isokinetic knee extension. *Japan J Phys Educ* 39: 426-436, 1995.
- Akima H, Takahashi H, Kuno S, Katsuta S. Coactivation pattern in human quadriceps during isokinetic knee-extension by muscle functional MRI. *Eur J Appl Physiol* 91: 7-14, 2004.
- Akima H, Takahashi H, Kuno S, Masuda K, Masuda T, Shimojo H, Anno I, Itai Y, Katsuta S. Early phase adaptations of muscle use and strength to isokinetic training. *Med Sci Sports Exerc* 31: 588-594, 1999.
- Akima H, Ushiyama JI, Kubo J, Tonosaki SI, Itoh M, Kawakami Y, Fukuoka H, Kanehisa H, Fukunaga T. Resistance training during unweighting maintains muscle size and function in human calf. *Med Sci Sports Exerc* 35: 655-662, 2003.
- Armstrong JB, Rose PK, Vanner S, Bakker GJ, Richmond FJR. Compartmentalization of motor units in the cat neck muscle, biventer cervicis. *J Neurophysiol* 60: 30-45, 1988.
- Bendahan D, Giannesini B, Cozzone PJ. Functional investigations of exercising muscle: a noninvasive magnetic resonance spectroscopy-magnetic resonance imaging approach. *Cell Mol Life Sci* 61: 1001-1015, 2004.
- Bernardi M, Felici F, Marchetti M, Montellanico F, Piacentini MF, Solomonow M. Force generation performance and motor unit recruitment strategy in muscles of contralateral limbs. *J Electromyogr Kinesiol* 9: 121-30, 1999.
- Bernardi M, Solomonow M, Nguyen G, Smith A, Baratta R. Motor unit recruitment

Chapter 8 Bibliography

- strategy changes with skill acquisition. *Eur J Appl Physiol Occup Physiol* 74: 52-59, 1996.
- Bigland-Ritchie B & Woods JJ. Integrated electromyogram and oxygen uptake during positive and negative work. *J Physiol* 260: 267-277, 1976.
- Bilodeau M, Goulet C, Nadeau S, Arsenault AB, Gravel D. Comparison of the EMG power spectrum of the human soleus and gastrocnemius muscles. *Eur J Appl Physiol Occup Physiol* 68: 395-401, 1994.
- Bodine SC, Roy RR, Eldred E, Edgerton VR. Maximal force as a function of anatomical features of motor units in the cat tibialis anterior. *J Neurophysiol* 57: 1730-1745, 1987.
- Bodine-Fowler S, Garfinkel A, Roy RR, Edgerton VR. Spatial distribution of muscle fibers within the territory of a motor unit. *Muscle Nerve* 13: 1133-1145, 1990.
- Bodurka J & Bandettini PA. Toward direct mapping of neuronal activity: MRI detection of ultraweak, transient magnetic field changes. *Magn Reson Med* 47: 1052-1058, 2002.
- Bonny JM, Zanca M, Boespflug-Tanguy O, Dedieu V, Joandel S, Renou JP. Characterization in vivo of muscle fiber types by magnetic resonance imaging. *Magn Reson Imaging* 16: 167-173, 1998.
- Bratton CB, Hopkins AL, Weinberg JW. Nuclear magnetic resonance studies of living muscle. *Science* 147: 738-739, 1965.
- Burke RE. Motor units: anatomy, physiology, and functional organization. In: *Handbook of Physiology. The Nervous System*. Bethesda, MD: American Physiological Society, p. 345-422, 1981.
- Burke RE, Levine DN, Zajac FE 3rd. Mammalian motor units:

Chapter 8 Bibliography

- physiological-histochemical correlation in three types in cat gastrocnemius. *Science* 174: 709-712, 1971.
- Burke RE & Tsairis P. Anatomy and innervation ratios in motor units of cat gastrocnemius. *J Physiol* 234: 749-765, 1973.
- Chanaud CM, Pratt CA, Loeb GE. Functionally complex muscles of the cat hindlimb. V. The roles of histochemical fiber-type regionalization and mechanical heterogeneity in differential muscle activation. *Exp Brain Res* 85: 300-313, 1991.
- Colliander EB, Dudley GA, Tesch PA. Skeletal muscle fiber type composition and performance during repeated bouts of maximal, concentric contractions. *Eur J Appl Physiol* 58: 81-86, 1988.
- Conley MS, Meyer RA, Bloomberg JJ, Feedback DL, Dudley GA. Noninvasive analysis of human neck muscle function. *Spine* 20: 2505-2512, 1995.
- Conley MS, Stone MH, Nimmons M, Dudley GA. Resistance training and human cervical muscle recruitment plasticity. *J Appl Physiol* 83: 2105-2111, 1997.
- Damon BM, Gregory CD, Hall KL, Stark HJ, Gulani V, Dawson MJ. Intracellular acidification and volume increases explain R (2) decreases in exercising muscle. *Magn Reson Med* 47: 14-23, 2002.
- De Luca CJ, LeFever RS, McCue MP, Xenakis AP. Behaviour of human motor units in different muscles during linearly varying contractions. *J Physiol* 329: 113-128, 1982.
- De Ruiter CJ, De Haan A, Sargeant AJ. Physiological characteristics of two extreme muscle compartments in gastrocnemius medialis of the anaesthetized rat. *Acta Physiol Scand* 153: 313-324, 1995.

Chapter 8 Bibliography

- DeRuiter CJ, De Haan A, Sargeant AJ. Fast-twitch muscle unit properties in different rat medial gastrocnemius muscle compartments. *J Neurophysiol* 75: 2243-2254, 1996.
- Dudley GA & Terjung RL. Influence of acidosis on AMP deaminase activity in contracting fast-twitch muscle. *Am J Physiol Cell Physiol* 248: C43-C50, 1985.
- Edgerton VR, Smith JL, Simpson DR. Muscle fibre type populations of human leg muscles. *Histochem J* 7: 259-266, 1975.
- Edström L & Kugelberg E. Histochemical composition, distribution of fibres and fatiguability of single motor units. Anterior tibial muscle of the rat. *J Neurol Neurosurg Psychiatry* 31: 424-433, 1968.
- Enoka RM. Single-joint system components. In: *Neuromechanics of Human Movement. The Motor System*. Champaign, IL: Human Kinetics, p. 209-360, 2001.
- Fisher MJ, Meyer RA, Adams GR, Foley JM, Potchen EJ. Direct relationships between proton T2 and exercise intensity in skeletal muscle MR images. *Invest Radiol* 25: 480-485, 1990.
- Fleckenstein JL, Canby RC, Parkey RW, Peshock RM. Acute effects of exercise on MR imaging of skeletal muscle in normal volunteers. *AJR Am J Roentgenol* 151: 231-237, 1988.
- Fleckenstein JL, Haller RG, Bertocci LA, Parkey RW, Peshock RM. Glycogenolysis, not perfusion, is the critical mediator of exercise-induced muscle modifications on MR images. *Radiology* 183: 25-27, 1992a.
- Fleckenstein JL, Haller RG, Lewis SF, Archer BT, Barker BR, Payne J, Parkey RW, Peshock RM. Absence of exercise-induced MRI enhancement of skeletal muscle in McArdle's disease. *J Appl Physiol* 71: 961-969, 1991.

Chapter 8 Bibliography

- Fleckenstein JL, Watumull D, Bertocci LA, Parkey RW, Peshock RM. Finger-specific flexor recruitment in humans: depiction by exercise-enhanced MRI. *J Appl Physiol* 72: 1974-1977, 1992b.
- Fleckenstein JL, Watumull D, McIntire DD, Bertocci LA, Chason DP, Peshock RM. Muscle proton T₂ relaxation times and work during repetitive maximal voluntary exercise. *J Appl Physiol* 74: 2855-2859, 1993.
- Friederich JA & Brand RA. Muscle fiber architecture in the human lower limb. *J Biomech* 23: 91-95, 1990.
- Fuglevand AJ & Segal SS. Simulation of motor unit recruitment and microvascular unit perfusion: spatial considerations. *J Appl Physiol* 83: 1223-1234, 1997.
- Fukunaga T, Roy RR, Shellock FG, Hodgson JA, Day MK, Lee PL, Kwong-Fu H, Edgerton VR. Physiological cross-sectional area of human leg muscles based on magnetic resonance imaging. *J Orthop Res* 10: 928-934, 1992.
- Fukunaga T, Roy RR, Shellock FG, Hodgson JA, Edgerton VR. Specific tension of human plantar flexors and dorsiflexors. *J Appl Physiol* 80: 158-165, 1996.
- Fung BM & Puon PS. Nuclear magnetic resonance transverse relaxation in muscle water. *Biophys J* 33: 27-37, 1981.
- Garnett RA, O'Donovan MJ, Stephens JA, Taylor A. Motor unit organization of human medial gastrocnemius. *J Physiol* 287: 33-43, 1979.
- Gerdle B, Henriksson-Larsen K, Lorentzon R, Wretling ML. Dependence of the mean power frequency of the electromyogram on muscle force and fibre type. *Acta Physiol Scand* 142: 457-465, 1991.
- Gravel D, Arsenault AB, Lambert J. Soleus-gastrocnemius synergies in controlled contractions produced around the ankle and knee joints: an EMG study.

Chapter 8 Bibliography

- Electromyogr Clin Neurophysiol* 27: 405-413, 1987.
- Green RA & Wilson DJ. A pilot study using magnetic resonance imaging to determine the pattern of muscle group recruitment by rowers with different levels of experience. *Skeletal Radiol* 29: 196-203, 2000.
- Hammond CG, Gordon DC, Fisher JT, Richmond FJ. Motor unit territories supplied by primary branches of the phrenic nerve. *J Appl Physiol* 66: 61-71, 1989.
- Hatakenaka M, Ueda M, Ishigami K, Otsuka M, Masuda K. Effects of aging on muscle T2 relaxation time: difference between fast- and slow-twitch muscles. *Invest Radiol* 36: 692-698, 2001.
- Henneman E & Mendell LM. Functional organization of motoneuron pool and its inputs. In: *Handbook of Physiology. The Nervous System*. Bethesda, MD: American Physiological Society, p. 423-507, 1981.
- Henneman E, Somjen G, Carpenter DO. Functional significance of cell size in spinal motoneurons. *J Neurophysiol* 28: 560-580, 1965.
- Hof AL & van den Berg J. Linearity between the weighted sum of the EMGs of the human triceps surae and the total torque. *J Biomech* 10: 529-539, 1977.
- Hutchison DL, Roy RR, Hodgson JA, Edgerton VR. EMG amplitude relationships between the rat soleus and medial gastrocnemius during various motor tasks. *Brain Res* 502: 233-244, 1989.
- Ichinose Y, Kanehisa H, Ito M, Kawakami Y, Fukunaga T. Morphological and functional differences in the elbow extensor muscle between highly trained male and female athletes. *Eur J Appl Physiol Occup Physiol* 78: 109-114, 1998.
- Ikai M & Fukunaga T. Calculation of muscle strength per unit cross-sectional area of human muscle by means of ultrasonic measurement. *Int Z Angew Physiol* 26:

Chapter 8 Bibliography

26-32, 1968.

Jacobs R & van Ingen Schenau GJ. Control of an external force in leg extensions in humans. *J Physiol* 457: 611-626, 1992.

Jenner G, Foley JM, Cooper TG, Potchen EJ, Meyer RA. Changes in magnetic resonance images of muscle depend on exercise intensity and duration, not work. *J Appl Physiol* 76: 2119-2124, 1994.

Johnson MA, Polgar J, Weightman D, Appleton D. Data on the distribution of fibre types in thirty-six human muscles: an autopsy study. *J Neurol Sci* 18: 111-129, 1973.

Kanda K, Hashizume K. Factors causing difference in force output among motor units in the rat medial gastrocnemius muscle. *J Physiol* 448: 677-695, 1992.

Kawakami Y, Ichinose Y, Fukunaga T. Architectural and functional features of human triceps surae muscles during contraction. *J Appl Physiol* 85: 398-404, 1998.

Kawakami Y, Ichinose Y, Kubo K, Ito M, Imai M, Fukunaga T. Architecture of contracting human muscles and its functional significance. *J Appl Biomech* 16: 88-98, 2000.

Kernell D. Organized variability in the neuromuscular system: a survey of task-related adaptations. *Arch Ital Biol* 130: 19-66, 1992.

Kinugasa R & Akima H. Neuromuscular activation of triceps surae using muscle functional MRI and EMG. *Med Sci Sports Exerc* 37: 593-598, 2005.

Kinugasa R, Akima H, Ota A, Ohta A, Sugiura K, Kuno SY. Short-term creatine supplementation does not improve muscle activation or sprint performance in humans. *Eur J Appl Physiol* 91: 230-237, 2004.

Kinugasa R, Hayashi S, Iino N, Tamura M, Oouchi T, Horii A. Recruitment pattern of

Chapter 8 Bibliography

- quadriceps femoris muscles during repetitive knee extension exercise by muscle functional MRI. *J Phys Exerc Sports Sci* 8: 1-6, 2002.
- Kinugasa R, Kawakami Y, Fukunaga T. Muscle activation and its distribution within human triceps surae muscles. *J Appl Physiol* 99: 1149-1156, 2005a.
- Kinugasa R, Kawakami Y, Fukunaga T. Quantitative assessment of skeletal muscle activation using muscle functional MRI. *Magn Reson Imaging* 24: 639-644, 2006.
- Kinugasa R, Kawashima S, Masuda K, Ajisaka R, Matsuda M, Kuno S. The time course of strength gain due to muscle recruitment and hypertrophic factors in middle-aged and elderly women. *Jpn J Phys Fitness Sports Med* 52 (Suppl): 105-118, 2003 (Japanese).
- Kinugasa R, Yoshida K, Watanabe T, Kuchiki K, Horii A. Skin cooling alters the activation patterns of different heads of the quadriceps. *Can J Appl Physiol* 30: 127-139, 2005b.
- Kukulka CG & Clamann HP. Comparison of the recruitment and discharge properties of motor units in human brachial biceps and adductor pollicis during isometric contractions. *Brain Res* 219: 45-55, 1981.
- Lan N & Crago PE. A noninvasive technique for in vivo measurement of joint torque of biarticular muscles. *J Biomech* 25: 1075-1079, 1992.
- LeBlanc A, Lin C, Shackelford L, Sinitsyn V, Evans H, Belichenko O, Schenkman B, Kozlovskaya I, Oganov V, Bakulin A, Hedrick T, Feedback D. Muscle volume, MRI relaxation times (T₂), and body composition after spaceflight. *J Appl Physiol* 89: 2158–2164, 2000.
- Lemos R, Epstein M, Herzog W, Wyvill B. Three-dimensional geometric model of

Chapter 8 Bibliography

- skeletal muscle. In: *Skeletal Muscle Mechanics: From Mechanisms to Function*. Chichester, WS: John Wiley & Sons, p. 179-206, 2000.
- Lieber RL. Physiological properties of muscle fiber types. In: *Skeletal muscle structure, function & plasticity*. Baltimore, MD: Lippincott Williams & Wilkins, p. 85-87, 2002.
- Livingston BP, Segal RL, Song A, Hopkins K, English AW, Manning CC. Functional activation of the extensor carpi radialis muscles in humans. *Arch Phys Med Rehabil* 82: 1164-1170, 2001.
- Loh EY, Agur AM, McKee NH. Intramuscular innervation of the human soleus muscle: a 3D model. *Clin Anat* 16: 378-382, 2003.
- McLean L & Goudy N. Neuromuscular response to sustained low-level muscle activation: within- and between-synergist substitution in the triceps surae muscles. *Eur J Appl Physiol* 91: 204-216, 2004.
- Meyer RA, Brown TR, Krilowicz BL, Kushmerick MJ. Phosphagen and intracellular pH changes during contraction of creatine depleted rat muscle. *Am J Physiol Cell Physiol* 250: C264-C274, 1986.
- Meyer RA & Prior BM. Functional magnetic resonance imaging of muscle. *Exerc Sport Sci Rev* 28: 89-92, 2000.
- Meyer RA, Prior BM, Siles RI, Wiseman RW. Contraction increases the T_2 of muscle in fresh water but not in marine invertebrates. *NMR Biomed* 14: 199-203, 2001.
- Milner-Brown HS, Stein RB, Yemm R. The contractile properties of human motor units during voluntary isometric contractions. *J Physiol* 228: 285-306, 1973.
- Monti RJ, Roy RR, Edgerton VR. Role of motor unit structure in defining function. *Muscle Nerve* 24: 848-866, 2001.

Chapter 8 Bibliography

- Moritani T & deVries HA. Reexamination of the relationship between the surface integrated electromyogram (IEMG) and force of isometric contraction. *Am J Phys Med* 57: 263-277, 1978.
- Moritani T & Muro M. Motor unit activity and surface electromyogram power spectrum during increasing force of contraction. *Eur J Appl Physiol* 56: 260-265, 1987.
- Moritani T, Oddsson L, Thorstensson A. Activation patterns of the soleus and gastrocnemius muscles during different motor tasks. *J Electromyogr Kinesiol* 1: 81-88, 1991.
- Muramatsu T, Muraoka T, Takeshita D, Kawakami Y, Hirano Y, Fukunaga T. Mechanical properties of tendon and aponeurosis of human gastrocnemius muscle in vivo. *J Appl Physiol* 90: 1671-1678, 2001.
- Murray MP, Guten GN, Baldwin JM, Gardner GM. A comparison of plantar flexion torque with and without the triceps surae. *Acta Orthop Scand* 47: 122-124, 1976.
- Nichols TR. A biomechanical perspective on spinal mechanisms of coordinated muscular action: an architectural principle. *Acta Anat (Basel)* 151: 1-13, 1994.
- Ochs RM, Smith JL, Edgerton VR. Fatigue characteristics of human gastrocnemius and soleus muscles. *Electroencephalogr Clin Neurophysiol* 17: 297-306, 1977.
- Ploutz LL, Tesch PA, Biro RL, Dudley GA. Effect of resistance training on muscle use during exercise. *J Appl Physiol* 76: 1675-1681, 1994.
- Ploutz-Snyder LL, Nyren S, Cooper TG, Potchen EJ, and Meyer RA. Different effects of exercise and edema on T2 relaxation in skeletal muscle. *Magn Reson Med* 37: 676-682, 1997.
- Ploutz-Snyder LL, Tesch PA, Crittenden DJ, Dudley GA. Effect of unweighting on skeletal muscle use during exercise. *J Appl Physiol* 79: 168-175, 1995.

Chapter 8 Bibliography

- Polak JF, Jolesz FA, Adams DF. NMR of skeletal muscle. Differences in relaxation parameters related to extracellular/intracellular fluid spaces. *Invest Radiol* 23: 107-112, 1988.
- Price TB, Kamen G, Damon BM, Knight CA, Applegate B, Gore JC, Eward K, Signorile JF. Comparison of MRI with EMG to study muscle activity associated with dynamic plantar flexion. *Magn Reson Imaging* 21: 853-861, 2003.
- Price TB, Kennan RP, Gore JC. Isometric and dynamic exercise studied with echo planar magnetic resonance imaging (MRI). *Med Sci Sports Exerc* 30: 1374-1380, 1998.
- Price TB, McCauley TR, Duleba AJ, Wilkens KL, Gore JC. Changes in magnetic resonance transverse relaxation times of two muscles following standardized exercise. *Med Sci Sports Exerc* 27: 1421-1429, 1995.
- Prior, BM, Foley JM, Jayaraman RC, Meyer RA. Pixel T2 distribution in functional magnetic resonance images of muscle. *J Appl Physiol* 87: 2107-2114, 1999.
- Prior BM, Ploutz-Snyder LL, Cooper TG, Meyer RA. Fiber type and metabolic dependence of T2 increases in stimulated rat muscles. *J Appl Physiol* 90: 615-623, 2001.
- Rafuse VF & Gordon T. Self-reinnervated cat medial gastrocnemius muscles. II. Analysis of the mechanisms and significance of fiber type grouping in reinnervated muscles. *J Neurophysiol* 75: 282-297, 1996.
- Reid RW, Foley JM, Jayaraman RC, Prior BM, Meyer RA. Effect of aerobic capacity on the T (2) increase in exercised skeletal muscle. *J Appl Physiol* 90: 897-902, 2001.
- Rusinek H & Chandra R. Brain tissue volume measurement from magnetic resonance

Chapter 8 Bibliography

- imaging. A phantom study. *Invest Radiol* 28: 890-895, 1993.
- Saltin B & Gollnick PD. Skeletal muscle adaptability: significance for metabolism and performance. In: *Handbook of Physiology. Skeletal Muscle*. Bethesda, MD: American Physiological Society, p. 555-631, 1983.
- Scott SH, Engstrom CM, Loeb GE. Morphometry of human thigh muscles. Determination of fascicle architecture by magnetic resonance imaging. *J Anat* 182: 249-257, 1993.
- Segal RL & Song AW. Nonuniform activity of human calf muscles during an exercise task. *Arch Phys Med Rehabil* 86: 2013-2017, 2005.
- Segal RL, Wolf SL, DeCamp MJ, Chopp MT, English AW. Anatomical partitioning of three multiarticular human muscles. *Acta Anat (Basel)* 142: 261-266, 1991.
- Shellock FG, Fukunaga T, Mink JH, Edgerton VR. Exertional muscle injury: evaluation of concentric versus eccentric actions with serial MR imaging. *Radiology* 179: 659-664, 1991.
- Signorile JF, Applegate B, Duque M, Cole N, Zink A. Selective recruitment of the triceps surae muscles with changes in knee angle. *J Strength Cond Res* 16: 433-439, 2002.
- Sloniger MA, Cureton KJ, Prior BM, Evans EM. Lower extremity muscle activation during horizontal and uphill running. *J Appl Physiol* 83: 2073-2079, 1997.
- Tamaki H, Kitada K, Akamine T, Sakou T, Kurata H. Electromyogram patterns during plantarflexions at various angular velocities and knee angles in human triceps surae muscles. *Eur J Appl Physiol Occup Physiol* 75: 1-6, 1997.
- Thompson CW & Floyd RT. The Ankle and Foot Joints. In: *Manual of Structural Kinesiology*. St Louis, MO: Mosby, p. 129-132, 1994.

Chapter 8 Bibliography

- Tötösy de Zepetnek JE, Zung HV, Erdebil S, Gordon T. Innervation ratio is an important determinant of force in normal and reinnervated rat tibialis anterior muscles. *J Neurophysiol* 67: 1385-1403, 1992.
- Trotter JA. Functional morphology of force transmission in skeletal muscle. A brief review. *Acta Anat (Basel)* 146: 205-222, 1993.
- Van Cutsem M, Feiereisen P, Duchateau J, Hainaut K. Mechanical properties and behaviour of motor units in the tibialis anterior during voluntary contractions. *Can J Appl Physiol* 22: 585-597, 1997.
- van Bolhuis BM, Gielen CCAM, van Ingen Schenau GJ. Activation patterns of mono- and bi-articular arm muscles as a function of force and movement direction of the wrist in humans. *J Physiol* 508: 313–324, 1998.
- van Ingen Schenau GJ, Boots PJ, de Groot G, Snackers RJ, van Woensel WW. The constrained control of force and position in multi-joint movements. *Neuroscience* 46: 197-207, 1992.
- van Ingen Schenau GJ, Dorssers WM, Welter TG, Beelen A, de Groot G, Jacobs R. The control of mono-articular muscles in multijoint leg extensions in man. *J Physiol* 484: 247-254, 1995.
- Vandenborne K, Walter G, Ploutz-Snyder L, Dudley G, Elliott MA, De Meirleir K. Relationship between muscle T_2^* relaxation properties and metabolic state: a combined localized ^{31}P -spectroscopy and ^1H -imaging study. *Eur J Appl Physiol* 82: 76-82, 2000.
- Wang CH, Chen JC, Liu RS. Development and evaluation of MRI based Bayesian image reconstruction methods for PET. *Comput Med Imaging Graph* 28: 177-184, 2004.

Chapter 8 Bibliography

- Warfield SK, Mulkern RV, Winalski CS, Jolesz FA, Kikinis R. An image processing strategy for the quantification and visualization of exercise-induced muscle MRI signal enhancement. *J Magn Reson Imaging* 11: 525-531, 2000.
- Weidman ER, Charles HC, Negro-Vilar R, Sullivan MJ, MacFall JR. Muscle activity localization with ^{31}P spectroscopy and calculated T_2 - weighted ^1H images. *Invest Radiol* 26: 309-316, 1991.
- Weishaupt D, Schweitzer ME, Morrison WB. Injuries to the distal gastrocnemius muscle: MR findings. *J Comput Assist Tomogr* 25: 677-682, 2001.
- Willison RG. Preservation of bulk and strength in muscles affected by neurogenic lesions. *Muscle Nerve* 1: 404-406, 1978.
- Windhorst U, Hamm TM, Stuart DG. On the function of muscle and reflex partitioning. *Behav Brain Sci* 12: 629-681, 1989.
- Wolf SL & Kim JH. Morphological analysis Morphological analysis of the human tibialis anterior and medial gastrocnemius muscles. *Acta Anat (Basel)* 158: 287-295, 1997.
- Wolf SL, Segal RI, English AW. Task-oriented EMG activity recorded from partitions in human lateral gastrocnemius muscle. *J Electromyogr Kinesiol* 3: 87-94, 1993.
- Yamashita N & Moritani T. Anticipatory changes of soleus H-reflex amplitude during execution process for heel raise from standing position. *Brain Res* 490: 148 –151, 1989.
- Yanagisawa O, Niitsu M, Yoshioka H, Goto K, Itai Y. MRI determination of muscle recruitment variations in dynamic ankle plantar flexion exercise. *Am J Phys Med Rehabil* 82: 760-765, 2003.
- Yue G, Alexander AL, Laidlaw DH, Gmitro AF, Unger EC, Enoka RM. Sensitivity of

Chapter 8 Bibliography

- muscle proton spin-spin relaxation time as an index of muscle activation. *J Appl Physiol* 77: 84-92, 1994.
- Zajac FE. Coupling of Recruitment Order to the Force Produced by Motor Units: The "Size Principle Hypothesis". In: *The segmental motor system*. New York, NY: Oxford University Press, p. 96-111, 1989.
- Zajac FE & Faden JS. Relationship among recruitment order, axonal conduction velocity, and muscle-unit properties of type-identified motor units in cat plantaris muscle. *J Neurophysiol* 53: 1303-1322, 1985.
- Zhu XP, Zhao S, Isherwood I. Magnetization transfer contrast (MTC) imaging of skeletal muscle at 0.26 Tesla--changes in signal intensity following exercise. *Br J Radiol* 65: 39-43, 1992.
- Zuurbier CJ, Everard AJ, van der Wees P, Huijing PA. Length-force characteristics of the aponeurosis in the passive and active muscle condition and in the isolated condition. *J Biomech* 27: 445-453, 1994.